Columbus Viaduct System

Nebraska Department of Roads (NDOR)

Project Number: P303

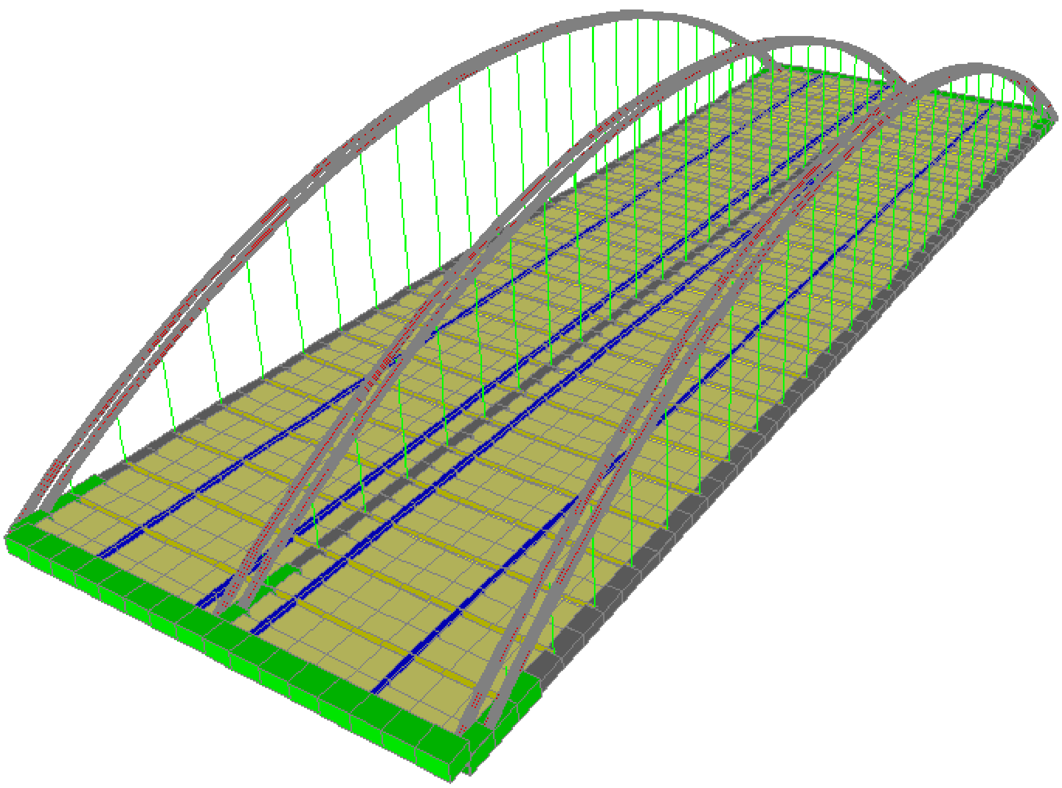

February 2009

Columbus Viaduct System

Nebraska Department of Roads (NDOR)

Project Number: P303

FINAL REPORT

PRINCIPAL INVESTIGATORS

George Morcous, Kromel Hanna, and Maher K. Tadros

SPONSORED BY

Nebraska Department of Roads

University of Nebraska - Lincoln

February 2009

TECHNICAL REPORT DOCUMENTATION PAGE

1. Report No.	2. Government Accession No.	3. Recipient's Catalog No.
1. Title and Subtitle Columbus Viaduct System		2. Report Date February, 2009
		3. Performing Organization Code
4. Author(s) George Morcous, Kromel Hanna, and Maher K. Tadros		5. Performing Organization Report No.
6. Performing Organization Name and Address Department of Civil Engineering University of Nebraska-Lincoln Omaha, Nebraska 68182-0178		7. Work Unit No. 8. Contract or Grant No. P303
9. Sponsoring Agency Name and Address Nebraska Department of Roads Bridge Division P. O. Box 94759 Lincoln, NE 68509-4759		10. Type of Report and Period Covered Draft Report 11. Sponsoring Agency Code
12. Supplementary Notes		

13. Abstract

Recently, the Bridge Division at Nebraska Department of Roads (NDOR) has added to its menu of bridge systems a new system, the tied arch system. This system would be suitable for overpasses where vertical clearance is restricted and center pier is undesirable or impractical, such as water crossings and railroad crossings. This system has been first applied to the construction of the Ravenna Viaduct in 2005 for a single span of 174 ft over a major railroad route with a structural depth of 35 in. and total width of 56.5 ft.

In this project, the tied arch system is applied to the construction of the Columbus Viaduct on US Hwy 30 in Platte County-Nebraska. The viaduct has a single span of 260 ft and total width of approximately 84 ft. Three tied arches are used to facilitate staging of construction while replacing the old bridge. The objective of this project is to provide technical support for the analysis, design, and detailing of the Columbus viaduct and prove the feasibility of the tied arch system in applications where spans over 250 ft are required and vertical clearance restrictions exist. The report presents the detailed analysis of the system at different construction phases as well as the design checks of its main components under various loading conditions. The finite element model developed to analyze the tie beam to arch connection and non-linear analysis performed for lateral stability of arches are also presented.

14. Keywords: Confinement, steel tube, Arch Bridge, Columbus, Post-Tensioning, FEA, interaction diagrams.		15. Distribution Statement	
16. Security Classification (of this report) Unclassified	17. Security Classification (of this page) Unclassified	18. No. of Pages 85	22. Price

Form DOT F1700.7 (8-72)

DISCLAIMER

The contents of this report reflect the views of the authors who are responsible for the facts and the accuracy of the data presented herein. The contents do not necessarily reflect the official views or policies of the Nebraska Department of Roads, nor of the University of Nebraska-Lincoln. This report does not constitute a standard, specification, or regulation. Trade or manufacturers' names, which may appear in this report, are cited only because they are considered essential to the objectives of the report. The United States (U.S.) government and the State of Nebraska do not endorse products or manufacturers.

ACKNOWLEDGEMENTS

This project was sponsored by the Nebraska Department of Roads (NDOR) and the University of Nebraska-Lincoln. The support of the technical advisory committee (TAC) members is gratefully acknowledged. The design team at NDOR Bridge Division is also acknowledged, they spent considerable time and effort in coordinating this project, discussing its technical direction, and inspiring the university researchers.

ABSTRACT

Recently, the Bridge Division at Nebraska Department of Roads (NDOR) has added to its menu of bridge systems a new system, the tied arch system. This system would be suitable for overpasses where vertical clearance is restricted and center pier is undesirable or impractical, such as water crossings and railroad crossings. This system was first applied to the construction of the Ravenna Viaduct in 2005 for a single span of 174 ft over a major railroad route with a structural depth of 35 in. and total width of 56.5 ft.

In this project, the tied arch system is included in the construction of the Columbus Viaduct on US Hwy 30 in Platte County-Nebraska. The viaduct has a single span of 260 ft and total width of approximately 84 ft. Three tied arches are used to facilitate staging of construction while replacing the old bridge. The objective of this project is to provide technical support for the analysis, design, and detailing of the Columbus viaduct and prove the feasibility of the tied arch system in applications where spans over 250 ft are required and vertical clearance restrictions exist. The report presents the detailed analysis of the system at different construction phases as well as the design checks of its main components under various loading conditions. The finite element model developed to analyze the tie beam to arch connection and non-linear analysis performed for lateral stability of arches are also presented.

TABLE OF CONTENTS

SECTION 1: INTRODUCTION

1.1 Background

The positive design and construction experience of the tied arch system in Ravenna Viaduct encouraged Nebraska Department of Roads (NDOR) to use this system in another project with a longer span. Columbus Viaduct on US Hwy 30 in Platte County-Nebraska has two spans; arch span of 260 feet, and beam span of 96 ft; and a width of approximately 84 feet. Figure 1.1.1 shows the proposed tied arch system that consists of concrete filled steel tubes for the arch, post-tensioned concrete filled steel tubes for the tie, threaded rod hangers, and steel floor beams composite with post-tensioned concrete deck. This system was proven to be the most efficient system from structural and economical points of view. The report focuses on the analysis and design of the main components of the arch span.

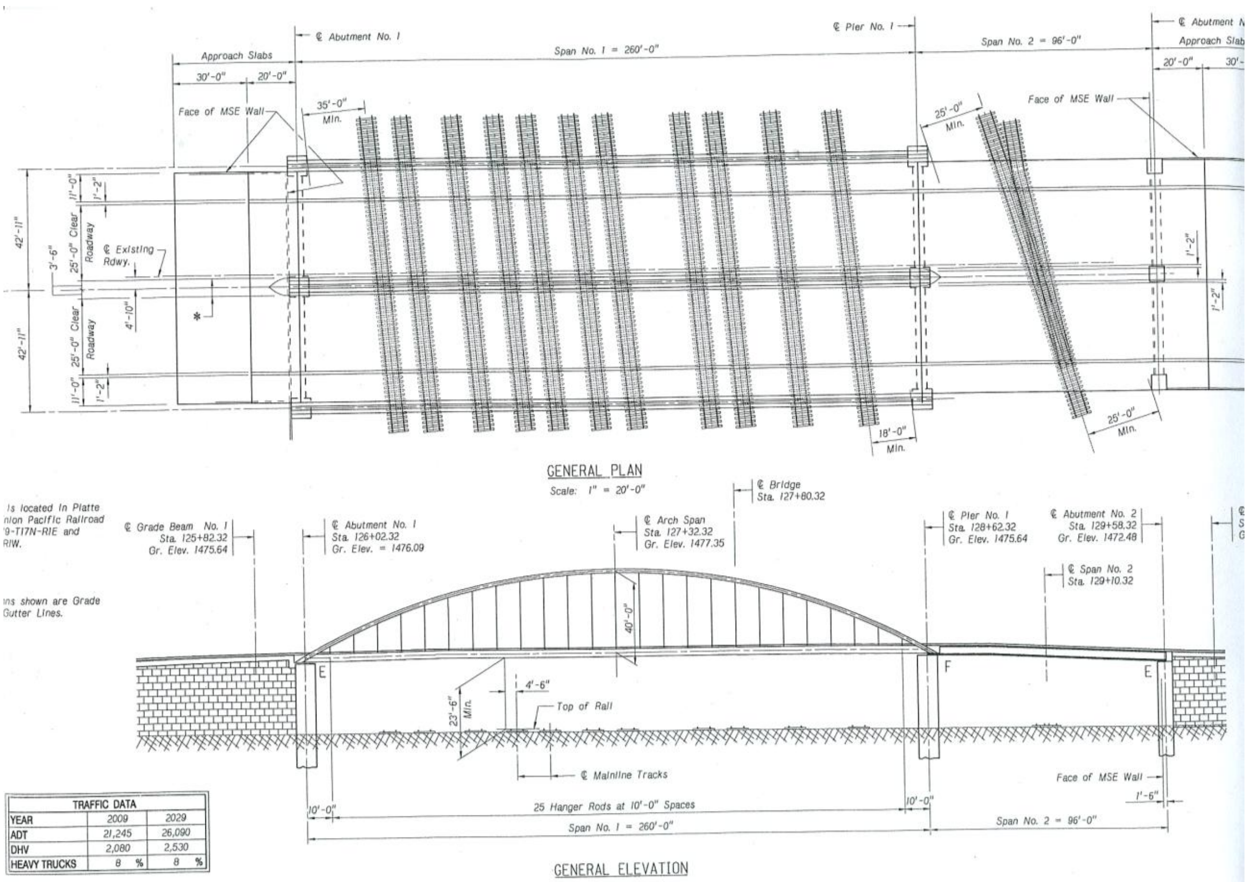

Figure 1.1.1: General plan and elevation of Columbus viaduct

The structural efficiency of this system is mainly due to: 1) the effects of confinement on the concrete capacity in compression members; 2) the use of post-tensioning to eliminate tensile stresses in the tie; 3) the significant reduction in bending moments through the use of top and bottom chords; 4) the composite action with a full width bridge deck to enhance the flexural capacity of the tie even without diaphragms. The economic efficiency of this system is mainly due to the optimal use of different materials (i.e. steel and concrete) and the prefabrication of the tied arch, which significantly saves the construction time and allows the replacement projects to be completed with minimal traffic disruption. Moreover, this system makes it possible to design a superstructure that provides the required overhead clearance for railroad lines. Also, the non-linear P-delta analysis of the tied arch system may indicate that cross braces are not necessary for lateral stability, which improves the aesthetics of the structure.

1.2 Objective

The immediate goal of this research is to provide technical support during the analysis, design, and detailing of the Columbus Viaduct Arch System. The results of the research will form the basis for standardizing the system for future use in applications where spans over 250 ft are required and vertical clearance restrictions exist.

1.3 Report Organization

This report is divided into four sections. Section one provides the background, objective, and report organization. Section two presents the models used for system analysis, section properties, loads, and analysis stages and results. Section three presents the design checks of the various system components including the arch, tie, hanger, cross beams, and connections as well as checks for lateral stability. Section four summarizes the analysis and design results and research conclusions

SECTION 2: SYSTEM ANALYSIS

2.1 Analysis Model

The structural analysis of the Columbus Viaduct is performed using the structural analysis software SAP2000 v.10.1.3. The viaduct is modeled as a 3-D structure using frame elements for ties, arches, cross beams, end beams, and rails; cable elements for hangers; tendon elements for post-tensioning strands; and shell elements for concrete deck. Figure 2.1 shows the plan and profile views of the model, its different components, and centerline dimensions.

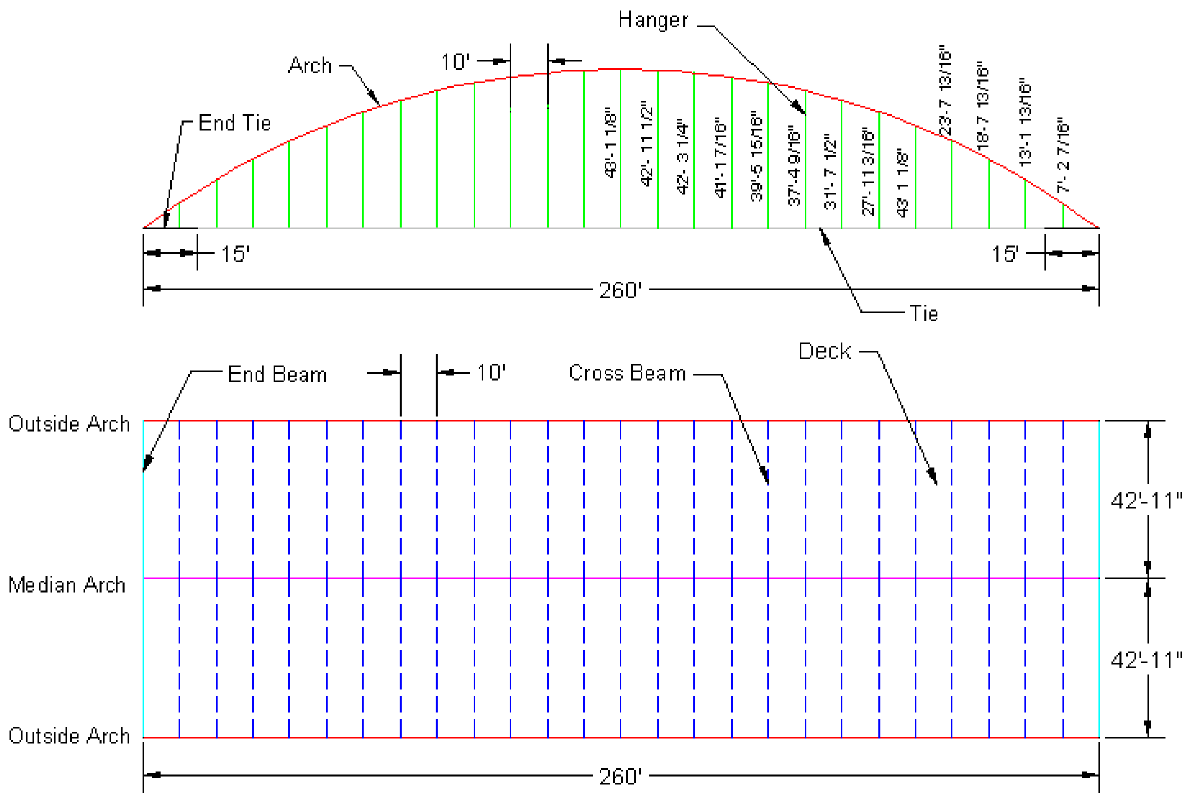

Figure 2.1.1: Plan and profile views of the viaduct model

2.2 Section Properties and Materials

Figure 2.2.1 shows the cross section of each element in the model. The geometric and mechanical properties of these elements are listed in Table 2.2.1. It should be noted that section properties are calculated for two different stages of construction: stage I: steel sections only, and stage II: steel sections filled with concrete. Appendix A shows in details the section properties used in developing the computer models.

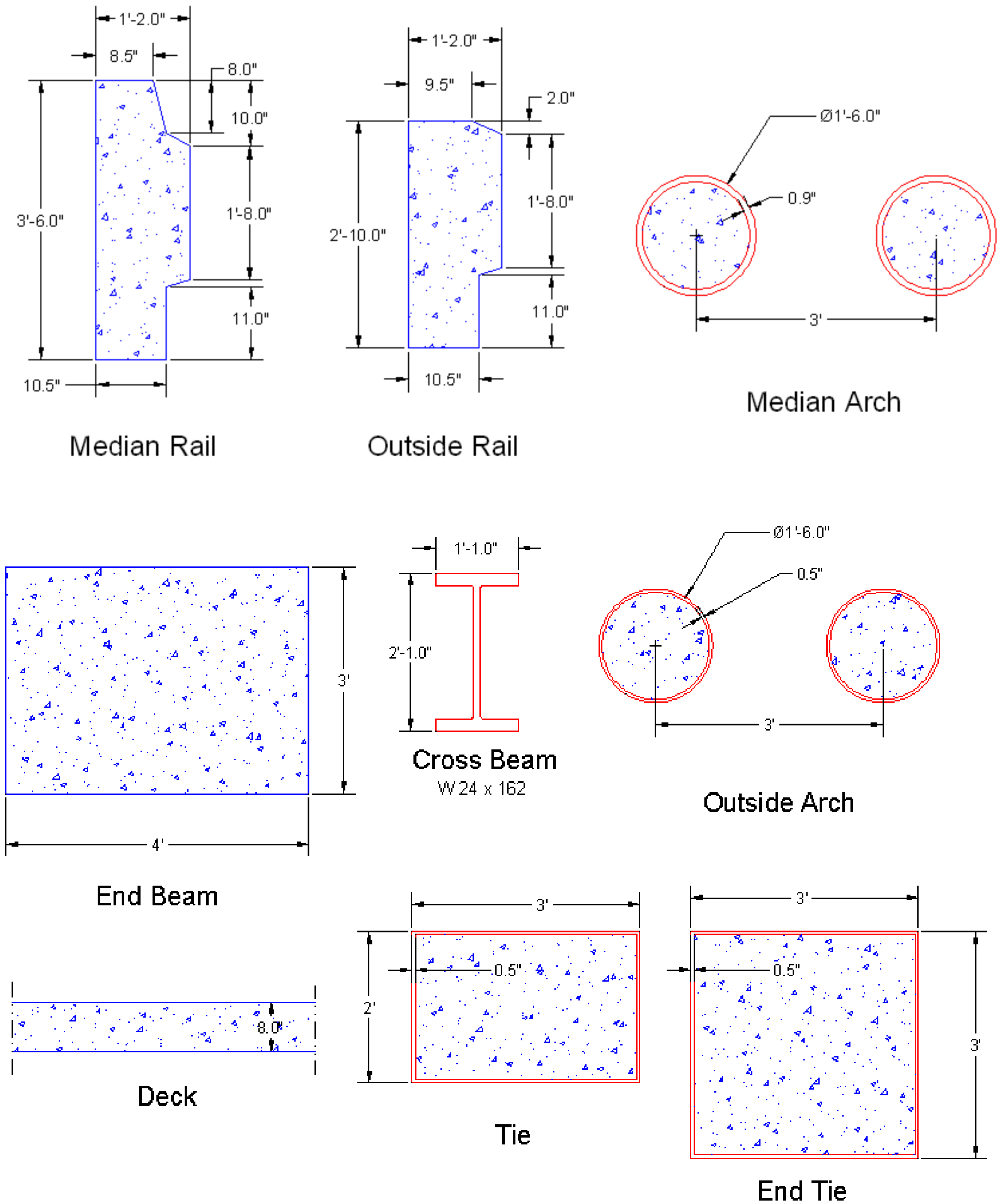

Figure 2.2.1: Cross section of different model elements

Table 2.2.1: Section properties of: a) median arch; b) outside arch; and c) other elements

a) Median Arch

Element	Dimensions		Property	E_{Steel}	$E_{Concrete}$	Equivalent	
	Parameter	Value (in)		29000	5098	Steel	Concrete
Arch (Schedule 80 steel pipe filled with 8 ksi SCC)	Outer Diameter	18	A (in^2)	101	408	172	980
	Spacing CL-to-CL	36	I_x (in^4)	3,670	6,636	4,837	27,513
	Thickness	0.938	I_y (in^4)	36,251	138,951	60,679	345,154
Tie (Grade 50W steel box filled with 8 ksi SCC)	Depth	24	A (in^2)	59	805	201	1,141
	Width	36	I_x (in^4)	5,985	35,487	12,224	69,531
	Thickness	0.5	I_y (in^4)	11,135	82,177	25,582	145,515
End Tie (Grade 50W steel box filled with 8 ksi SCC)	Depth	36	A (in^2)	71	1,225	286	1,629
	Width	36	I_x (in^4)	14,916	125,052	36,900	209,897
	Thickness	0.500	I_y (in^4)	14,916	125,052	36,900	209,897

b) Outside Arch

Element	Dimensions		Property	E_{Steel}	$E_{Concrete}$	Equivalent	
	Parameter	Value (in)		29000	5098	Steel	Concrete
Arch (Extra heavy steel pipe filled with 8 ksi SCC)	Outer Diameter	18	A (in^2)	55	454	135	767
	Spacing CL-to-CL	36	I_x (in^4)	2,106	8,200	3,548	20,181
	Thickness	0.5	I_y (in^4)	19,919	155,283	47,218	268,588
Tie (Grade 50W steel box filled with 8 ksi SCC)	Depth	24	A (in^2)	59	805	201	1,141
	Width	36	I_x (in^4)	5,985	35,487	12,224	69,531
	Thickness	0.5	I_y (in^4)	11,135	82,177	25,582	145,515
End Tie (Grade 50W steel box filled with 8 ksi SCC)	Depth	36	A (in^2)	71	1,225	286	1,629
	Width	36	I_x (in^4)	14,916	125,052	36,900	209,897
	Thickness	0.50	I_y (in^4)	14,916	125,052	36,900	209,897

c) Other Elements

Element	Material	A (in^2)	I_x (in^4)	I_y (in^4)
End Beam	4 ksi Concrete	1,728.0	186,624	331,776
Cross Beam	Structural Grade 50W weathering steel	47.7	5,170	443
Hanger	1 ¾ in diameter Grade 150 ksi steel rods	2.4	0	0
Median Rail	4 ksi Concrete	508.3	65,137	7,136
Outside Rail	4 ksi Concrete	431.3	38,930	6,195

2.3 Loads

Table 2.3.1 lists the own weight of different viaduct components used in the model analysis. In addition to the own weight, the following loads are considered:

- Post-tensioning of ties is calculated assuming 2 tendons of 19-0.6" strands in the outside arch and 2 tendons of 37-0.6" strands in the median arch. Deck is also longitudinally post-tensioned using 0.6" mono strands at 12" spacing. Jacking Stress force is assumed to be 210.6 ksi (0.78*270) and an anchor set of 0.25". Force after anchor set is 41 kip per strand.
- Vehicular live load is calculated in accordance to AASHTO LRFD Section 3.6.1.2, which includes the design truck shown in Figure 2.3.1 in addition to a lane load of 0.64 klf uniformly distributed over 10 ft width. Multiple presence factors are used based on the number of loaded lanes (maximum of 4 traffic lanes and 2 pedestrian lanes) according to AASHTO LRFD Section 3.6.1.1. Dynamic load allowance of 33% is used in accordance to AASHTO LRFD Section 3.6.2.
- Pedestrian live load is calculated in accordance to AASHTO LRFD Section 3.6.1.6, which includes a uniform load of 0.075 ksf over pedestrian lands with no multiple presence factor or dynamic load allowance.
- Fatigue load is calculated in accordance to AASHTO LRFD Section 3.6.1.4, which includes a fatigue truck that has a 30 ft fixed distance between the two 32 kips axles shown below. Load factor of 1.5 (0.75 x 2) is used for infinite life check. Dynamic load allowance of 15% is used in accordance to AASHTO LRFD Section 3.6.2.

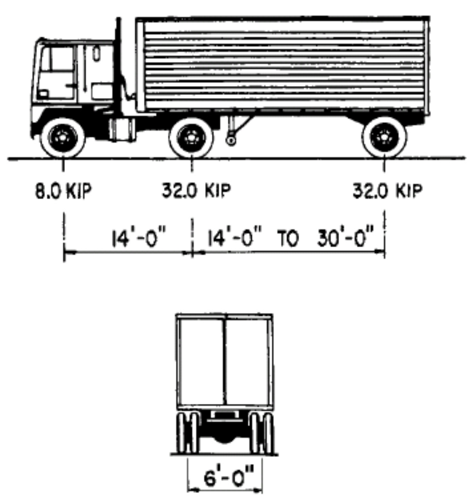

Figure 2.3.1: Characteristics of the design truck

Table 2.3.1: Own weight values of different viaduct components

Own Weight	Value	Unit
Median Arch (Steel Only)	0.342	kip/ft
Outside Arch (Steel Only)	0.187	kip/ft
Tie (Steel Only)	0.201	kip/ft
End Tie (Steel Only)	0.242	kip/ft
Median Arch Concrete	0.425	kip/ft
Outside Arch Concrete	0.473	kip/ft
Tie Concrete	0.839	kip/ft
End Tie Concrete	1.276	kip/ft
Cross Beam	0.162	kip/ft
Metal Deck	0.004	kip/ft^2
Future Wearing Surface	0.020	kip/ft^2
Pedestrian Wearing Surface	0.038	kip/ft^2
Deck Slab	0.100	kip/ft^2
Median Rail	0.530	kip/ft
Outside Rail	0.450	kip/ft
Pedestrian Fence	0.025	kip/ft

2.4 Analysis Stages and Results

Due to the proposed construction sequence of the Columbus viaduct, three analysis stages are performed as follows:

Stage I:

- Structure: Arch and tie (steel only) and cross beams.
- Loads: Own weight of arch, tie, cross beams, metal decking and filling concrete.

Stage II:

- Structure: Arch and tie (filled with concrete) and cross beams.
- Loads: Post-tensioning of ties and own weight of concrete deck.

Stage III:

- Structure: Arch and tie (filled with concrete), cross beams, and 7.5" concrete deck composite with tie beams and cross beams
- Loads: Post-tensioning of deck.

Stage IV:

- Structure: Arch and tie (filled with concrete), cross beams, and 7.5" concrete deck composite with tie and cross beams
- Loads: Railing, wearing surface, moving live load (truck + impact and lane load), pedestrian load, and fatigue load.

A summary of analysis results for each load case are listed in Table 2.4.1, and the analysis results for service and strength limit states are listed in Table 2.4.2. The six critical sections listed in these tables are defined as shown in Figure 2.4.1. Appendix B shows the detailed presentation of the model used in each stage along with the loads applied and the resulted deformation, bending moment, and axial force.

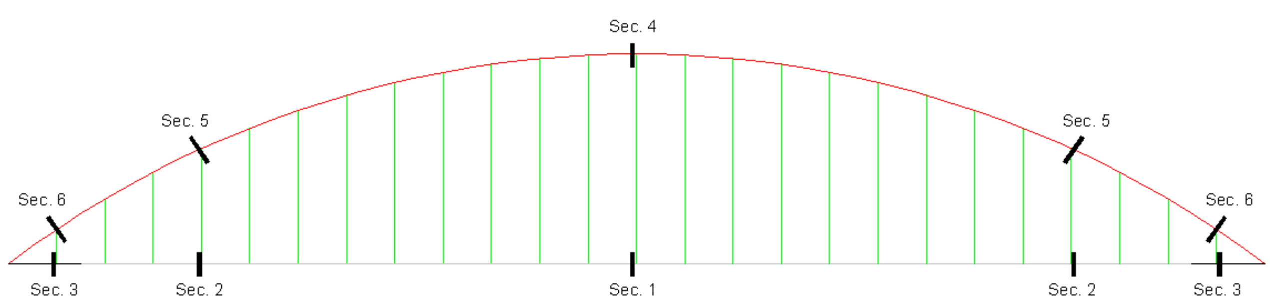

Figure 2.4.1: Location of the critical section

Table 2.4.1: Analysis results for different load cases

a) Median Arch

Section		Sec. 1		Sec. 2		Sec. 3		Sec. 4		Sec. 5		Sec. 6			Hanger	Mid-Point Deflection Δ (in)	Support Reaction (kip)
Stage	Limit State	P (kip)	M (kip.in)	P (kip)	M (kip.in)	P (kip)	M (kip.in)	P (kip)	M (kip.in)	P (kip)	M (kip.in)	P (kip)	M (kip.in)	V (kip)	T (kip)		
I	Own Weight	280	1560	280	-1494	280	-1476	-280	1094	-311	-982	-336	-774	11.3	12.7	2.5	186
	Filling Concrete	247	1135	247	-1150	247	-950	-247	845	-274	-746	-298	-580	9.7	10.1	2.0	174
II	Tie Post-Tensioing	-2613	3131	-2856	-5392	-2729	1484	43	1165	46	-2054	56	-438	3.7	-3.4	0.3	0
	Deck Weight	825	5517	825	-5364	825	-5028	-825	2682	-920	-2342	-995	-1954	30.8	49.3	4.0	536
III	Deck Post-Tensioning	-306	-2935	-302	3608	-187	15545	-51	-1116	-55	1321	-63	2041	0.5	2.2	-1.9	0
IV	Railing	239	621	239	-655	239	-892	-257	440	-286	-326	-310	-482	9.2	15.8	0.8	197
	Wearing Surface	167	510	167	-553	167	-593	-175	334	-195	-262	-211	-330	6.5	10.8	0.6	139
	Live Load + Impact	509	11373	509	-8638	509	-3830	-559	4246	-622	-3294	-673	-1329	23.5	35	4.3	452
	Pedestrian Load	68	310	68	-348	68	-230	-64	171	-71	-148	-77	-125	2.5	3.8	0.3	56
TOTAL (Service)		**-584**	**21,222**	**-823**	**-19,986**	**-581**	**4,030**	**-2,415**	**9,861**	**-2,688**	**-8,833**	**-2,907**	**-3,971**	**98**	**136**	**12.7**	**1,740**
TOTAL (Strength)		**330**	**32,448**	**91**	**-29,168**	**333**	**-1,398**	**-3,372**	**14,606**	**-3,753**	**-12,645**	**-4,060**	**-6,174**	**136**	**193**		**2,464**

a) Outside Arch

Section		Sec. 1		Sec. 2		Sec. 3		Sec. 4		Sec. 5		Sec. 6			Hanger	Mid-Point Deflection Δ (in)	Support Reaction (kip)
Stage	Limit State	P (kip)	M (kip.in)	P (kip)	M (kip.in)	P (kip)	M (kip.in)	P (kip)	M (kip.in)	P (kip)	M (kip.in)	P (kip)	M (kip.in)	V (kip)	T (kip)		
I	Own Weight	165	1138	165	-1082	165	-1006	-165	474	-184	-420	-200	-338	5.4	8.1	1.8	110
	Filling Concrete	257	1446	257	-1383	257	-1121	-257	624	-285	-558	-310	-466	8.5	10.7	2.5	181
II	Tie Post-Tensioing	-1342	1751	-1467	-2992	-1401	672	22	479	24	-825	28	-133	1.1	-1.6	0.2	0
	Deck Weight	413	3007	413	-2900	413	-2660	-413	1113	-460	-950	-499	-831	13.2	25.1	2.2	268
III	Deck Post-Tensioning	-307	-2732	-288	3487	-200	11302	-32	-771	-35	930	-40	1096	-0.4	1.6	-1.7	0
IV	Railing	72	384	72	-421	72	-161	-63	155	-70	-133	-76	-101	2.2	3.8	0.3	34
	Wearing Surface	95	432	95	-470	95	-297	-92	189	-102	-155	-111	-151	3	5.6	0.4	54
	Live Load + Impact	97	2837	97	-6170	97	-4668	-78	860	-87	-1660	-93	-531	4.1	4.3	1.4	57
	Pedestrian Load	110	433	110	-458	110	-451	-112	203	-125	-159	-136	-191	3.5	6.9	0.4	71
TOTAL (Service)		**-440**	**8,696**	**-546**	**-12,389**	**-392**	**1,610**	**-1,190**	**3,326**	**-1,324**	**-3,930**	**-1,437**	**-1,646**	**41**	**65**	**7.6**	**775**
TOTAL (Strength)		**-11**	**12,858**	**-117**	**-19,042**	**38**	**-3,615**	**-1,603**	**4,809**	**-1,784**	**-5,887**	**-1,936**	**-2,697**	**55**	**88**		**1,046**

Table 2.4.2: Analysis results for service and strength limit states

a) Median Arch

Section		Sec. 1		Sec. 2		Sec. 3		Sec. 4		Sec. 5		Sec. 6		Hanger	Mid-Point Deflection	Support Reaction
Stage	Limit State	P (kip)	M (kip.in)	P (kip)	M (kip.in)	P (kip)	M (kip.in)	P (kip)	M (kip.in)	P (kip)	M (kip.in)	P (kip)	M (kip.in)	T (kip)	Δ (in)	(kip)
I	Service I	527	2695	527	-2644	527	-2426	-527	1939	-585	-1728	-634	-1354	23	4.4	360
	Strength I	659	3369	659	-3305	659	-3033	-659	2424	-731	-2160	-793	-1693	29		450
II	Service I	-1788	8648	-2031	-10756	-1904	-3544	-782	3847	-874	-4396	-939	-2392	46	4.3	536
	Strength I	-1582	10027	-1825	-12097	-1697	-4801	-989	4517	-1104	-4981	-1188	-2881	58		670
III	Service I	-306	-2935	-302	3608	-187	15545	-51	-1116	-55	1321	-63	2041	2.2	-1.9	0
	Strength I	-306	-2935	-302	3608	-187	15545	-51	-1116	-55	1321	-63	2041	2.2		0
IV	Service I	983	12814	983	-10193	983	-5544	-1054	5191	-1174	-4029	-1270	-2266	65	5.8	843
	Strength I	1559	21987	1559	-17372	1559	-9108	-1672	8780	-1863	-6832	-2014	-3642	104		1343
	Fatigue	117	3806	117	-2362	117	-918	-129	1182	-143	-897	-155	-312	8.2		115
TOTAL (Service I)		**-584**	**21,222**	**-823**	**-19,985**	**-581**	**4,031**	**-2,414**	**9,861**	**-2,688**	**-8,832**	**-2,906**	**-3,971**	**136**	**12.6**	**1,739**
TOTAL (Strength I)		**330**	**32,448**	**91**	**-29,166**	**334**	**-1,397**	**-3,371**	**14,605**	**-3,753**	**-12,652**	**-4,058**	**-6,175**	**193**		**2,463**

a) Outside Arch

Section		Sec. 1		Sec. 2		Sec. 3		Sec. 4		Sec. 5		Sec. 6		Hanger	Mid-Point Deflection	Support Reaction
Stage	Limit State	P (kip)	M (kip.in)	P (kip)	M (kip.in)	P (kip)	M (kip.in)	P (kip)	M (kip.in)	P (kip)	M (kip.in)	P (kip)	M (kip.in)	T (kip)	Δ (in)	(kip)
I	Service I	422	2584	422	-2465	422	-2127	-422	1099	-469	-978	-510	-804	19	4.4	291
	Strength I	528	3230	528	-3081	528	-2659	-528	1374	-586	-1223	-638	-1005	24		364
II	Service I	-929	4757	-1054	-5890	-989	-1987	-391	1592	-436	-1775	-471	-964	24	2.4	268
	Strength I	-826	5508	-951	-6615	-886	-2652	-494	1870	-551	-2012	-596	-1172	30		335
III	Service I	-307	-2732	-288	3487	-200	11302	-32	-770	-35	930	-40	1096	1.6	-1.7	0
	Strength I	-307	-2732	-288	3487	-200	11302	-32	-770	-35	930	-40	1096	1.6		0
IV	Service I	374	4085	374	-7518	374	-5575	-345	1406	-384	-2106	-416	-975	21	2.6	217
	Strength I	594	6851	594	-12829	594	-9603	-549	2337	-612	-3581	-662	-1618	33		349
	Fatigue	93	5876	93	-3451	93	-1822	-93	1452	-103	-945	-111	-291	7		54
TOTAL (Service I)		**-440**	**8,694**	**-546**	**-12,386**	**-393**	**1,613**	**-1,190**	**3,327**	**-1,324**	**-3,929**	**-1,437**	**-1,647**	**66**	**7.7**	**776**
TOTAL (Strength I)		**-12**	**12,857**	**-118**	**-19,038**	**36**	**-3,612**	**-1,603**	**4,811**	**-1,784**	**-5,886**	**-1,936**	**-2,699**	**88**		**1,048**

SECTION 3: DESIGN CHECKS

3.1 Arch

The increase in the flexural capacity of a steel pipe when filled with concrete was estimated experimentally in an earlier research. Two 10 in. diameter 21 ft long specimens were purchased from Scoco Supply in Omaha, NE. One hollow specimen was tested as a 20 ft simply supported beam with point load at the midspan. The other specimen was tested exactly the same way after being filled with self-consolidating concrete that has a 30" spread and 28-day compressive strength of 7 ksi. To ensure that the second specimen was fully filled with concrete, concrete was pumped from bottom to top while the specimen was leaning at a steep angle. Both specimens were tested at the PKI Structures Lab using a single 110 kip hydraulic jack for loading and a LVDT at the midspan for measuring deflections as shown in Figure 3.1.1. The load-deflection curves of the two specimens were plotted as shown in Figure 3.1.2. The hollow specimen had an ultimate load of 39.8 kip, corresponding deflection of 6.83 in, and ultimate deflection of 10.7 in. The concrete filled specimen had an ultimate load of 55.3 kips and corresponding ultimate deflection of 14 in. By comparing load and deflection values of the two specimens, it can be concluded that filling a steel pipe with concrete increased its flexural capacity and ductility approximately 40% and 60% respectively. The measured flexural capacity of the hollow pipe (199 kip.ft) is very close to the theoretical flexure capacity of a steel pipe calculated using plastic section properties (189 kip.ft). On the other hand, the measured flexure capacity of the concrete-filled pipe (277 kip.ft) is similarly close to the theoretical flexure capacity calculated for a circular concrete section uniformly reinforced along its perimeter with a steel area equal to that of the surrounding pipe.

Service design checks at the critical sections of the outside and median arches before being filled with concrete are listed in Appendix C. Figures 3.1.3 and 3.1.4 show the stress-strain diagram of the confined concrete for the outside and median arches and the corresponding calculations using the theory of confinement. The estimated confined concrete compressive strength is used to develop the interaction diagrams shown in Appendix D using the computer program PCA Column version 4.0. These diagrams were used to perform strength design checks at the critical sections. It should be noted that all design checks are done on a single pipe, while the analysis results listed in Tables 2.4.1 and 2.4.2 are for the full section (i.e. two pipes)

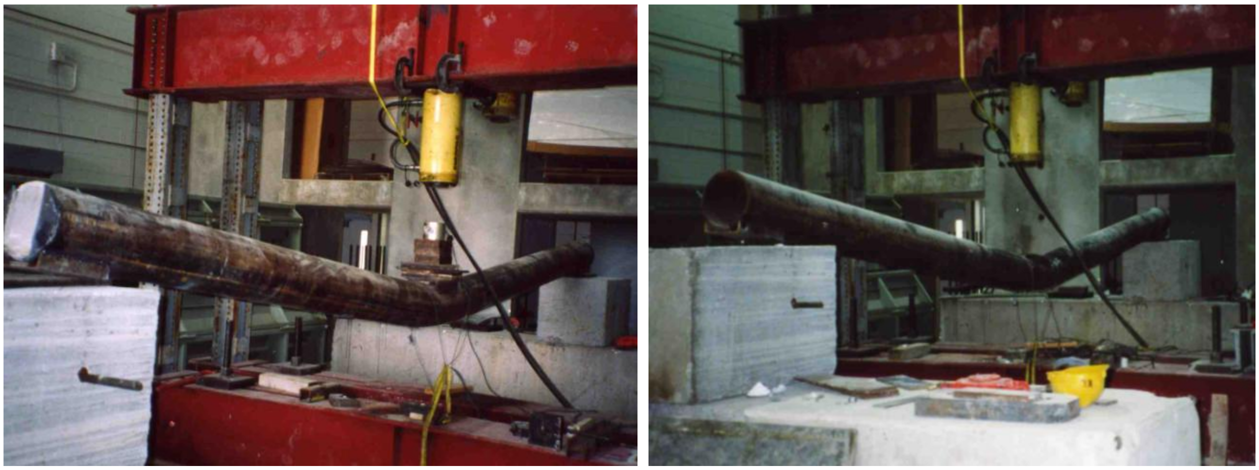

Figure 3.1.1: Test setup for hollow and concrete-filled pipes

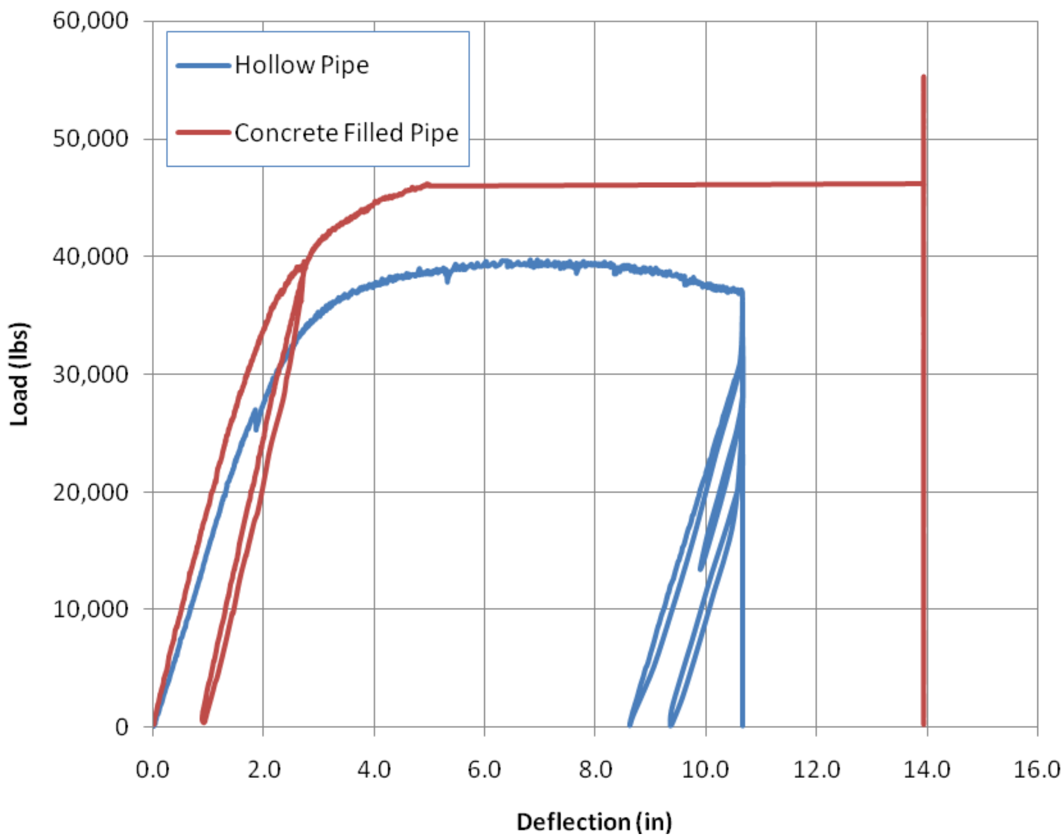

Figure 3.1.2: Load-deflection relationships for hollow and concrete-filled pipes

Compressive Strength of Confined Concrete (Median Arch)

Area of Spirals A_{sp} (in^2)	0.938	Use t x S in case of a tube
Spacing of Spirals S (in)	1	
Diameter of Spirals d_{sp} (in)	18	
Spirals Yield Strength f_y (ksi)	46	
Steel Modulus of Elasticity E_s (ksi)	29000	
Unconfined Compressive Strength f_{c0} (ksi)	8	
Unconfined Concrete Strain ε_{c0}	0.00201	
Initial Stress in Spirals f_{sp} (ksi)	46.00	
Strain in Spirals ε_{ct2}	0.01083	
Actual Stress in Spirals (ksi)	46.00	
Confining Stress f_{22} (ksi)	4.79	
Confined Compressive Strength f_{c2} (ksi)	27.66	
Confined Concrete Strain ε_{c2}	0.0266652	

$$\varepsilon_{ct2} = \varepsilon_{c0}\left(0.3 + 17\frac{A_{sp} f_{sp}}{d_{sp} s f_{c0}}\right)$$

$$f_{22} = \frac{2A_{sp}}{d_{sp} s} f_{sp}$$

$$f_{c2} = f_{c0} + 4 f_{22}$$

$$\varepsilon_{c2} = \varepsilon_{c0}\left(5\frac{f_{c2}}{f_{c0}} - 4\right)$$

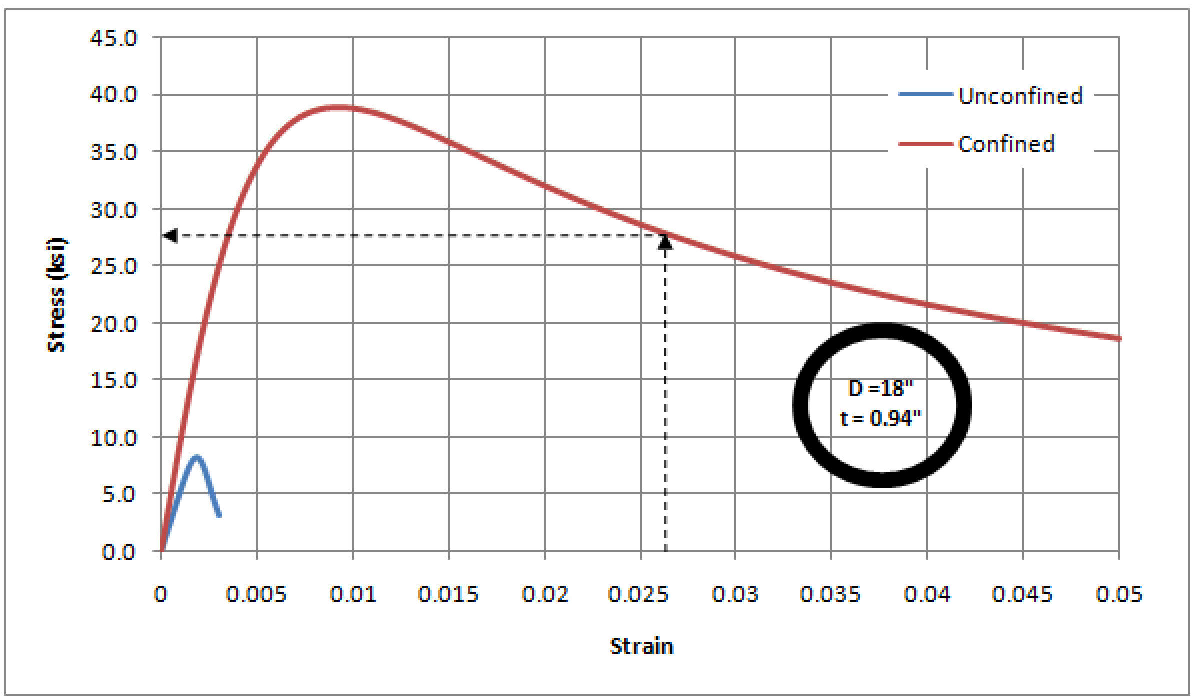

Figure 3.1.3: Stress-strain diagram of confined concrete (median arch)

Compressive Strength of Confined Concrete (Outside Arch)

Area of Spirals A_{sp} (in^2)	0.5	Use t x S in case of a tube
Spacing of Spirals S (in)	1	
Diameter of Spirals d_{sp} (in)	18	
Spirals Yield Strength f_y (ksi)	46	
Steel Modulus of Elasticity E_s (ksi)	29000	
Unconfined Compressive Strength f_{co} (ksi)	8	
Unconfined Concrete Strain ε_{co}	0.00201	
Initial Stress in Spirals f_{sp} (ksi)	46.00	
Strain in Spirals ε_{ct2}	0.00605	
Actual Stress in Spirals (ksi)	46.00	
Confining Stress f_{22} (ksi)	2.56	
Confined Compressive Strength f_{c2} (ksi)	18.48	
Confined Concrete Strain ε_{c2}	0.0151511	

$$\varepsilon_{ct2} = \varepsilon_{c0}\left(0.3 + 17\frac{A_{sp}f_{sp}}{d_{sp}sf_{c0}}\right)$$

$$f_{22} = \frac{2A_{sp}}{d_{sp}s}f_{sp}$$

$$f_{c2} = f_{c0} + 4f_{22}$$

$$\varepsilon_{c2} = \varepsilon_{c0}\left(5\frac{f_{c2}}{f_{c0}} - 4\right)$$

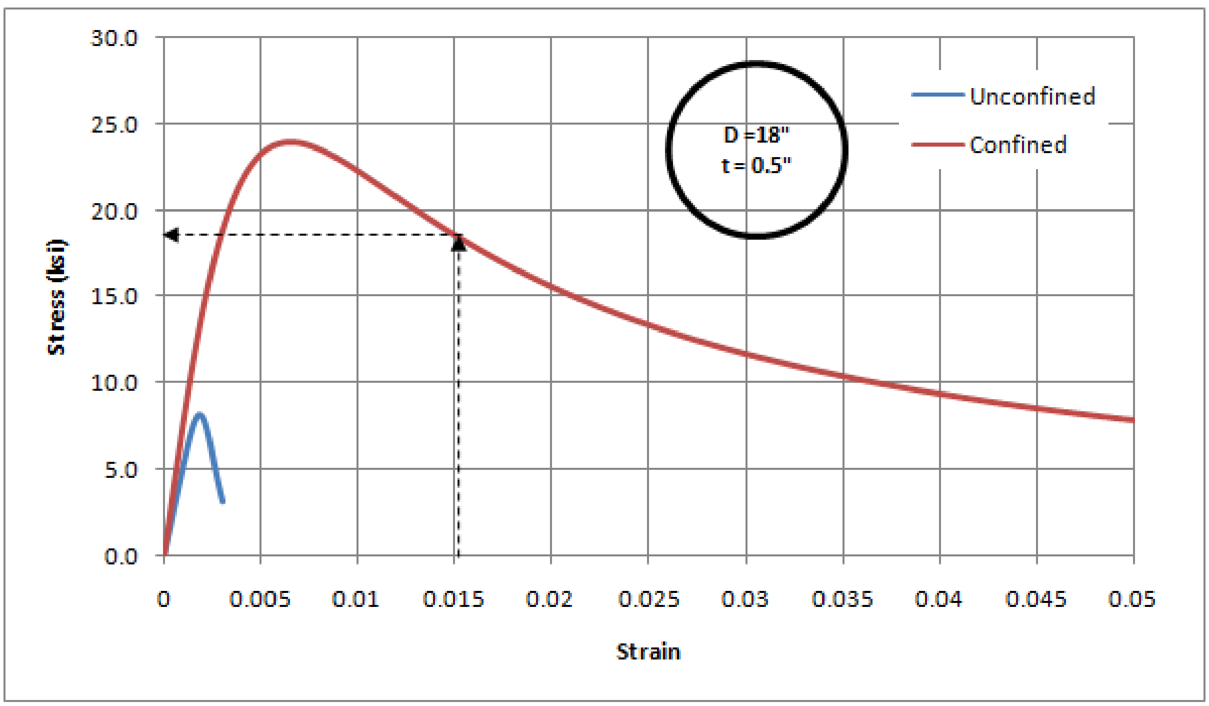

Figure 3.1.4: Stress-strain diagram of confined concrete (outside arch)

3.2 Tie

Due to the uniqueness of the tie design, an experimental investigation was carried out in an earlier study to estimate the flexural capacity of the post-tensioned concrete filled steel tube. A 40 ft long steel tube was fabricated at Capital Contractors in Lincoln, NE and shipped to PKI Structures Lab for testing. The tube is 24” x 24” and consists of four welded plates that are ½” thick. The top plate of the tube was left off to facilitate the installation of the post-tensioning hardware. End plates had two holes that were 6 ½” in diameter to fit post-tensioning anchorages. DSF post-tensioning hardware, which includes wedge plates, wedges, anchorage plates, duct couplers, ducts, and grouting accessories, that can accommodate two 19-0.6” strands were installed and properly fastened in the steel tube. The 4” diameter ducts were installed so that the center of the ducts is 4” from the bottom of the tube. Duct chairs were used to maintain 2” concrete cover below the duct and #4 bars were placed directly on top of the ducts at 3 ft spacing to prevent the upward movement of the ducts by buoyant forces when concrete is poured. In addition, 2” x 2” stiffeners were added with 1” clearance from each corner to help stiffening the plates and achieving the composite actions between the concrete and surrounding steel. The top plate was then welded to close the steel box. The top plate has two 4” diameter holes at each end for concrete pumping and twelve 1” diameter holes spaced at 3 ft for venting and quality assurance. A self-consolidating concrete (SCC) with 30” spread and specified 28-day strength of 7000 psi was pumped into the steel tube. Only 20 strands (10 per suck) were used and post-tensioned at 202.5 ksi using mono-strand jack after the filling concrete strength has reached 4000 psi. After all strands were tensioned, “lift off” tests were performed to determine the true level of prestressing after initial losses. This was found to be averaged at 170.5 ksi, which means 16% initial losses. Following post-tensioning, the two ducts were grouted using a very simple grout consisting of Type I cement and water (w/c = 0.44). Toggle bolts and washers were used to block the 9 additional holes in the anchor plate (only 10 strands in a 19-strand plate) and 2” diameter pipe fitting were used to block the grout access holes.

The specimen was tested using two 300 kip hydraulic jacks spaced 12’ from each other because of the fixed support locations in the lab floor. The span of the specimen from centerline to centerline was 39’ 3” and the loading points were located at 13’ 7.5” from each support as shown in Figure 3.2.1.

Figure 3.2.1: Tie specimen during loading

Figure 3.2.2 plots the load-deflection curve of the tested specimen. The ultimate load was found to be 445 kip, which corresponds to a moment of 3032 kip.ft, and the ultimate deflection at the mid-span was 4.5 in. The ultimate moment capacity of the specimen was calculated using strain compatibility was found to be 2979 kip.ft, which is very close to the measured value. Therefore, strain compatibility concept was used to determine the capacity of the outside and median ties for the Columbus Viaduct project.

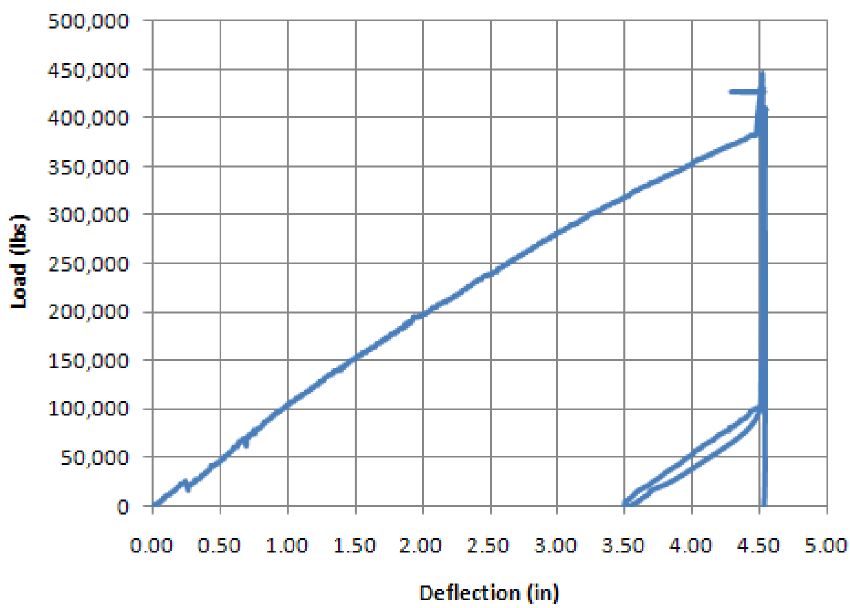

Figure 3.2.2: Load-deflection relationship of the tie specimen

Service design checks at the critical sections of the outside and median ties before being filled with concrete are listed in Appendix C. Table 3.2.1 summarizes the stress ratio at all the critical sections of the tie and arch during construction stage I. All the listed values are well below 1.0

Table 3.2.1: Stress ratio at critical sections for construction stage I

Section #	Stress Ratio	
	Median Arch	Outside Arch
1	0.52	0.45
2	0.52	0.44
3	0.38	0.31
4	0.35	0.43
5	0.35	0.45
6	0.34	0.45

The interaction diagrams for four tie sections (mid-section in outside tie, end-section in outside tie, mid-section in median tie, end-section in median tie) were developed using strain compatibility. For each section, diagrams were developed for two construction stages: non-composite tie for construction stage II, and composite tie for construction stage III. Based on the results of an earlier experimental investigation, the effective deck width for composite sections was taken as the distance between the centerlines of the deck panels between ties. Appendix D presents the interaction diagrams developed using 19, 27, and 37 strands per tendon. Plotting the bending moment and axial force values obtained from Tables 2.4.1 and 2.4.2 on these interaction diagrams indicate that using 19 strands per tendon for the outside tie and 37 strands per tendon for the median tie is adequate.

3.3 Hangers

Hangers are designed as tension members made of 150 ksi high strength rods that have a minimum yield strength of 120 ksi. All the rods are 1 ¾" in diameter with a variable length. According to the analysis results shown in Tables 2.4.1 and 2.4.2, the hangers of the median arch are more critical than those of the outside arch. The maximum tension force for the service limit state is 128 kips, which results in a working stress of 53 ksi; and the maximum tension force for the strength limit state is 179 kips, which results in an ultimate stress of 75 ksi. These stresses are well below the allowable stresses (0.6 F_y, and φ F_y respectively). Based on the results of the testing performed earlier on one of the hangers and its connection to the arch at the PKI structural lab, the ultimate capacity of the rod is 385 kips as shown in Figure 3.3.1. This provides a capacity-to-demand ratio of 2.15.

The maximum tension force in the hanger rod due to the fatigue truck is 10 kips, which results in a fatigue stress of 4.2 ksi. This stress is well below the limiting fatigue stress (16/2 ksi for detail category B). The fatigue testing performed earlier on the hanger-arch connection has indicated that both the hanger rod and the connection can withstand two million cycles under a cyclic load from 65 kips – 85 kips, which is twice the load that the hanger rod is subjected to in this project.

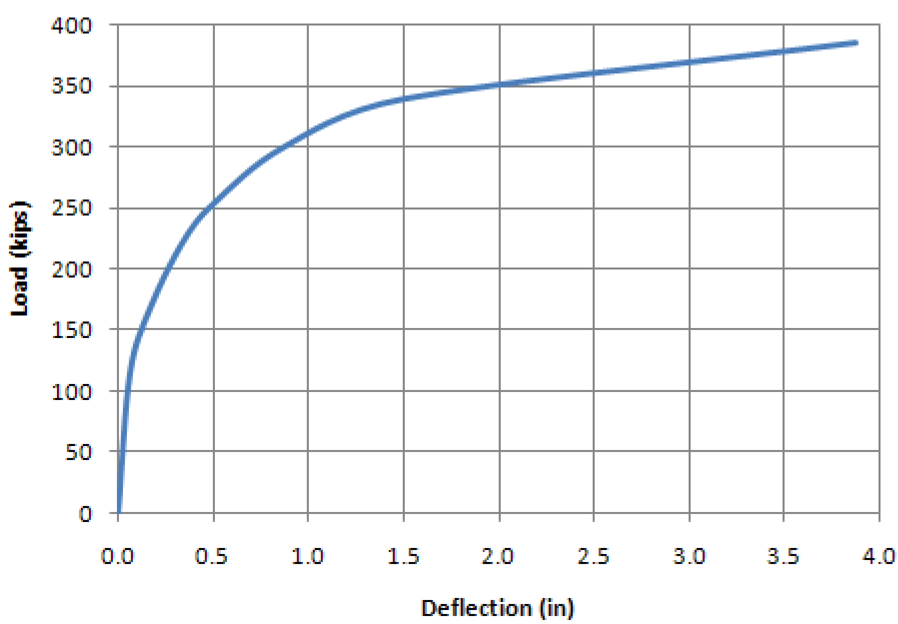

Figure 3.3.1: Load-deflection relationship of a 1 ¾ in. diameter hanger

3.4 Cross Beams

Cross beams are designed as 39' 11" simply supported beams that have 10' spacing and a cross section of W24x162. Figure 3.4.1 shows the different load cases and the corresponding bending moment, shear force, and mid-span deflection values. Table 3.4.1 shows the design check calculations for both the non-composite and composite sections.

Own Weight	
M (kip.ft)	32.3
V (kip)	3.2
Δ (ft)	0.0053
Deck Weight	
M (kip.ft)	199
V (kip)	19.96
Δ (ft)	0.0328
Wearing Surface	
M (kip.ft)	46.7
V (kip)	4.3
Δ (ft)	0.0078
Rail	
M (kip.ft)	31.2
V (kip)	6.5
Δ (ft)	0.0055
Lane Load	
M (kip.ft)	103.4
V (kip)	10.4
Δ (ft)	0.017
Truck Load + Impact	
M (kip.ft)	635
V (kip)	47.6
Δ (ft)	0.098
Σ M (kip.ft)	**1047.6**
Σ V (kip)	**92.0**
Σ Δ (in)	**2.00**

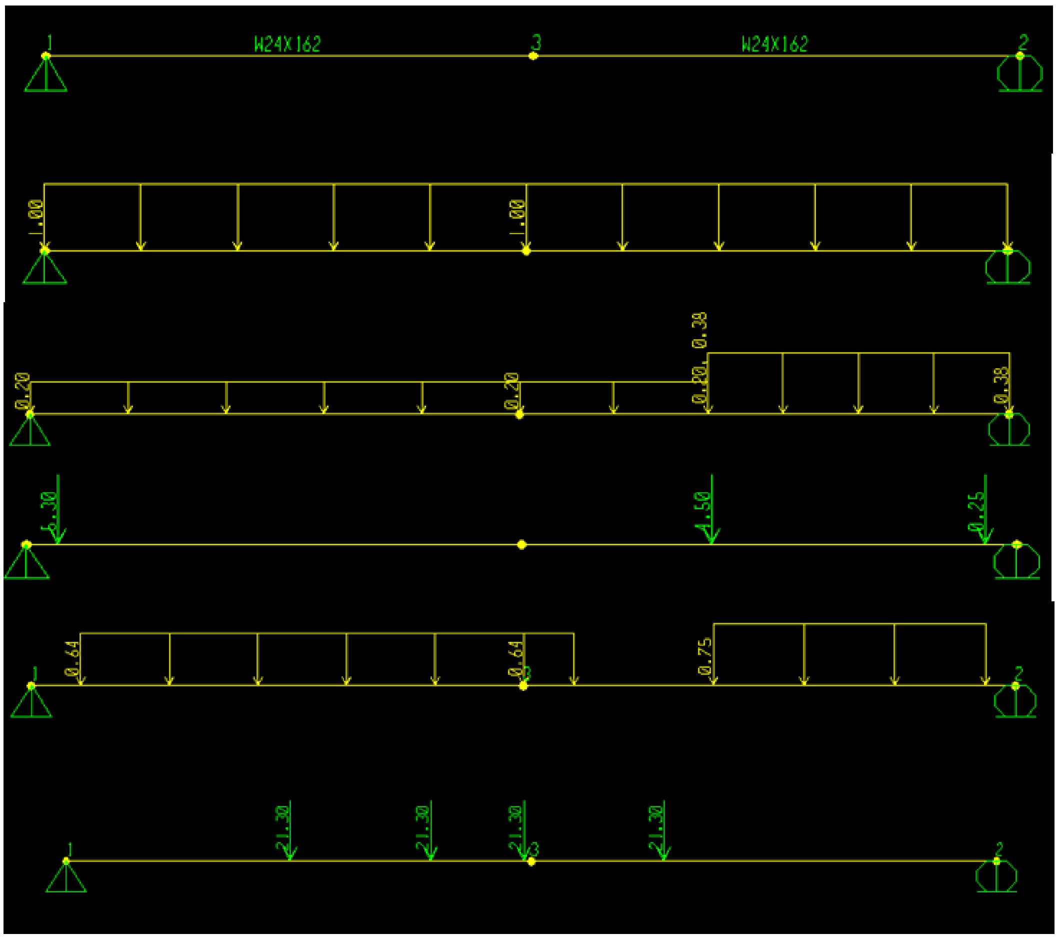

Figure 3.4.1: Load cases of the cross beams

Table 3.4.1: Stress calculations for cross beams under different loading conditions

Description	W24x162	Units		
Beam Area	47.7	in^2		
Beam Weight	0.162	kip/ft		
Beam Moment of Inertia	5,170.00	in^4		
Beam Height	25.00	in		
Top Flange Width	13	in		
Y_b	12.5	in		
Section Modulus	413.6	in^3		
Beam Span	39.92	ft		
Beam Spacing	10.00	ft		
Structural Deck Thickness	7.50	in		
Total Deck Thickness	8.00	in		
Haunch Thickness	1.0	in		
Deck Compressive Strength	4000	psi		
$M_{(non\text{-}composite)}$	2776	kip.in		
Bottom Stress on Non-Composite	**6.71**	**ksi**		
Modular Ratio	8.04	N/A		
Transformed Deck Width	14.92	in		
Transformed Deck Area	111.88	in^2		
$Y_{b\ (composite)}$	24.59	in		
$I_{(composite)}$	15,646	in^4		
$S_{(composite)}$	636	in^3		
$M_{(composite)}$	12,082	kip.in		
Bottom Stress on Composite	**18.99**	ksi	**Limit (ksi)**	
Unfactored Total Stress	**25.70**	ksi	**30**	ok
Factored Total stress	**34.82**	ksi	**50**	ok
Fatigue Stress	**8.98**	ksi	**12**	ok

3.5 Arch-Tie Connection

The connection between the tie and arch of the median arch is considered the most critical connection in the structure. Thus, a detailed finite element (FE) model was developed using structural analysis program ANSYS 11.0 to determine the principle stresses at the connection location. Figure 3.5.1 shows the dimensions of the connection that has been considered for the analysis.

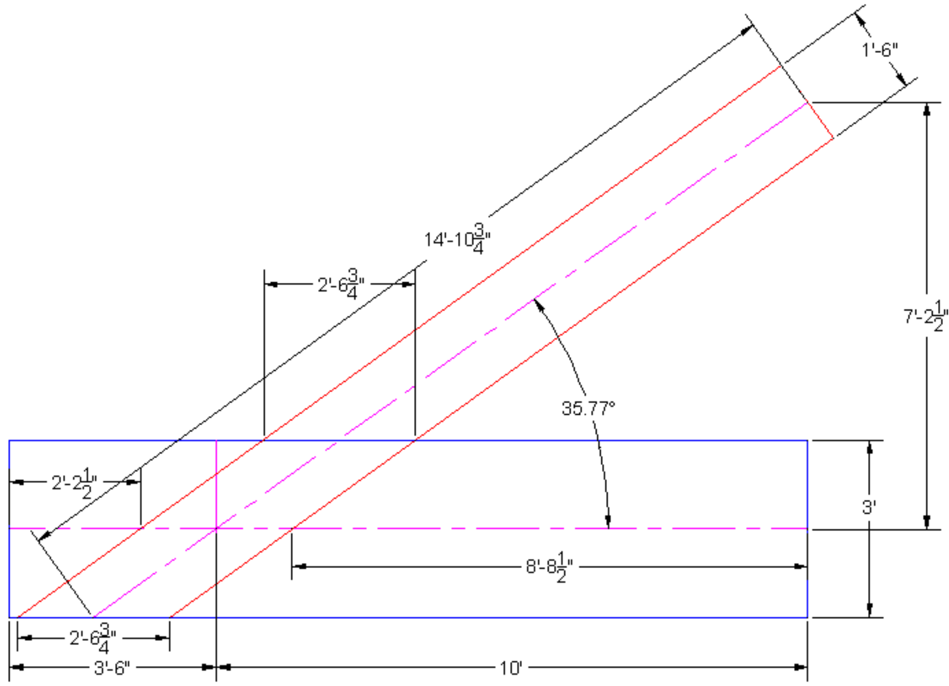

Figure 3.5.1: Dimensions of the arch-tie connection

Figure 3.5.2 shows the SHELL43 element used for modeling both the tie and the arc. SHELL 43 is well suited to model linear, warped, moderately-thick shell structures. The element has six degrees of freedom at each node: translations in the nodal x, y, and z directions and rotations about the nodal x, y, and z axes. The deformation shapes are linear in both in-plane directions. The complete 3D FE model of the joint is shown in Figure 3.5.3.

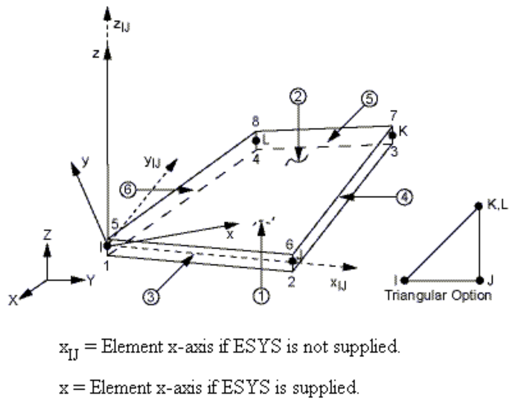

Figure 3.5.2: Shell element used for the analysis (SHELL43)

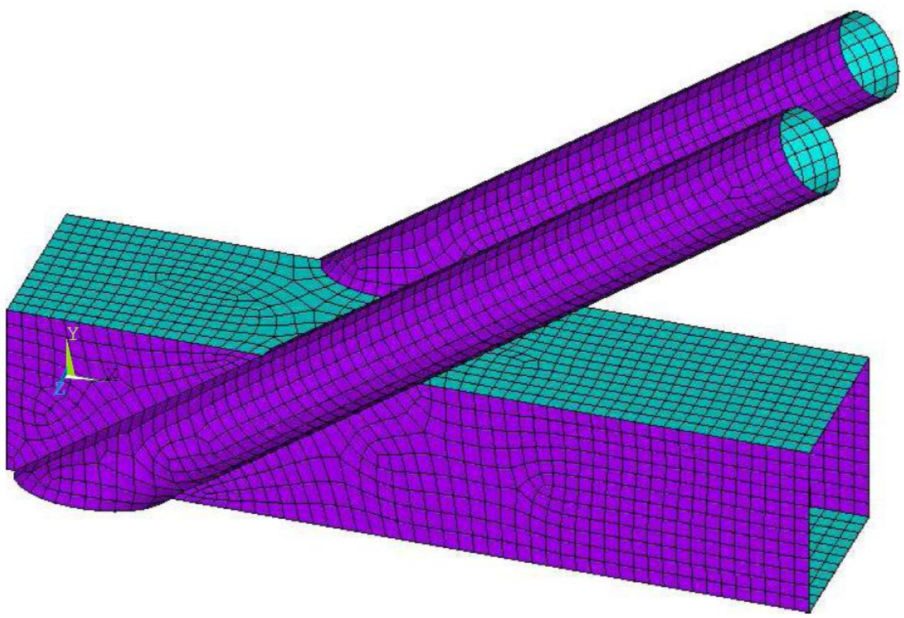

Figure 3.5.3: FE model of the connection

The loads applied to this connection were obtained from Table 2.4.1 and factored according to the 2007 AASHTO LRFD. These loads include dead load, post-tensioning force, super imposed dead load and live loads. Figures 3.5.4 and 3.5.5 show the principle stresses at the connection and welding locations respectively. Based on the presented stress contours, it can be concluded that the average principle stresses at the weld location is less than 20 ksi. Higher stress values occur at very few locations (i.e. the intersection of the pipe and box) due to stress concentrations. However, these stresses are still below the ultimate strength of the steel section and the weld used (i.e. Fy = 46 ksi)

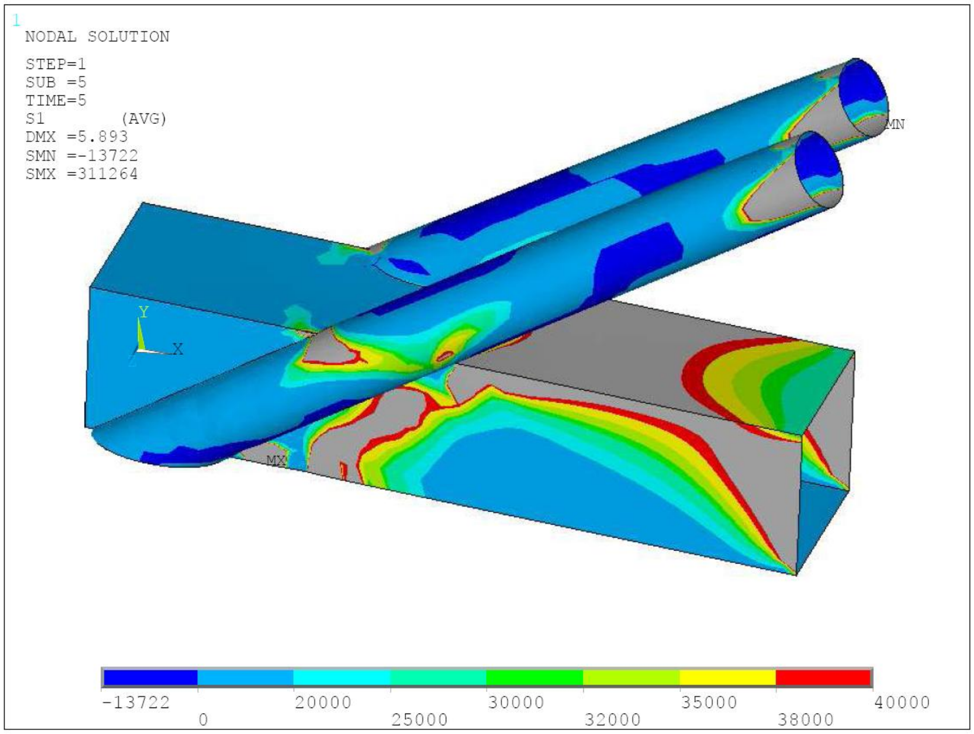

Figure 3.5.4: FE model for the Joint

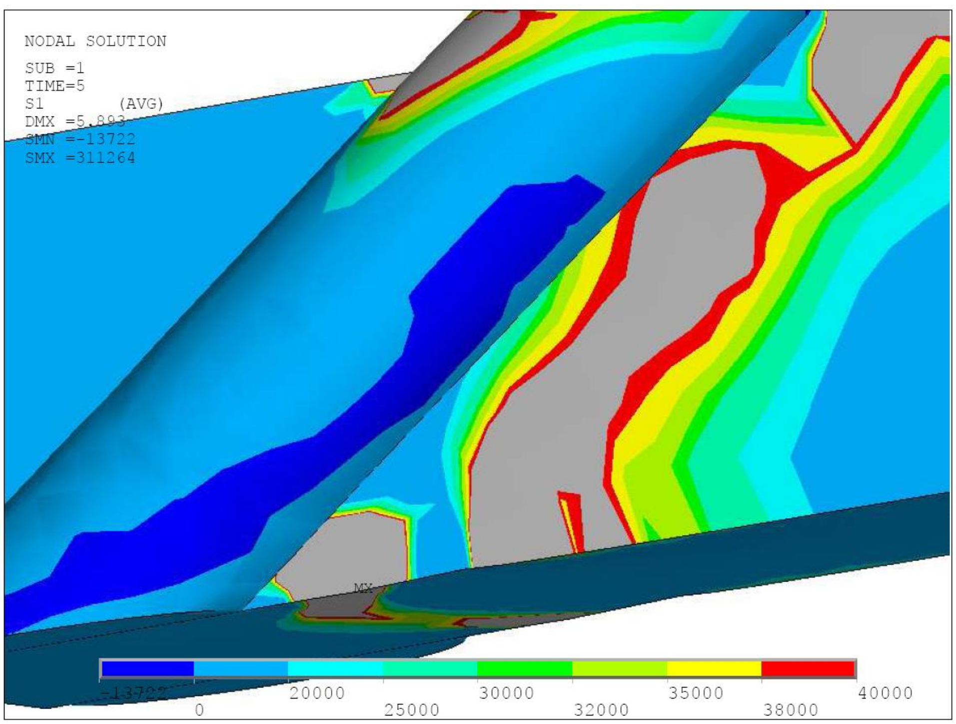

Figure 3.5.5: FE model for the Joint

3.6 Lateral Stability

Lateral stability analysis was performed to confirm the stability of the three arches of the Columbus viaduct in the transverse direction when subjected to wind loads. Non-linear static analysis (i.e. due to geometric nonlinearity) was applied to the three dimensional model developed earlier using SAP2000 version 10.1.3 to account for P-delta effects on the arch elements. Arches, ties, cross beams, and rails were modeled using frame element, hangers were modeled using cable elements, post-tensioning strands were modeled using tendon elements, and concrete deck was modeled using shell elements that have both bending and membrane capabilities. Wind load was calculated according to AASHTO LRFD Section 3.8.1.2, which is 50 psf in windward direction, and 25 psf in the leeward direction on the arch components. The calculated values should not be less than 300 plf in the plane of windward chord, and 150 plf in the plane of leeward chord. Figure 3.6.1 shows the forces applied to the model to represent the calculated wind load. Figure 3.6.2 shows the deformed shape of the structure when only wind load is applied. This deformed shape does not account for the P-delta effects of the axial force in the arch elements.

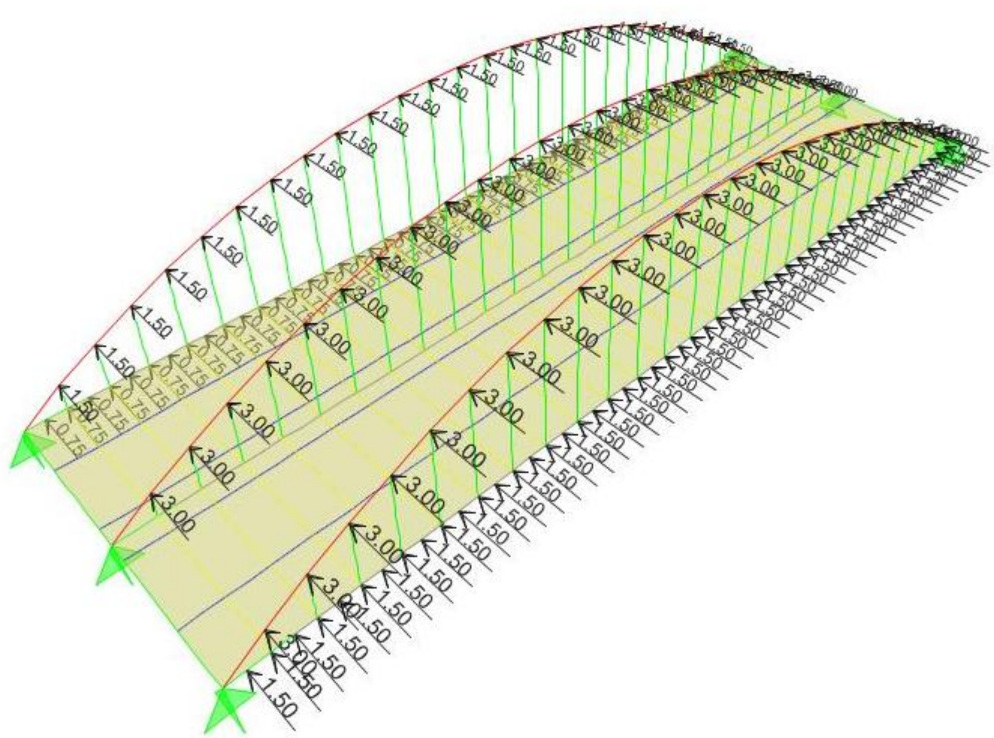

Figure 3.6.1: Wind load applied to the model for lateral stability analysis

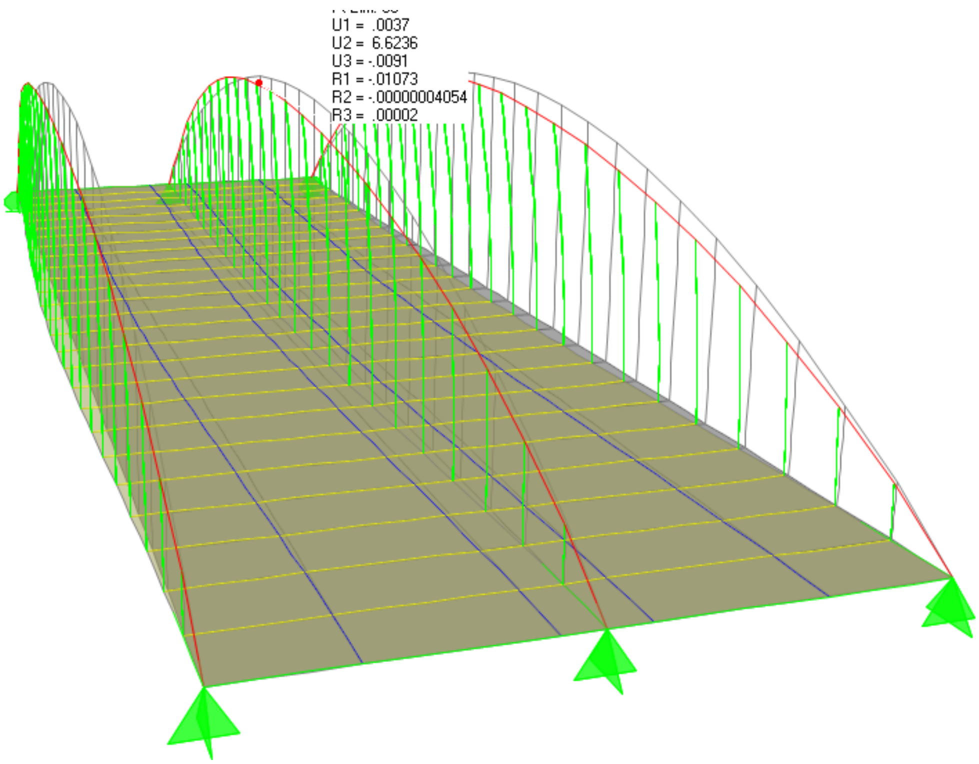

Figure 3.6.2: Deformed shape of the structure due to wind load only

To check the lateral stability of Columbus viaduct arches, wind load is applied while increasing the dead load gradually until lateral instability (i.e. buckling) occur. P-delta effects due to the compressive force in the arches will increase as the dead load increases. These effects are calculated in several iterations until the solution converge. Figure 3.6.3 shows the increase of the lateral deflection of the median and outside arches when dead load multiplier ranges from 0 to 4. In all these cases, the arches remain stable as the solution converges. Lateral instability occurred when a dead load multiplier of 5 is used. A converging solution could not be reached. A dead load multiplier of 4 confirms that the structure is very stable under the static design wind load with a factor of safety of 4. Figure 3.6.4 shows the deformed shape of the structure when wind load in applied in conjunction with four times the dead load.

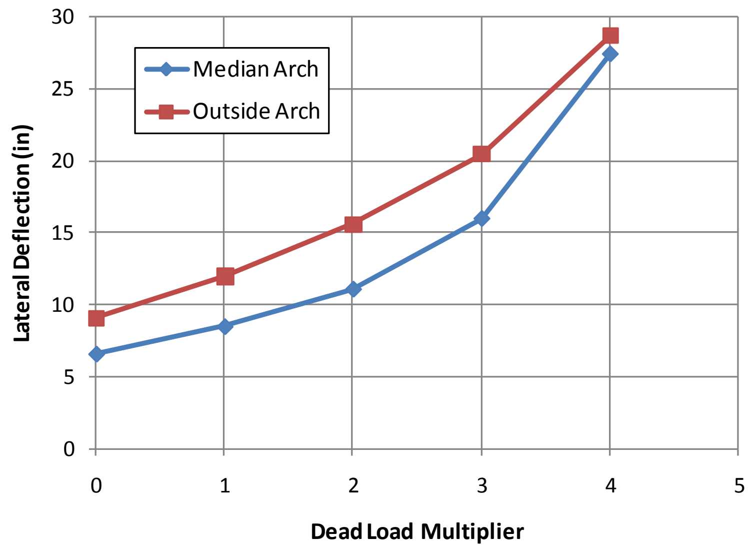

Figure 3.6.3 Lateral deflections calculated using nonlinear analysis with P-delta effects

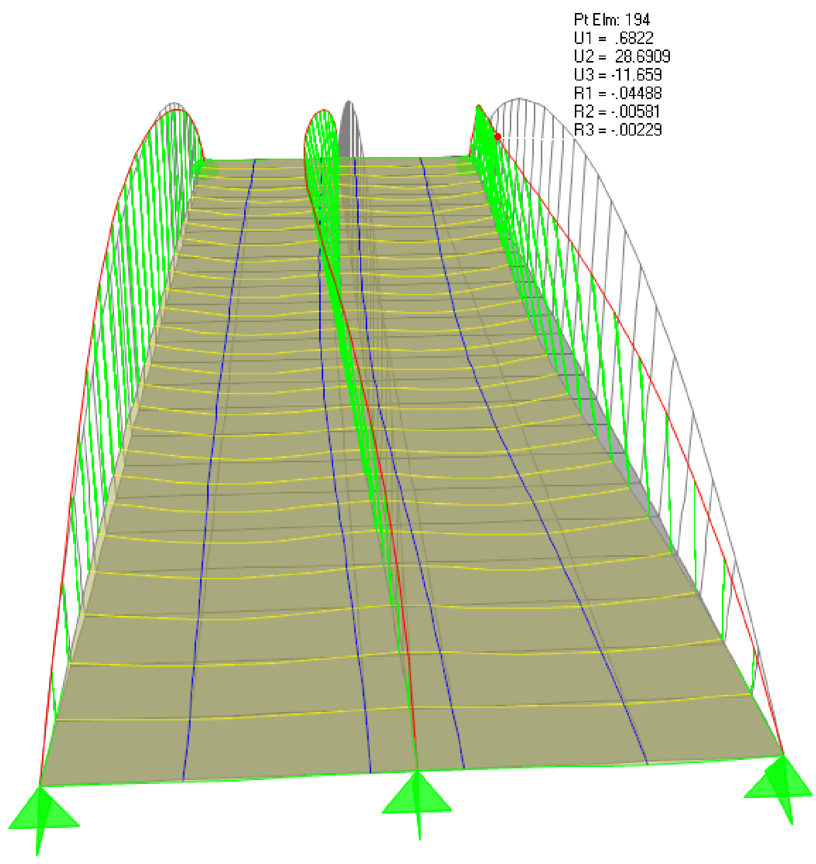

Figure 3.6.4 Lateral deflections due to wind load + 4 x dead load

SECTION 4: SUMMARY AND COLCLUSIONS

The tied arch system provides a unique solution to the several challenges associated with the construction of railroad overpasses, such as restricted vertical clearance, inadequate space for intermediate piers, and very limited traffic control during construction. The system was first applied to the construction of the Ravenna viaduct to provide a structural depth less than 35 in. while crossing a span of 174 ft without any intermediate piers. Additionally, most of the assembly and construction was done before the bridge was over the railroad, which kept worker time over the railroad and rail traffic disruption to a minimum.

In this project, the analysis and design of Columbus viaduct using the tied arch system was investigated. Although the system has the same components of that used in the Ravenna viaduct, it is considered significantly different due to the use of three parallel tied arches instead of two and spanning 260 ft instead of 174 ft. Three-dimensional models were developed for the structural analysis of the viaduct at different construction stages. The models consist of frame elements (i.e. tie, arch, cross beams, and end beams), cable elements (i.e. hangers), and shell elements (i.e. deck). Design loads were calculated according to the 2007 AASHTO LRFD specifications. Theory of confinement and strain compatibility were used to develop the interaction diagrams required to check the design of the tie and arch at the most critical sections. A finite element model was also developed to check the stresses at the arch-to-tie connection of the median arch. P-delta analysis was performed to check lateral stability of the outside and median arches due to design wind loads.

All these checks have indicated that the current design of the Columbus Viaduct developed by NDOR bridge engineers is adequate for the specified loads.

APPENDIXES

APPENDIX A: SECTION PROPERTIES

Section Name 2Pipes

Properties

Cross-section (axial) area	54.9779	Section modulus about 3 axis	234.0377
Torsional constant	4005.5916	Section modulus about 2 axis	737.747
Moment of Inertia about 3 axis	2106.3397	Plastic modulus about 3 axis	298.8368
Moment of Inertia about 2 axis	19919.17	Plastic modulus about 2 axis	973.4035
Shear area in 2 direction	37.2023	Radius of Gyration about 3 axis	6.1897
Shear area in 3 direction	126.7192	Radius of Gyration about 2 axis	19.0345

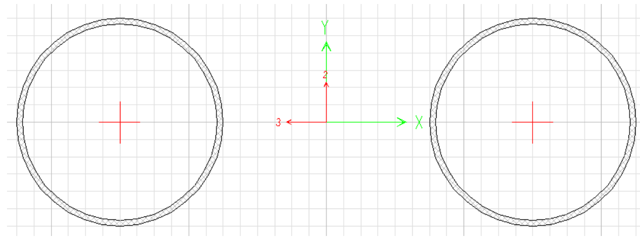

Section Name 2PipesMid

Properties

Cross-section (axial) area	100.5571	Section modulus about 3 axis	407.8032
Torsional constant	10521.383	Section modulus about 2 axis	1342.6193
Moment of Inertia about 3 axis	3670.2289	Plastic modulus about 3 axis	533.2979
Moment of Inertia about 2 axis	36250.72	Plastic modulus about 2 axis	1780.4002
Shear area in 2 direction	66.284	Radius of Gyration about 3 axis	6.0414
Shear area in 3 direction	227.1701	Radius of Gyration about 2 axis	18.9868

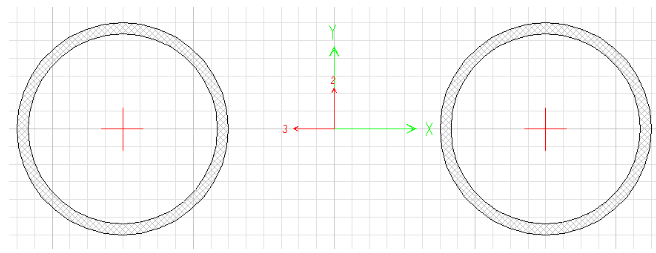

Section Name Box

Properties

Cross-section (axial) area	59.	Section modulus about 3 axis	498.7431
Torsional constant	11960.107	Section modulus about 2 axis	618.6065
Moment of Inertia about 3 axis	5984.9167	Plastic modulus about 3 axis	555.25
Moment of Inertia about 2 axis	11134.917	Plastic modulus about 2 axis	732.25
Shear area in 2 direction	23.8121	Radius of Gyration about 3 axis	10.0717
Shear area in 3 direction	35.1174	Radius of Gyration about 2 axis	13.7378

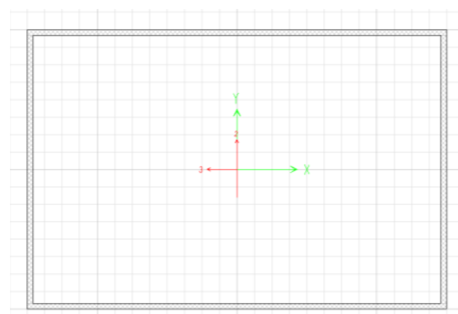

Section Name BoxEND

Properties

Cross-section (axial) area	71.	Section modulus about 3 axis	828.662
Torsional constant	22634.807	Section modulus about 2 axis	828.662
Moment of Inertia about 3 axis	14915.917	Plastic modulus about 3 axis	945.25
Moment of Inertia about 2 axis	14915.917	Plastic modulus about 2 axis	945.25
Shear area in 2 direction	35.5227	Radius of Gyration about 3 axis	14.4943
Shear area in 3 direction	35.5227	Radius of Gyration about 2 axis	14.4943

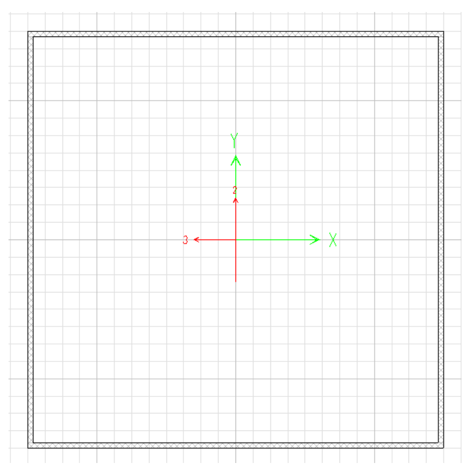

Section Name 2Pipes

Properties

Cross-section (axial) area	134.8122	Section modulus about 3 axis	394.2609
Torsional constant	19879.692	Section modulus about 2 axis	1749.1672
Moment of Inertia about 3 axis	3548.348	Plastic modulus about 3 axis	1896.4269
Moment of Inertia about 2 axis	47227.51	Plastic modulus about 2 axis	9010.9356
Shear area in 2 direction	113.4685	Radius of Gyration about 3 axis	5.1304
Shear area in 3 direction	313.7306	Radius of Gyration about 2 axis	18.7169

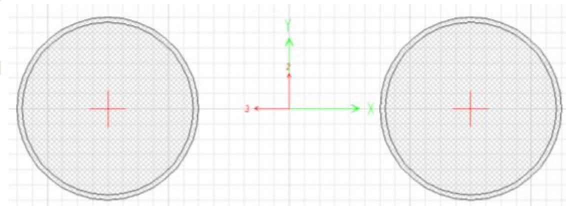

Section Name 2PipesMID

Properties

Cross-section (axial) area	172.3402	Section modulus about 3 axis	537.339
Torsional constant	9672.1016	Section modulus about 2 axis	2247.195
Moment of Inertia about 3 axis	4836.0508	Plastic modulus about 3 axis	1895.4127
Moment of Inertia about 2 axis	60674.26	Plastic modulus about 2 axis	9007.3485
Shear area in 2 direction	119.0754	Radius of Gyration about 3 axis	5.2973
Shear area in 3 direction	119.0754	Radius of Gyration about 2 axis	18.7633

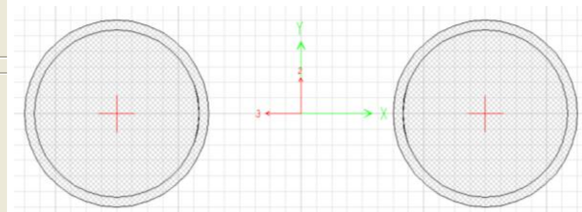

Section Name Box

Properties

Cross-section (axial) area	200.569	Section modulus about 3 axis	1018.8124
Torsional constant	98996.33	Section modulus about 2 axis	1421.486
Moment of Inertia about 3 axis	12225.749	Plastic modulus about 3 axis	5184.
Moment of Inertia about 2 axis	25586.749	Plastic modulus about 2 axis	7776.
Shear area in 2 direction	156.9875	Radius of Gyration about 3 axis	7.8074
Shear area in 3 direction	162.6403	Radius of Gyration about 2 axis	11.2947

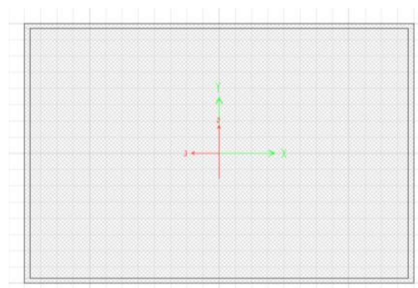

Section Name BoxEND

Properties

Cross-section (axial) area	286.431	Section modulus about 3 axis	2050.4353
Torsional constant	239436.27	Section modulus about 2 axis	2050.4353
Moment of Inertia about 3 axis	36907.83	Plastic modulus about 3 axis	11664.
Moment of Inertia about 2 axis	36907.83	Plastic modulus about 2 axis	11664.
Shear area in 2 direction	231.4441	Radius of Gyration about 3 axis	11.3514
Shear area in 3 direction	231.4441	Radius of Gyration about 2 axis	11.3514

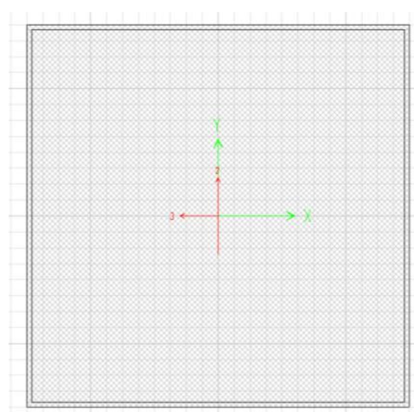

Section Name W24X162

Properties

Cross-section (axial) area	47.7	Section modulus about 3 axis	413.6
Torsional constant	18.5	Section modulus about 2 axis	68.1538
Moment of Inertia about 3 axis	5170.	Plastic modulus about 3 axis	468.
Moment of Inertia about 2 axis	443.	Plastic modulus about 2 axis	105.
Shear area in 2 direction	17.625	Radius of Gyration about 3 axis	10.4108
Shear area in 3 direction	26.4333	Radius of Gyration about 2 axis	3.0475

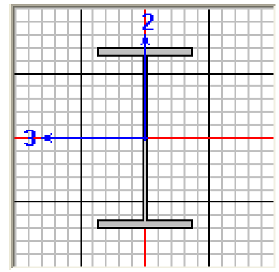

Section Name HANG

Properties

Cross-section (axial) area	2.4053	Section modulus about 3 axis	0.5262
Torsional constant	0.9208	Section modulus about 2 axis	0.5262
Moment of Inertia about 3 axis	0.4604	Plastic modulus about 3 axis	0.8932
Moment of Inertia about 2 axis	0.4604	Plastic modulus about 2 axis	0.8932
Shear area in 2 direction	2.1648	Radius of Gyration about 3 axis	0.4375
Shear area in 3 direction	2.1648	Radius of Gyration about 2 axis	0.4375

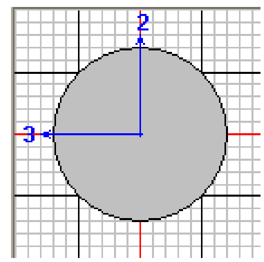

Section Name ENDBEAM

Properties

Cross-section (axial) area	1728.	Section modulus about 3 axis	10368.
Torsional constant	403076.9	Section modulus about 2 axis	13824.
Moment of Inertia about 3 axis	186624.	Plastic modulus about 3 axis	15552.
Moment of Inertia about 2 axis	331776.	Plastic modulus about 2 axis	20736.
Shear area in 2 direction	1440.	Radius of Gyration about 3 axis	10.3923
Shear area in 3 direction	1440.	Radius of Gyration about 2 axis	13.8564

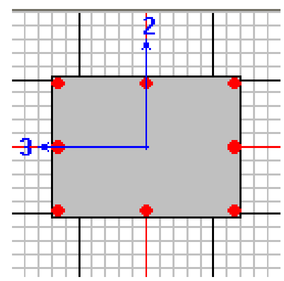

APPENDIX B: ANALYSIS DIAGRAMS

Stage I: Own Weight

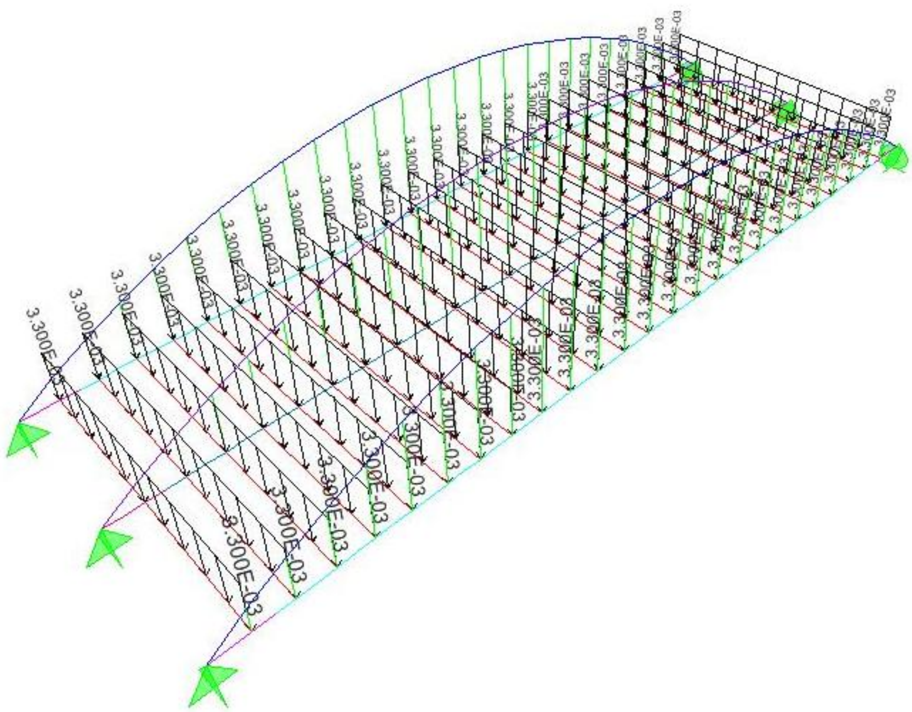

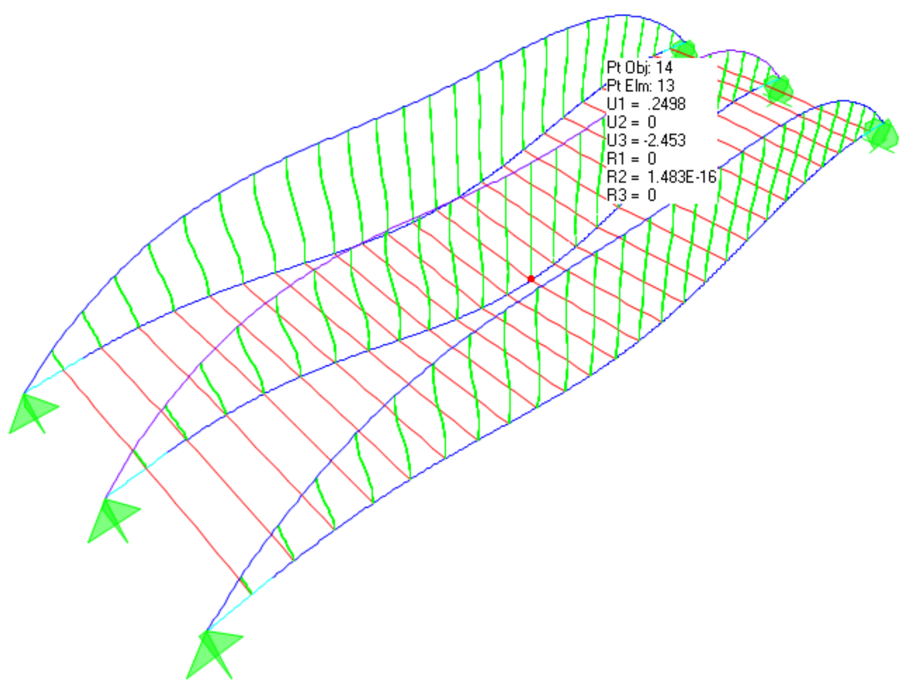

- Median Arch

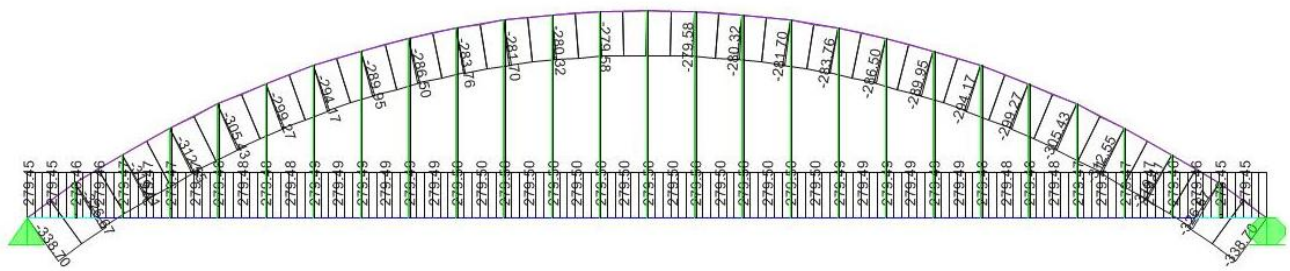

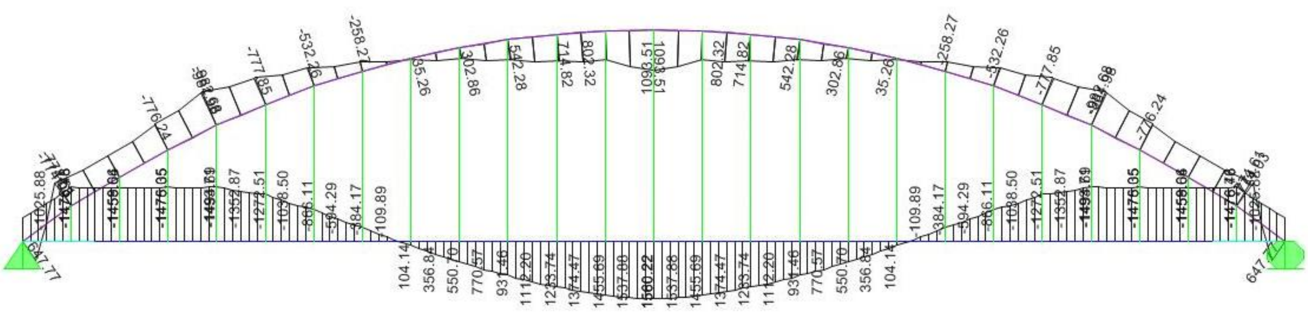

- Outside Arch

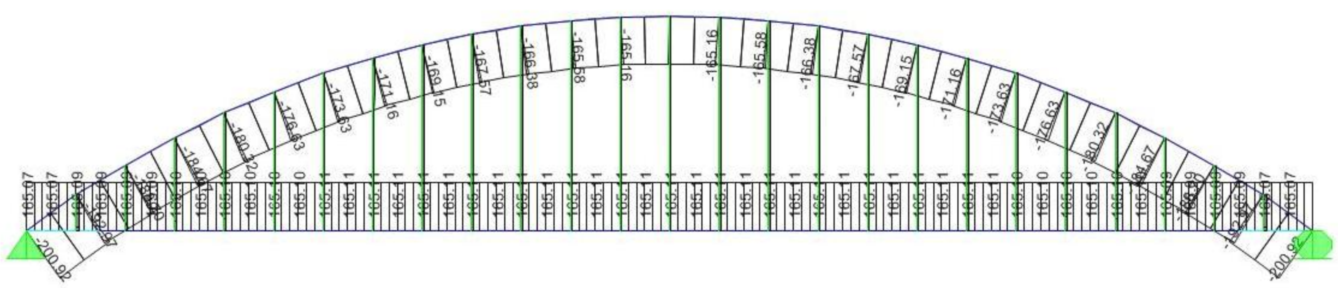

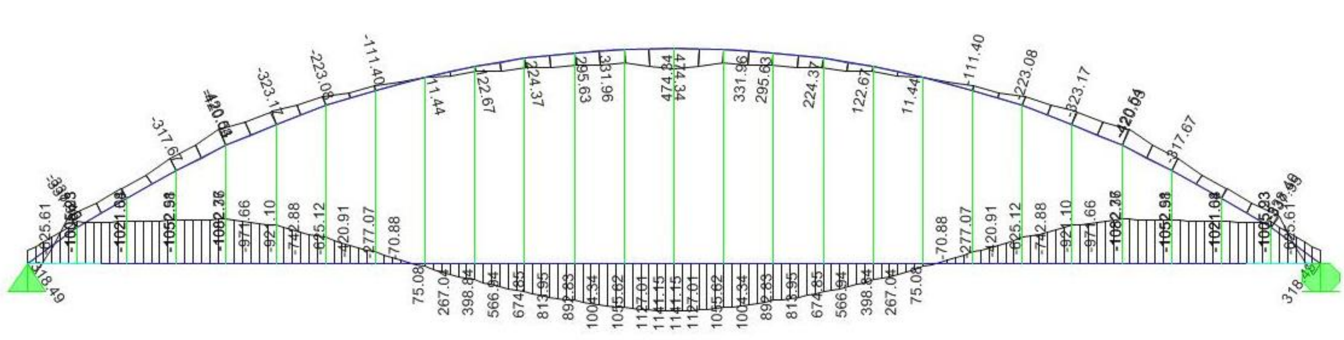

<u>Stage I: Filling Concrete</u>

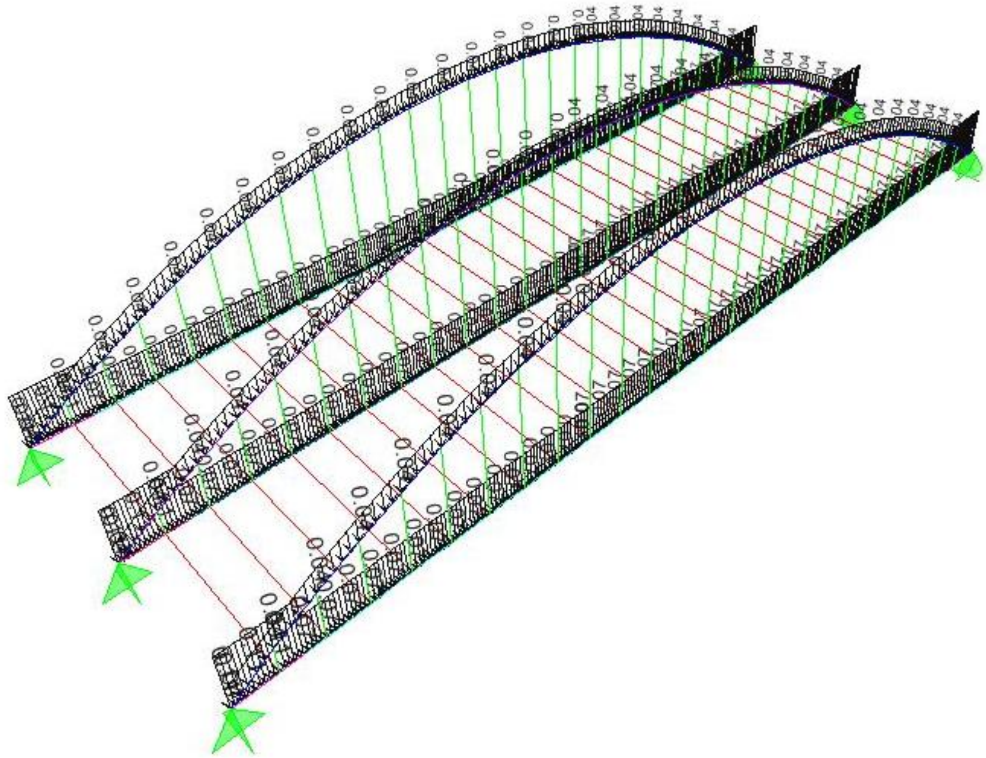

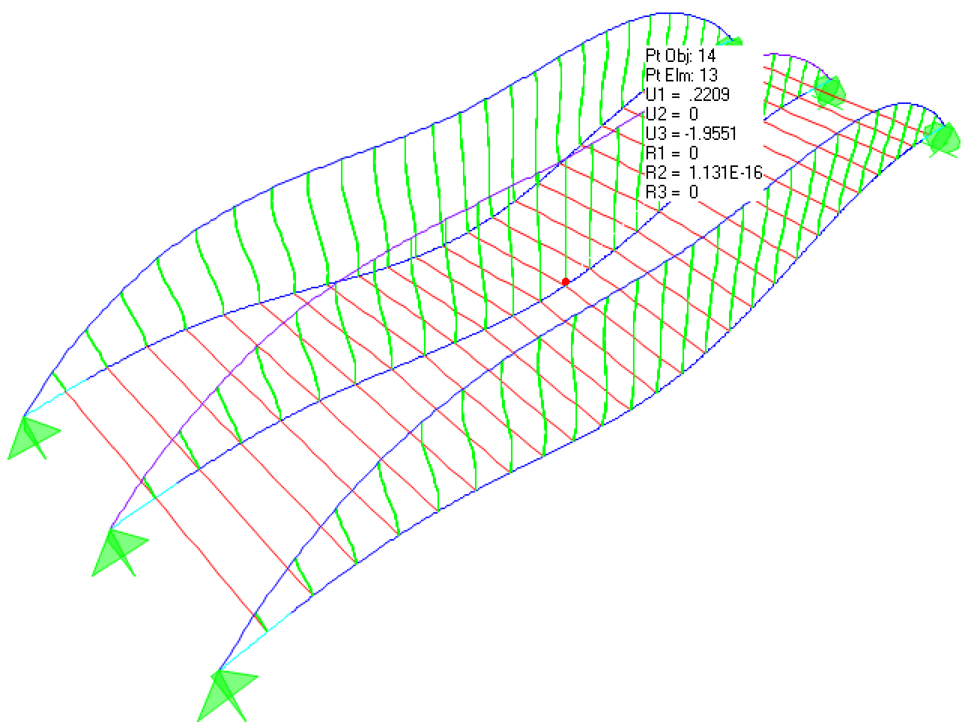

- Median Arch

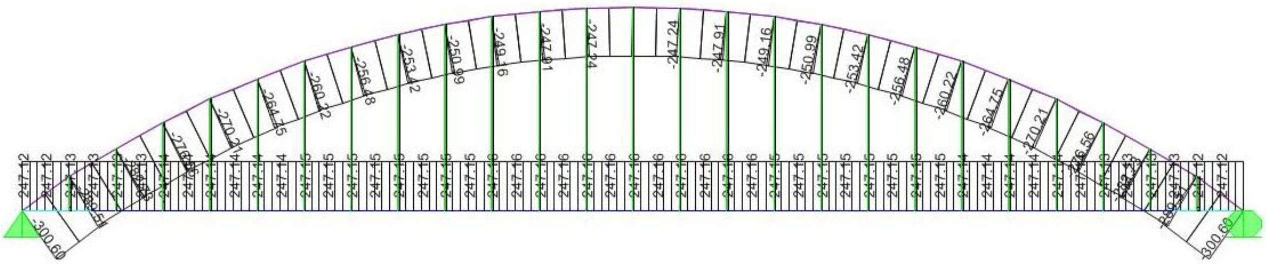

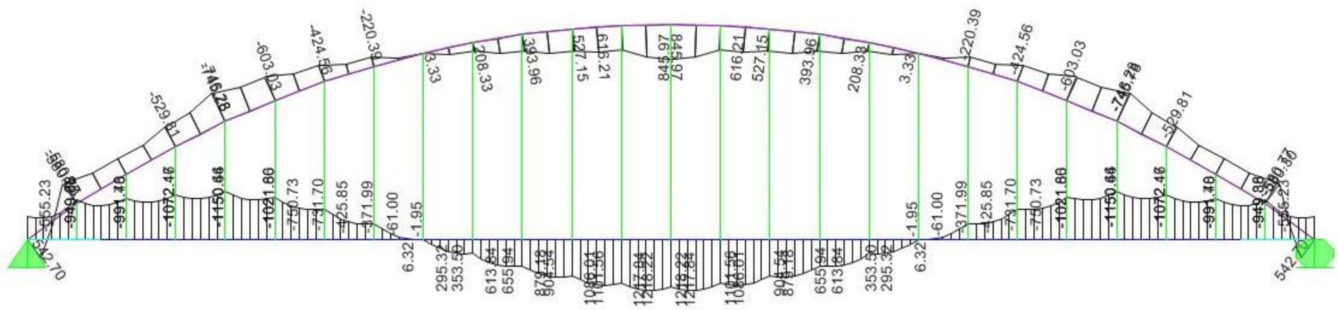

- Outside Arch

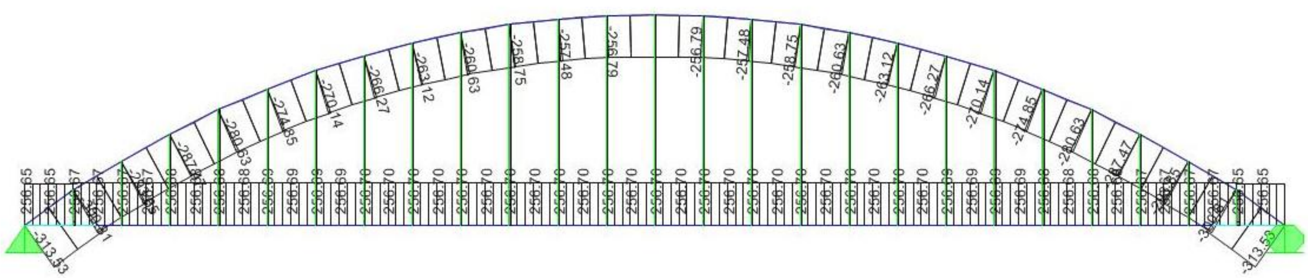

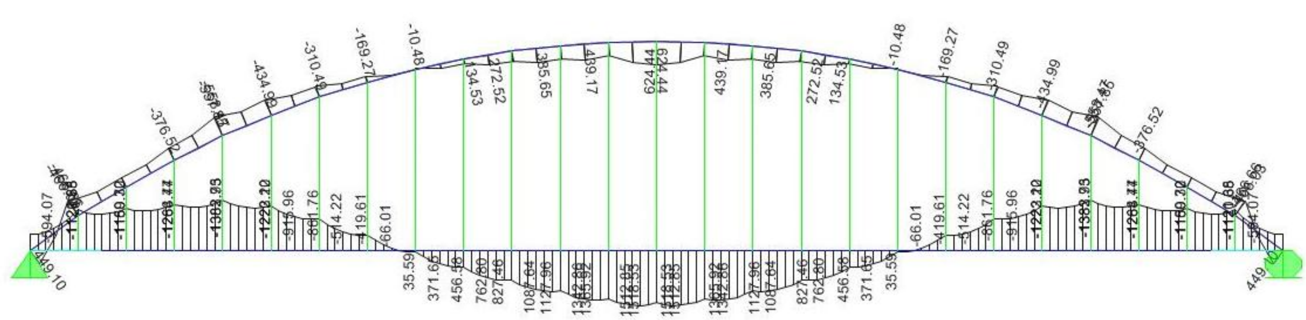

Stage I: Service I Combination

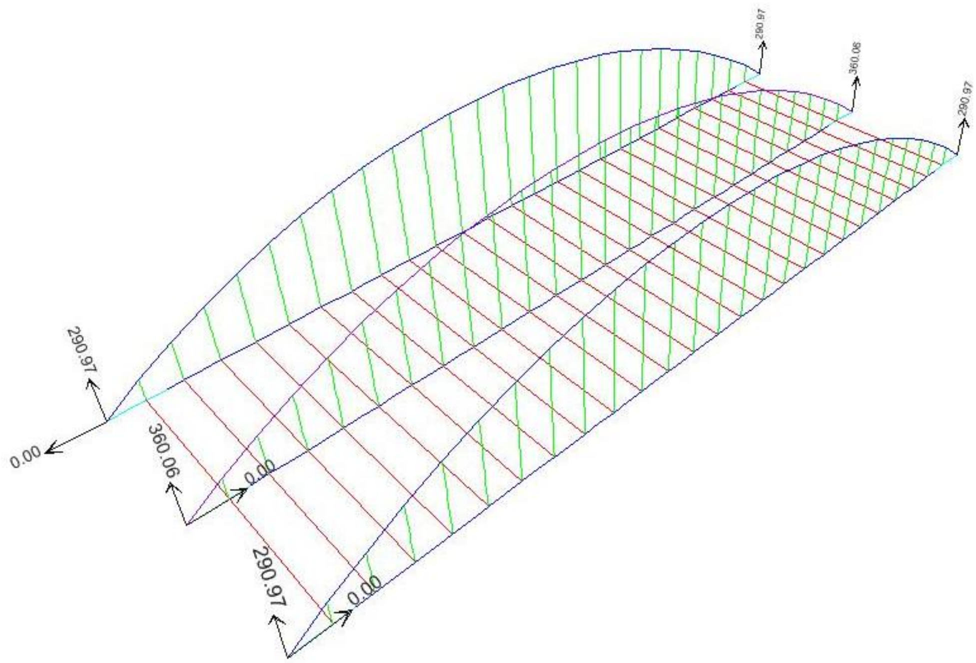

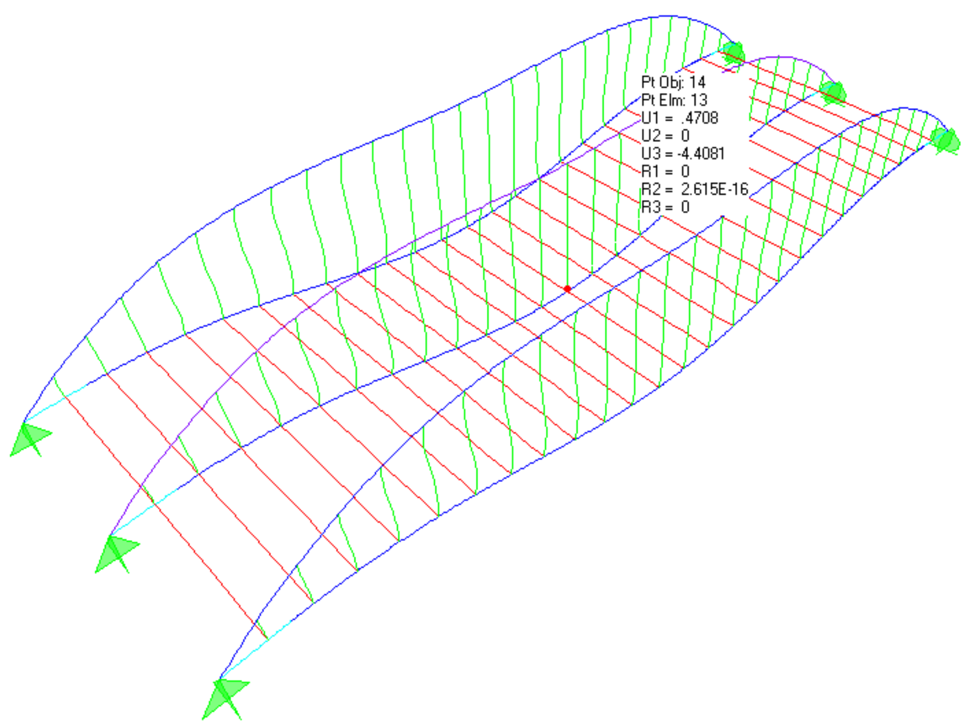

- Median Arch

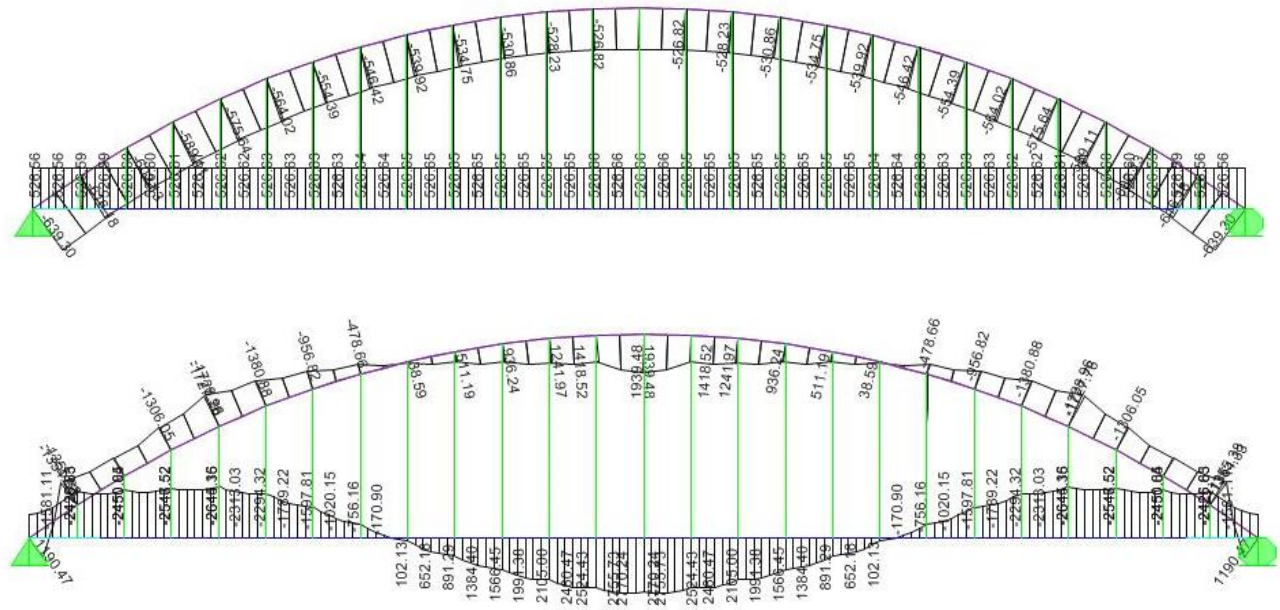

- Outside Arch

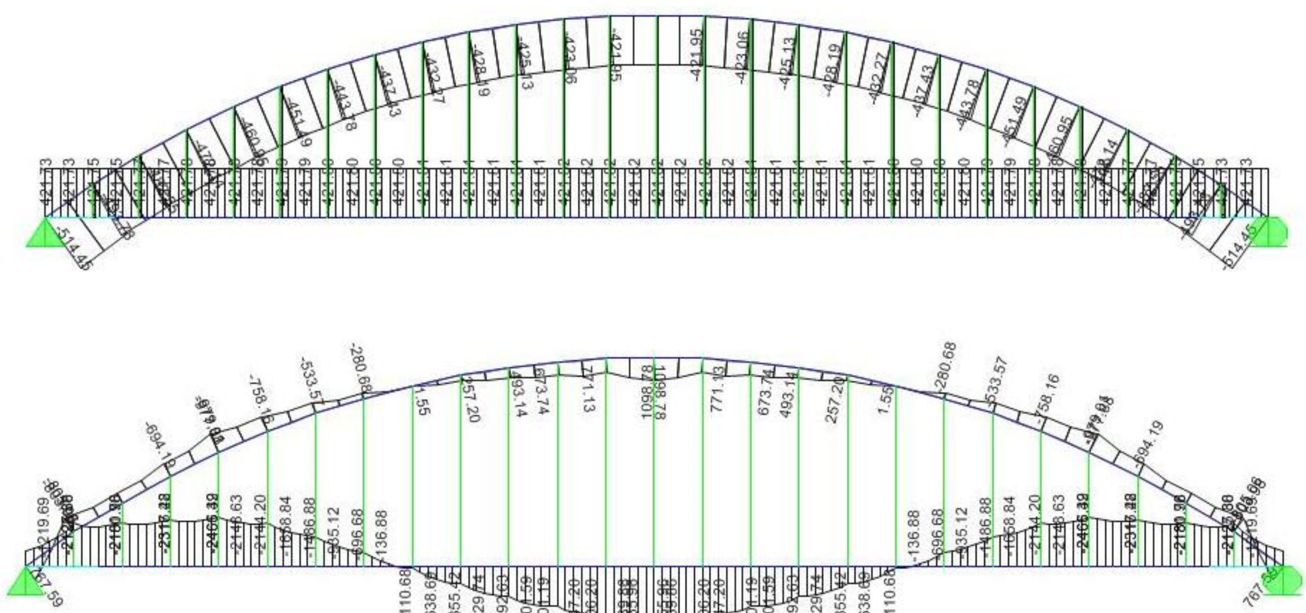

<u>Stage I: Strength I Combination</u>

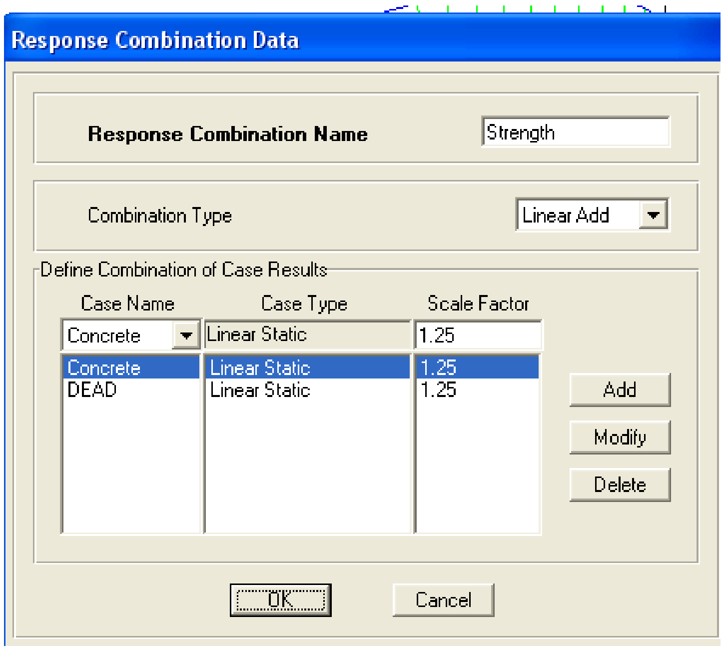

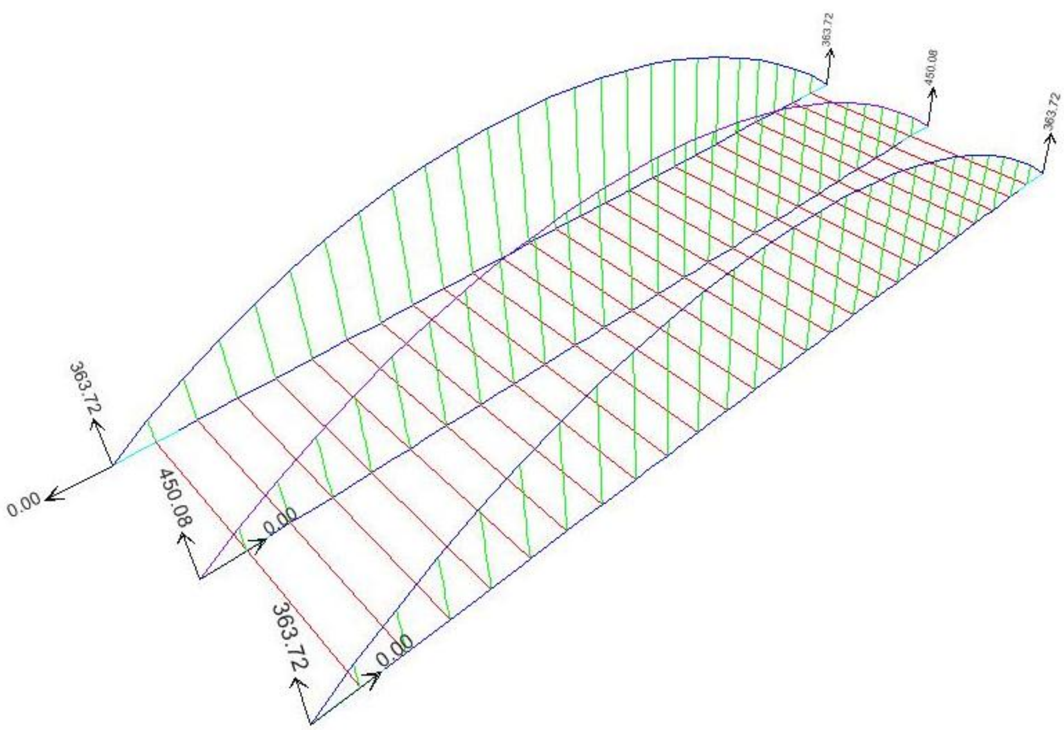

- Median Arch

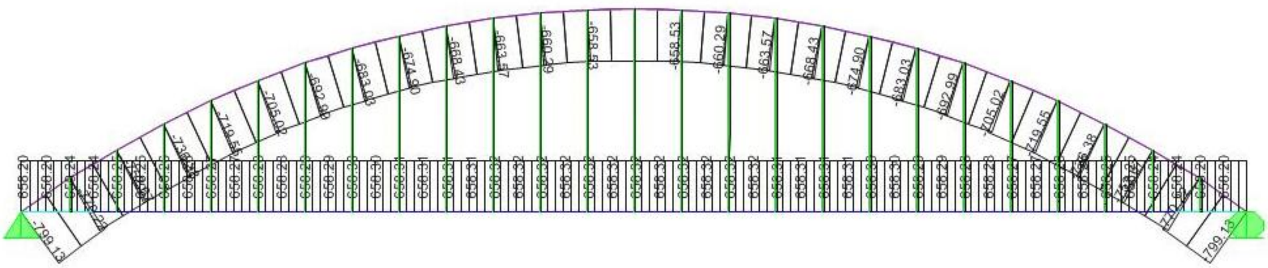

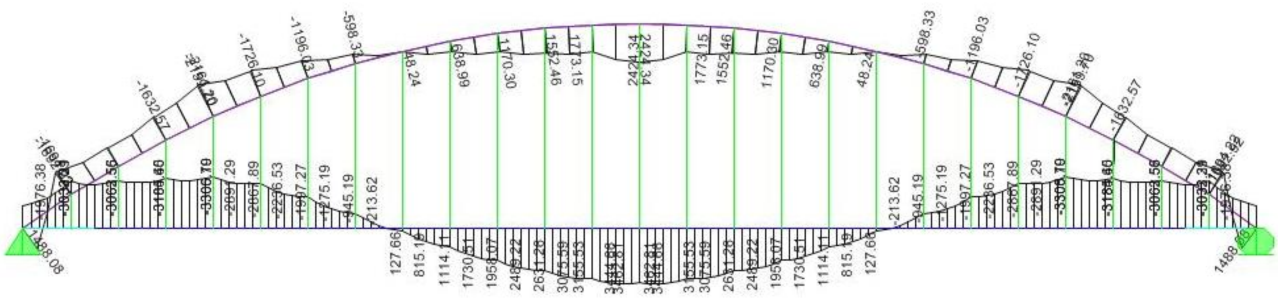

- Outside Arch

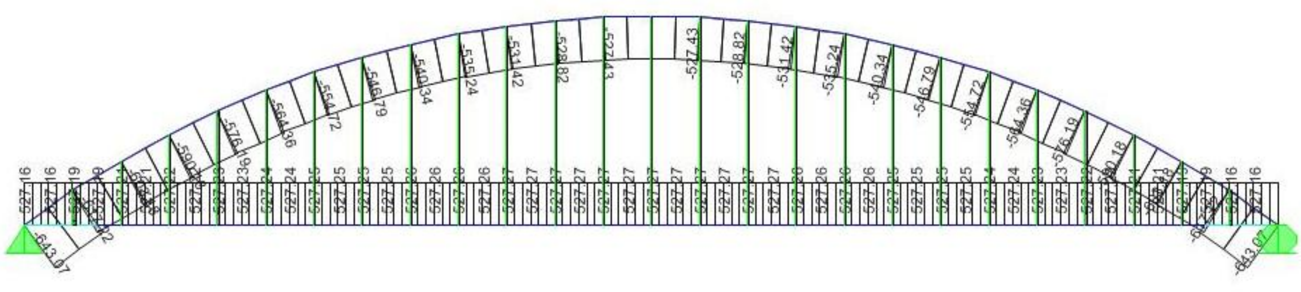

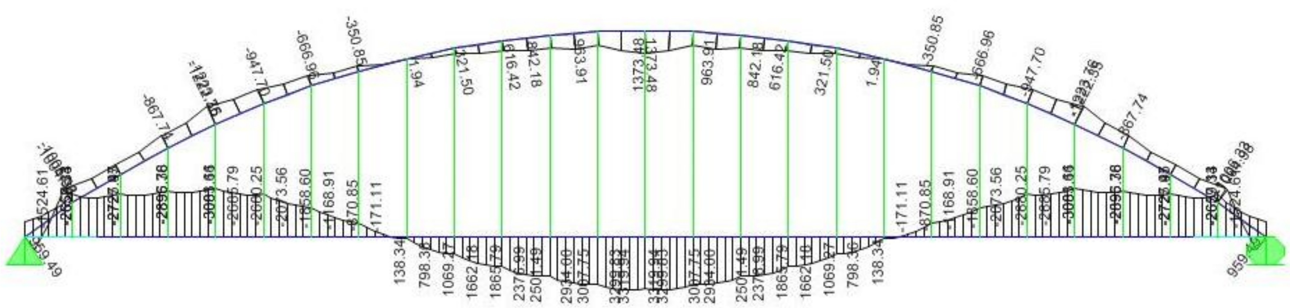

Stage II: Tie Post-Tensioning

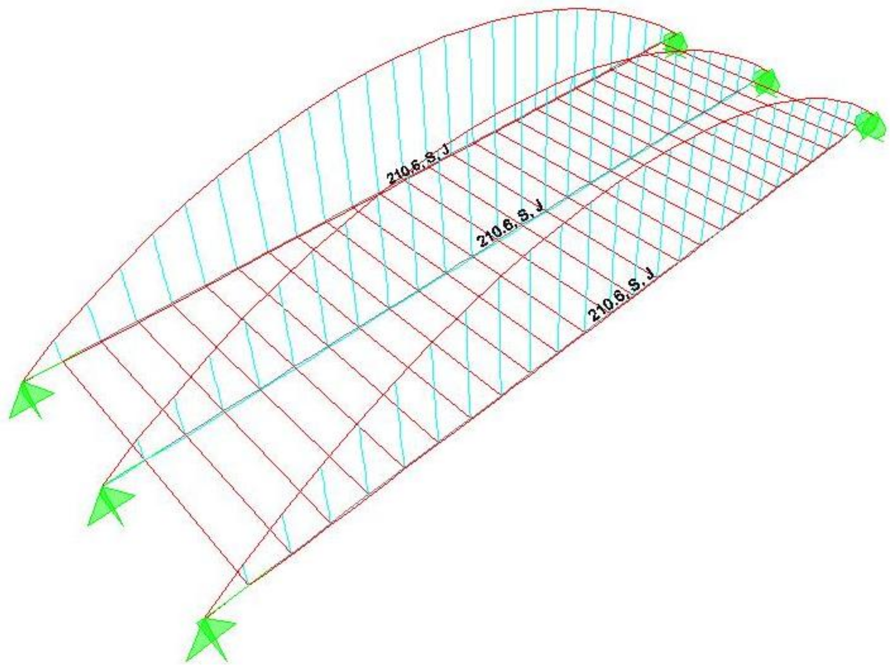

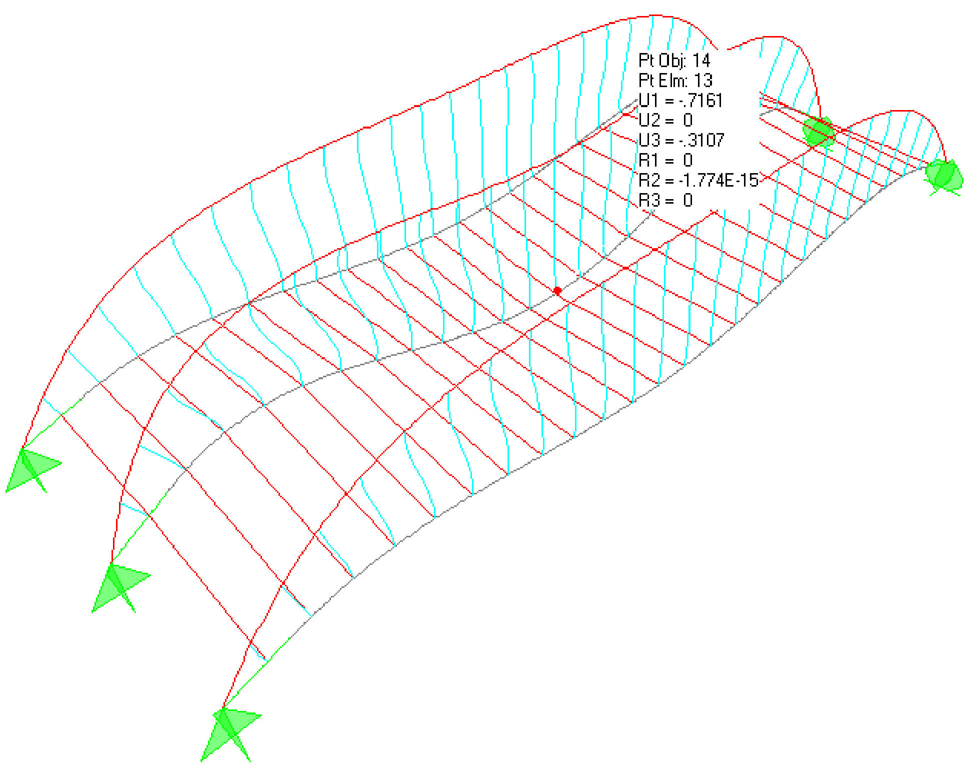

- Median Arch

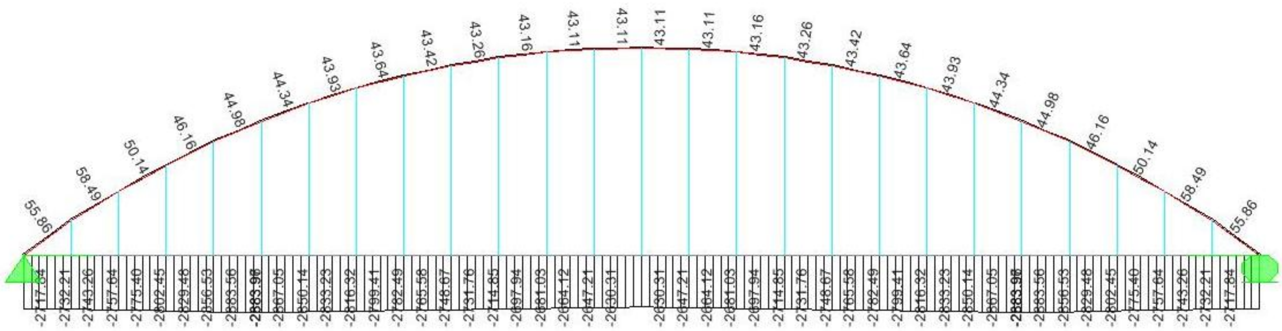

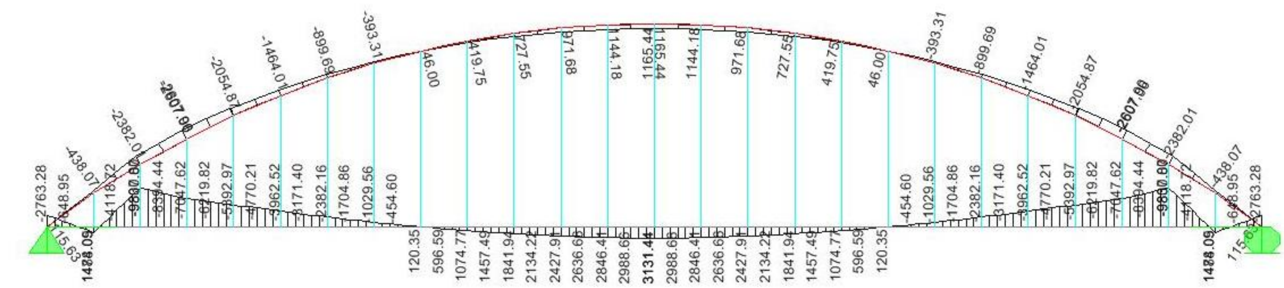

- Outside Arch

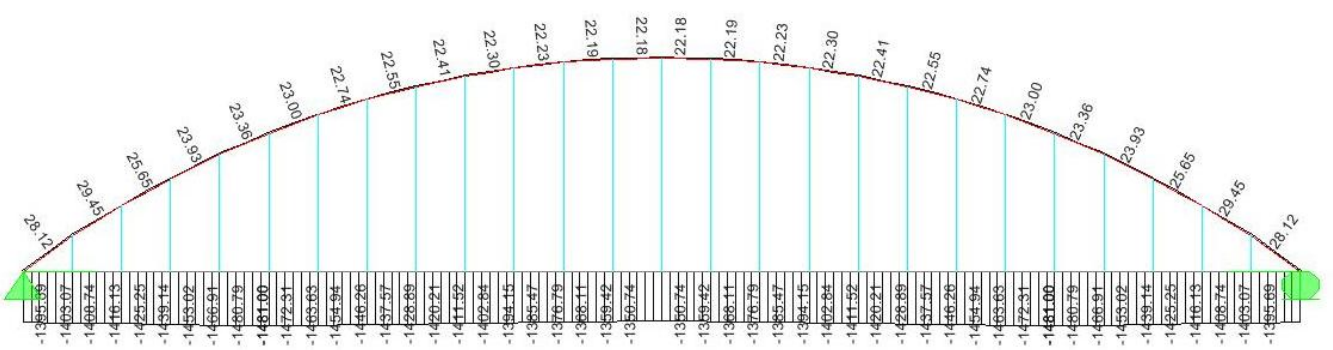

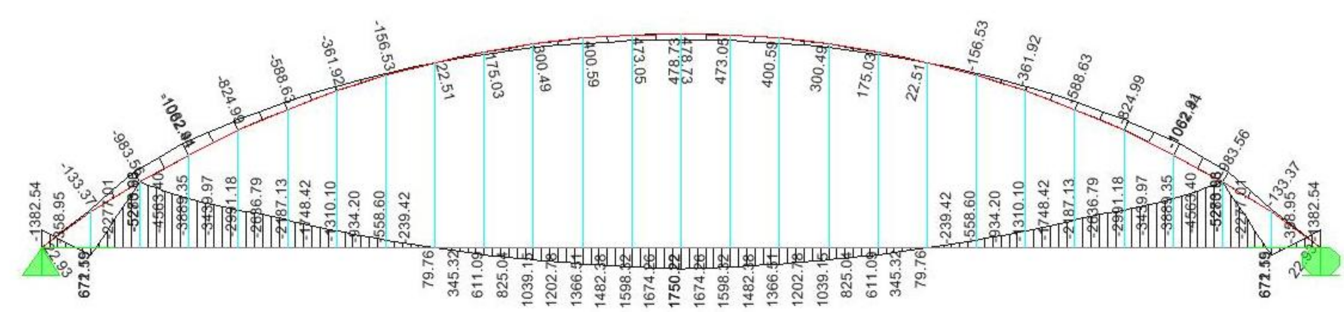

Stage II: Deck Weight

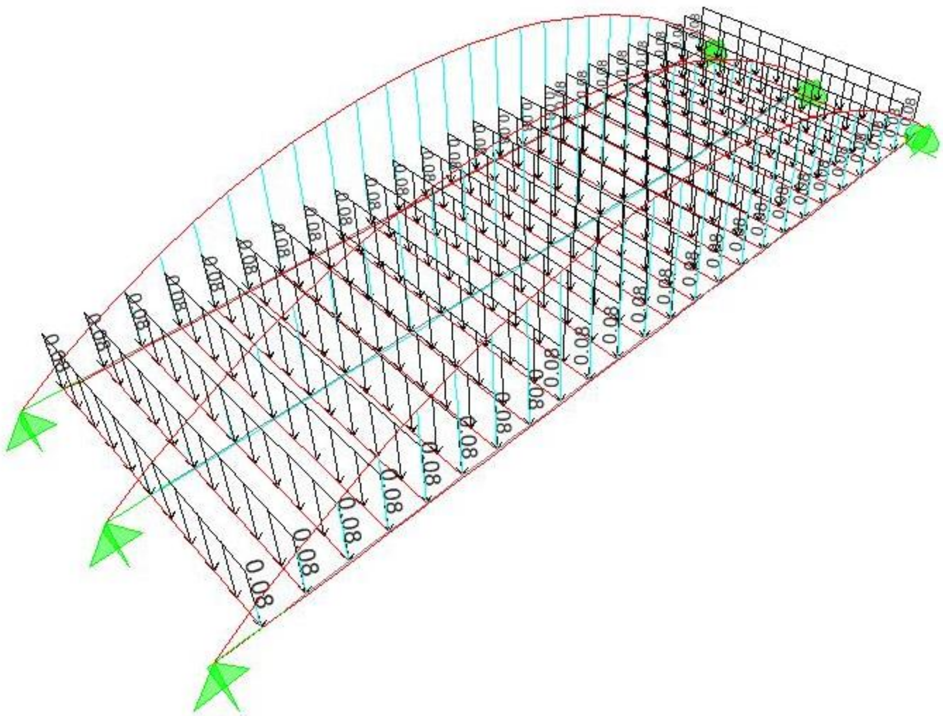

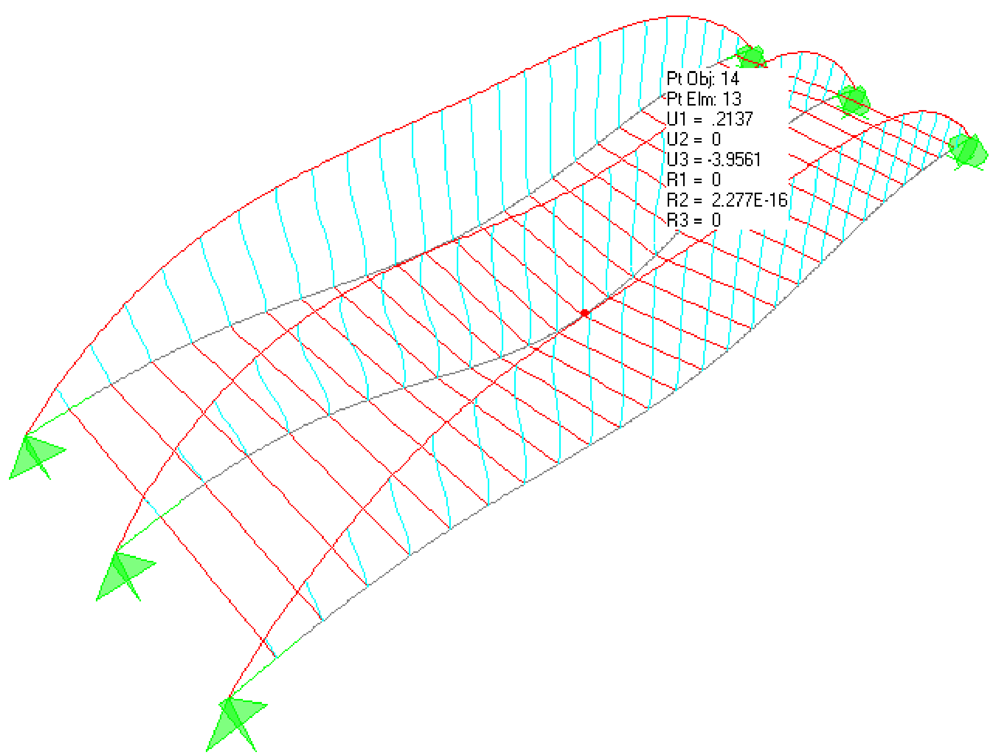

- Median Arch

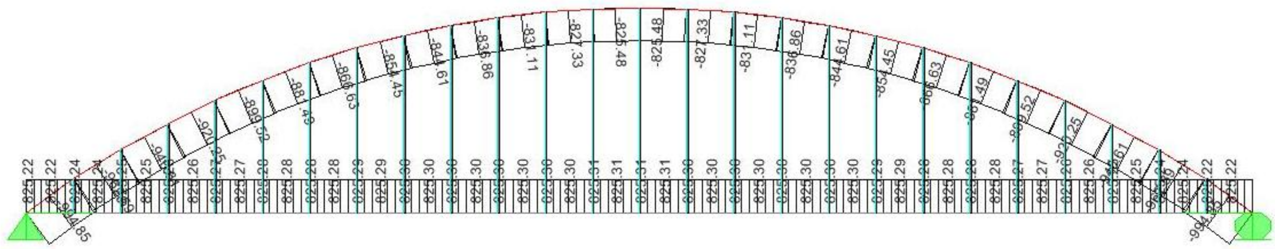

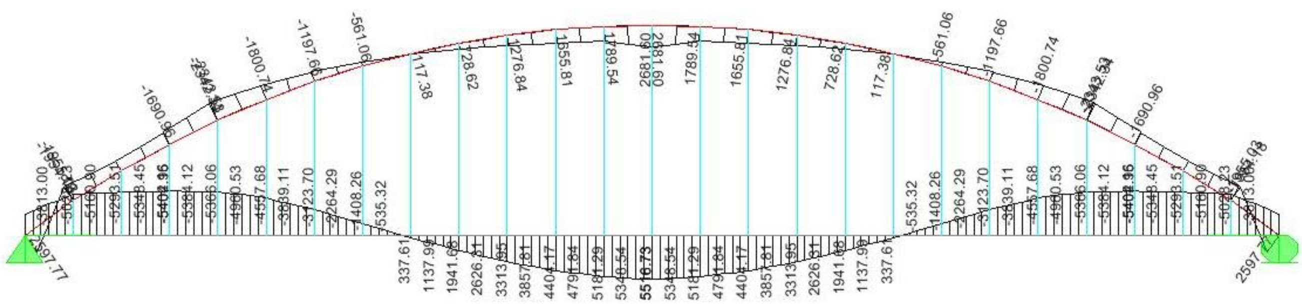

- Outside Arch

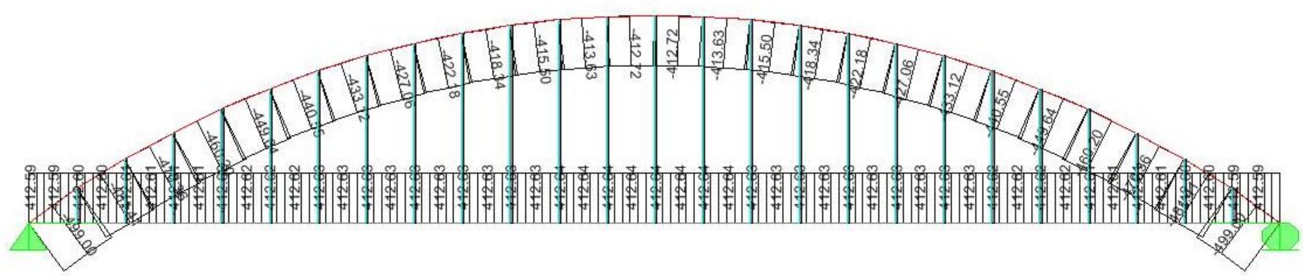

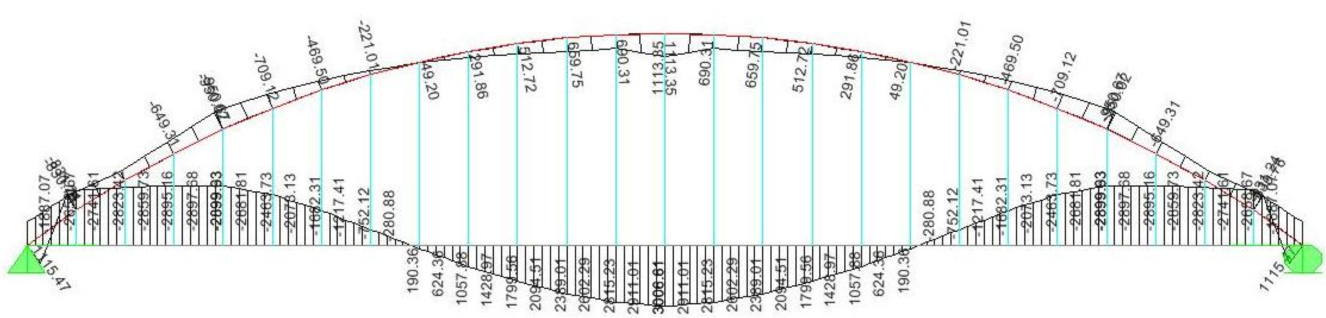

Stage II: Service I Combination

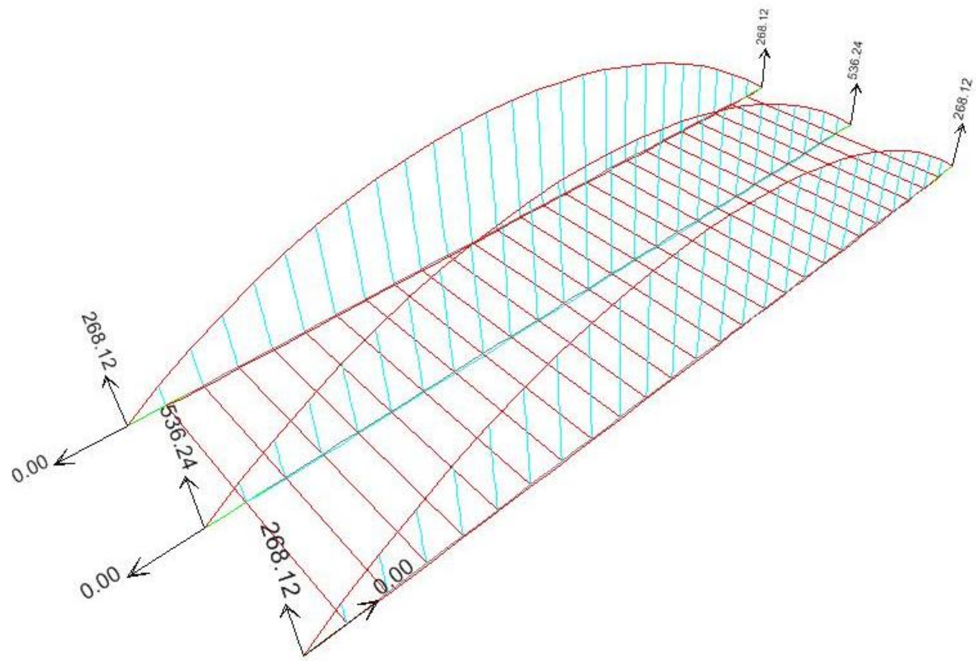

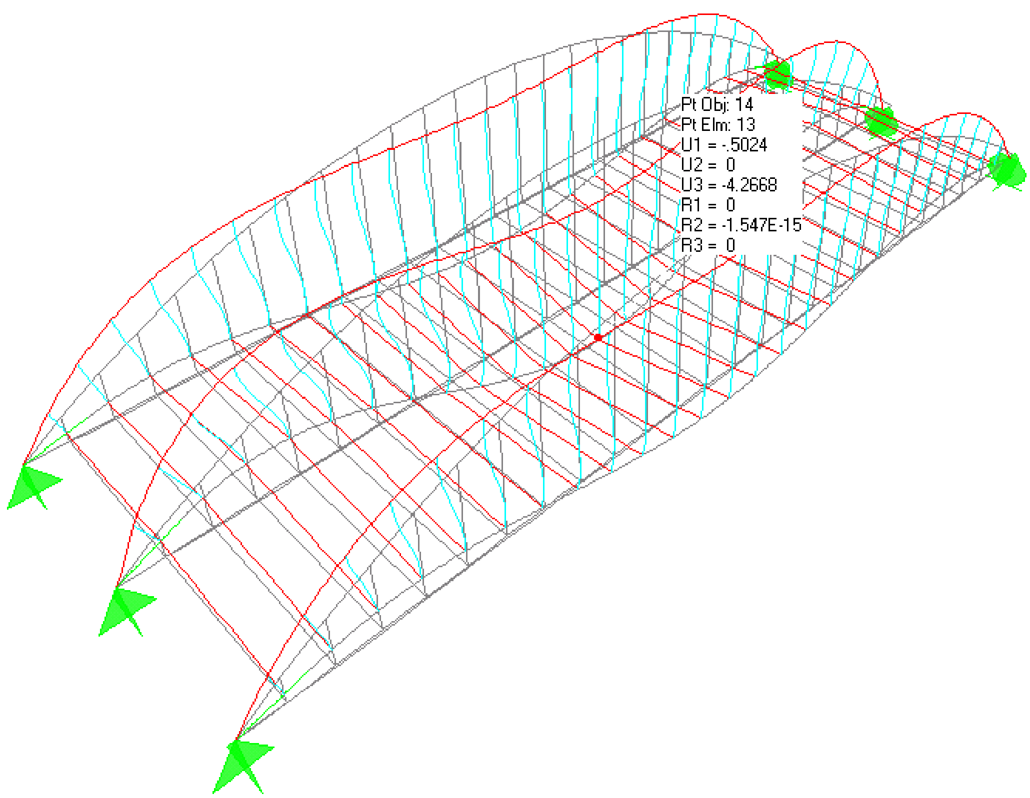

- Median Arch

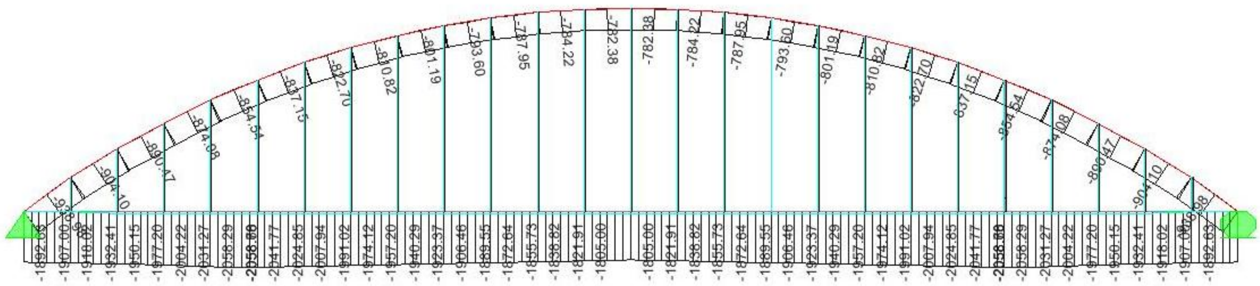

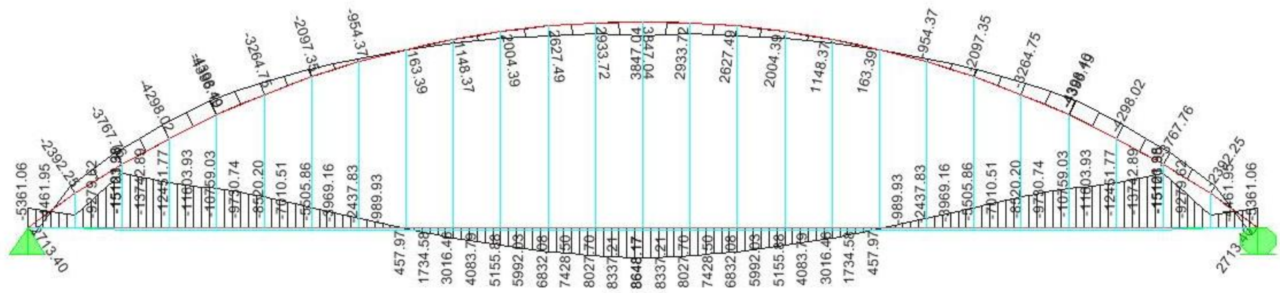

- Outside Arch

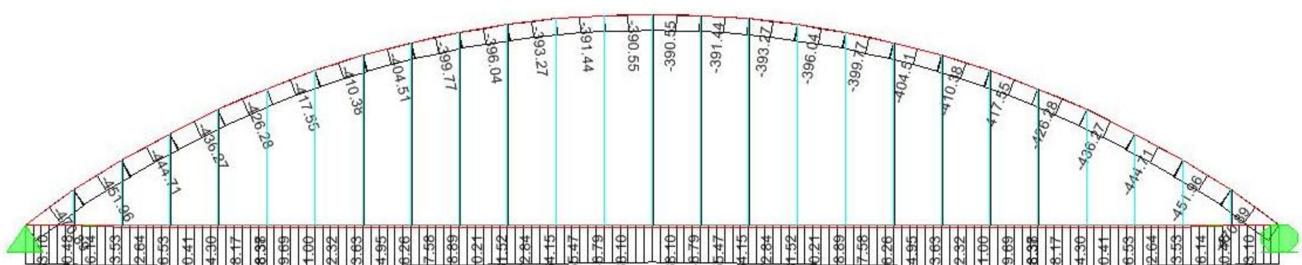

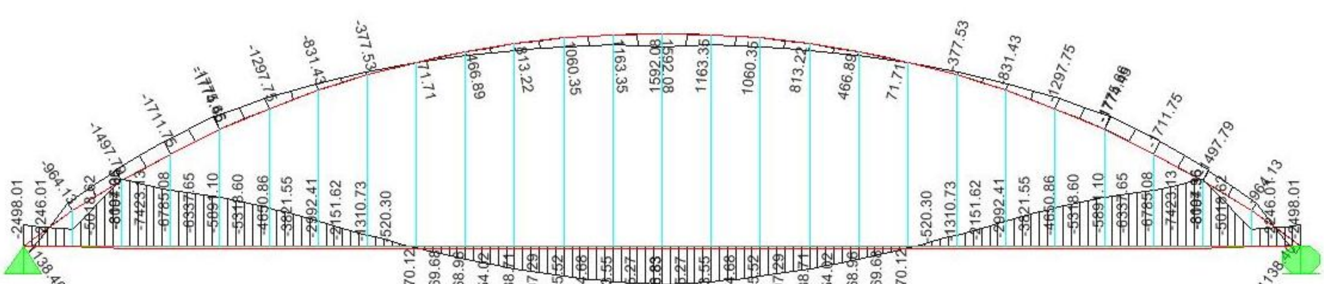

Stage II: Strength I Combination

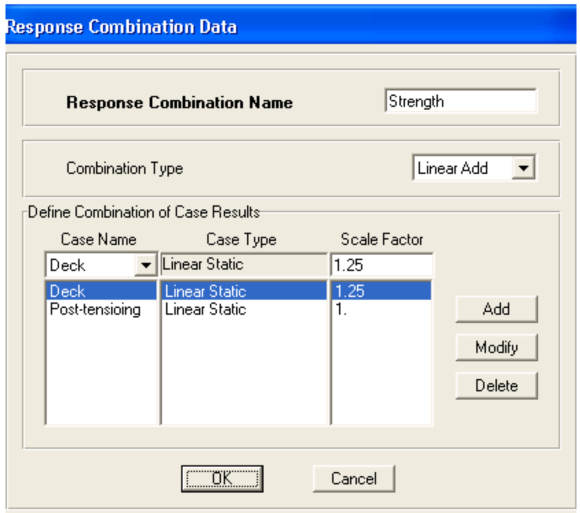

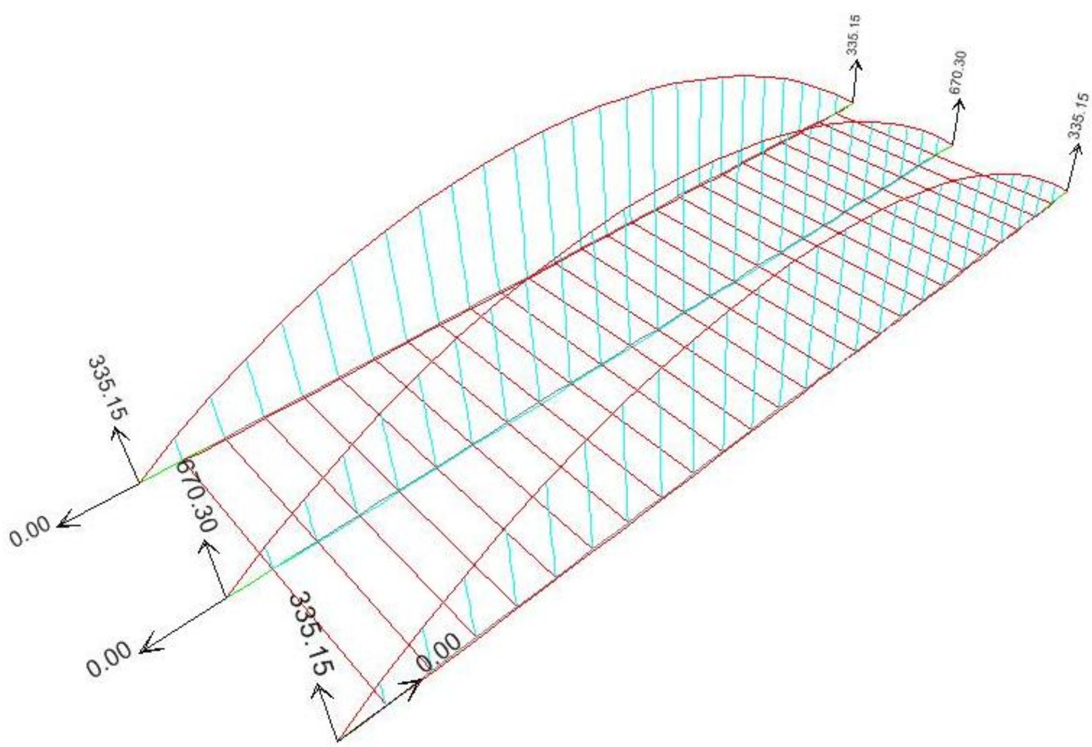

- Median Arch

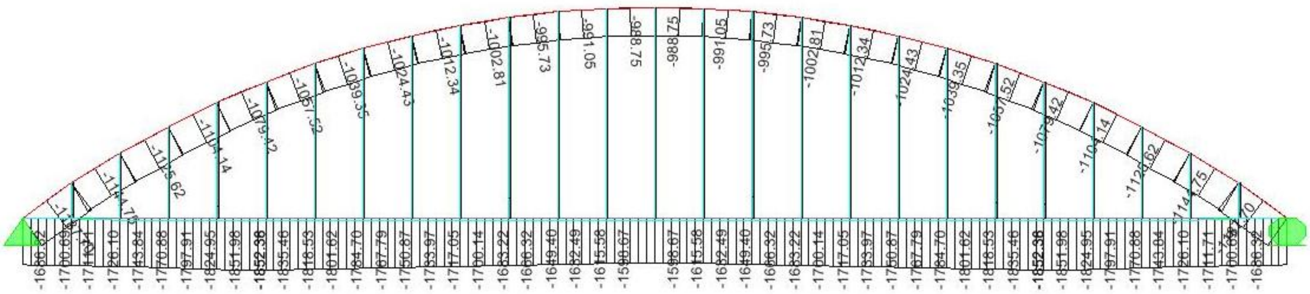

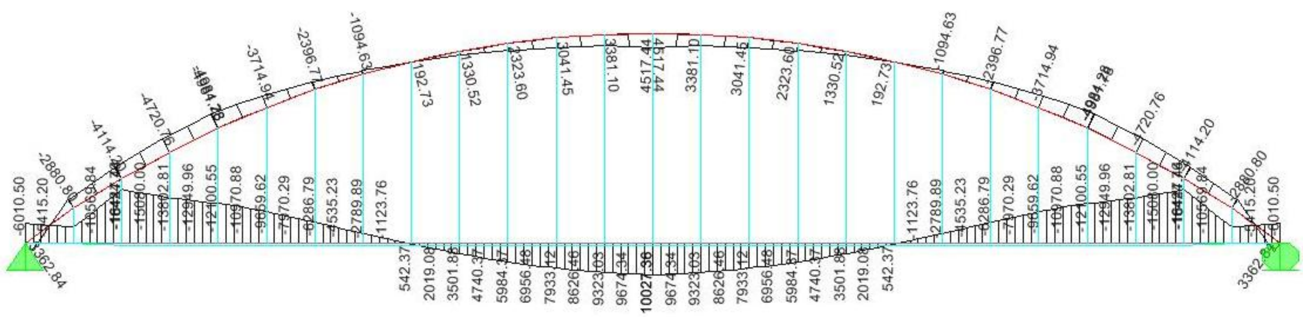

- Outside Arch

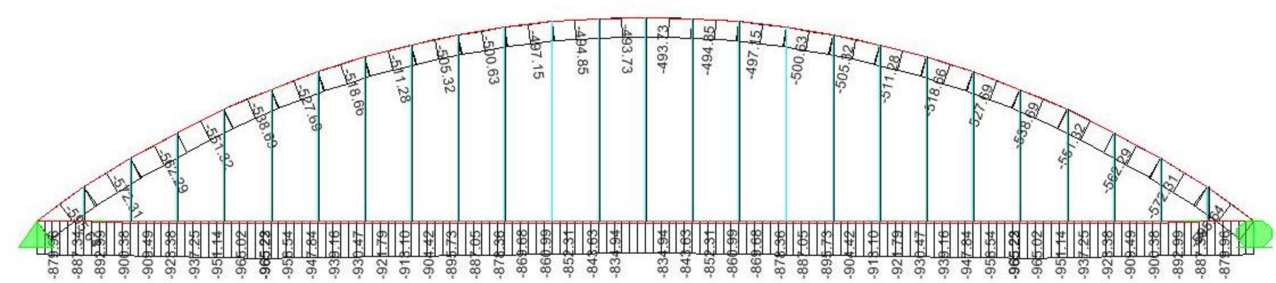

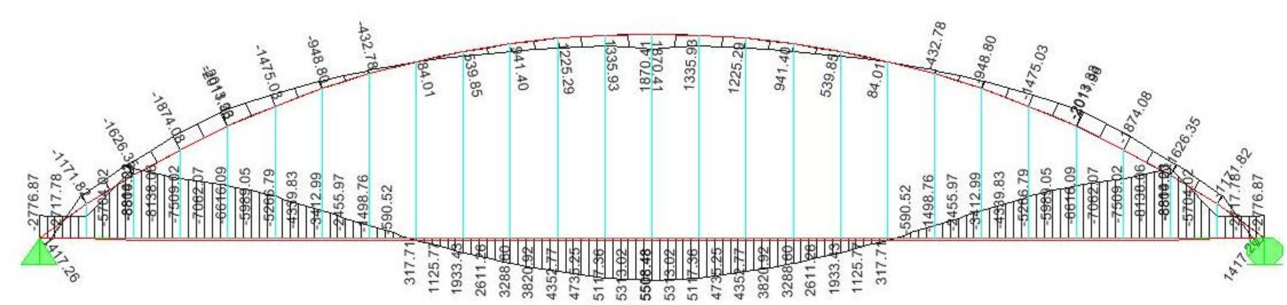

Stage III: Deck Post-Tensioning

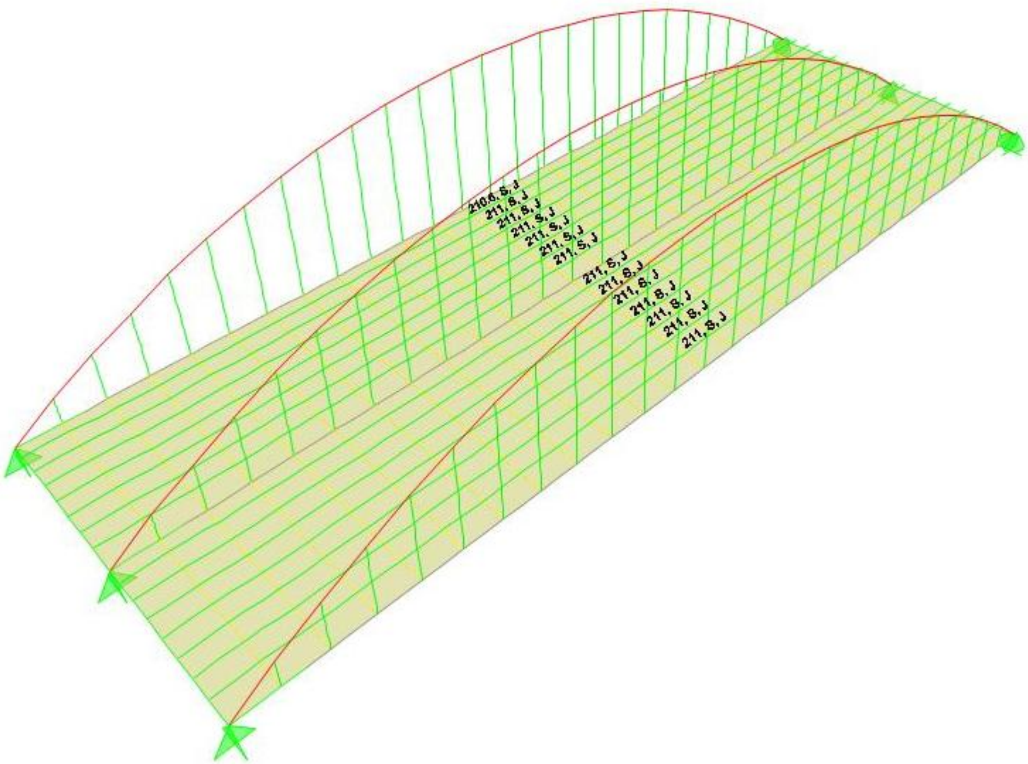

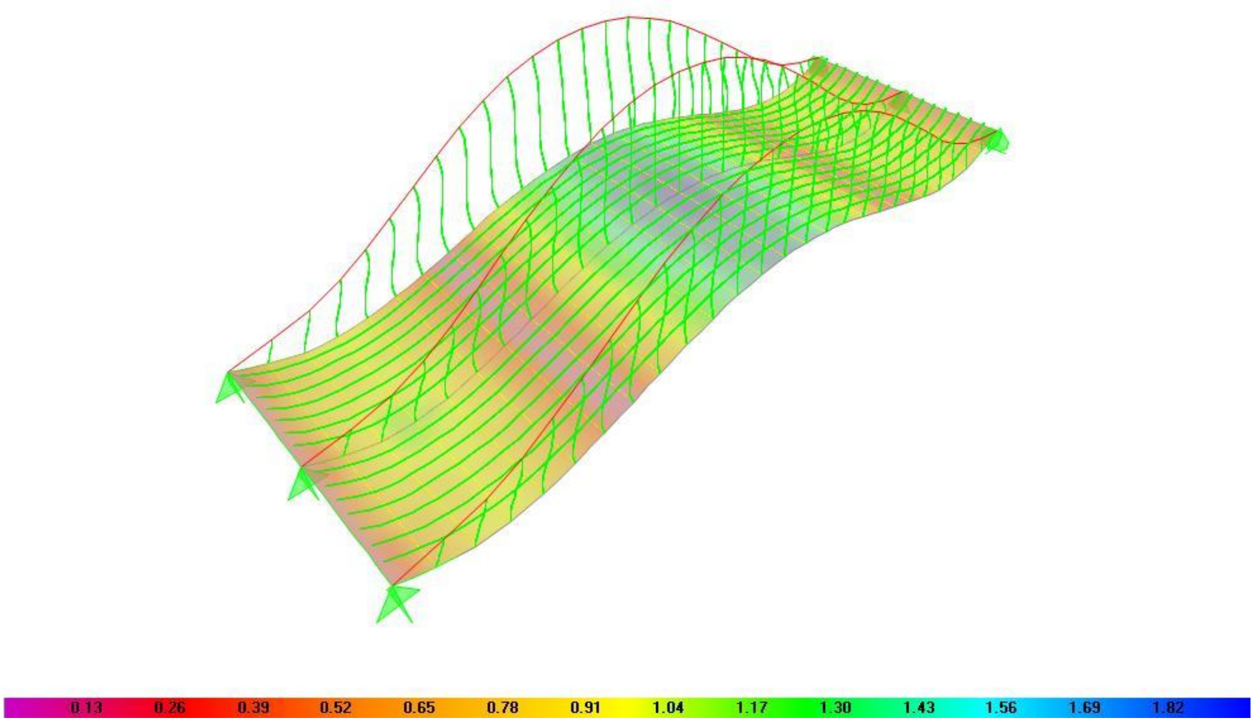

- Median Arch

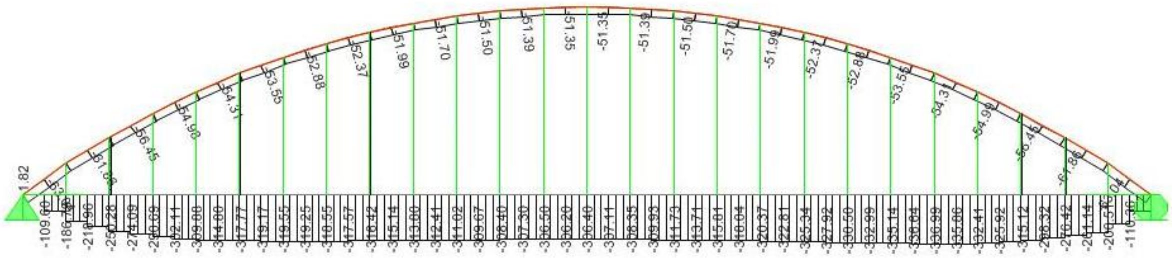

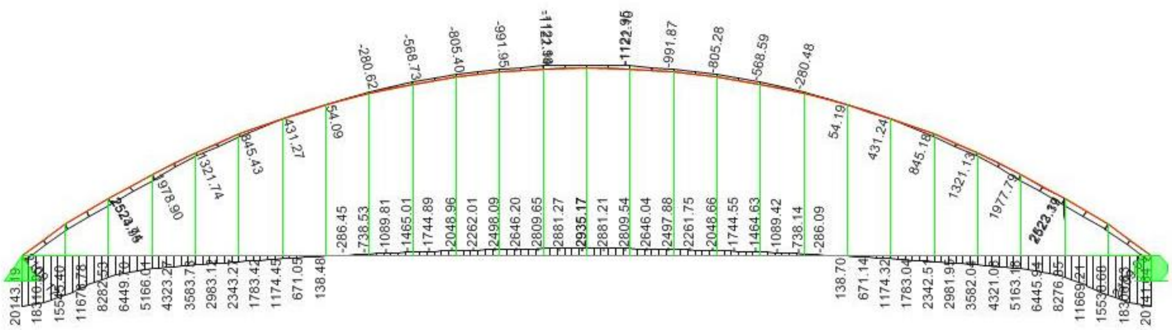

- Outside Arch

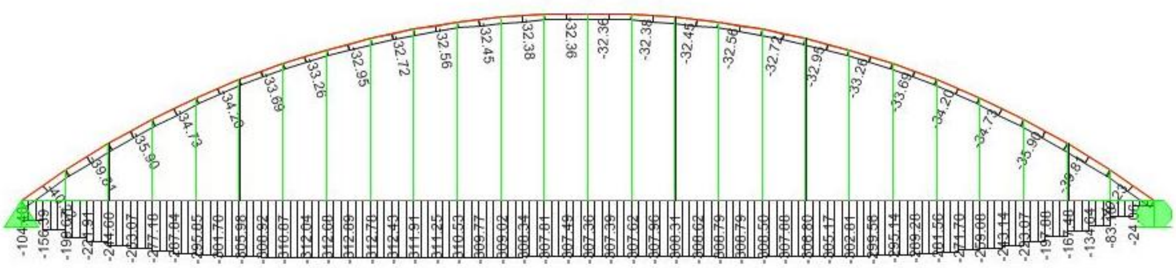

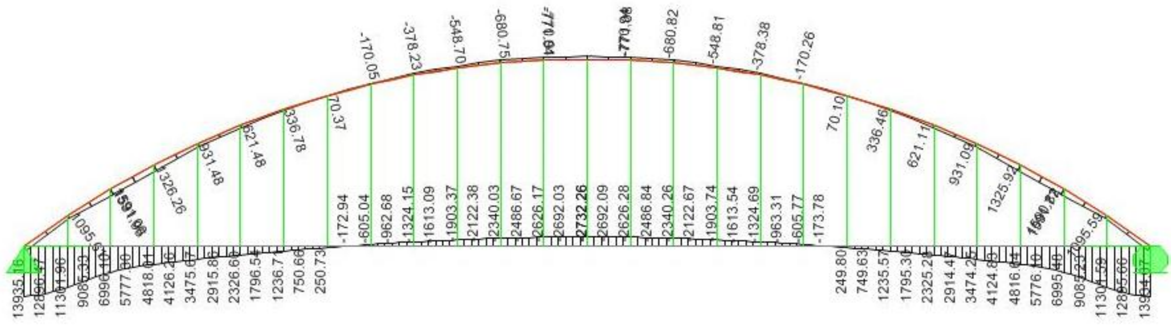

- Longitudinal Stresses in the Deck

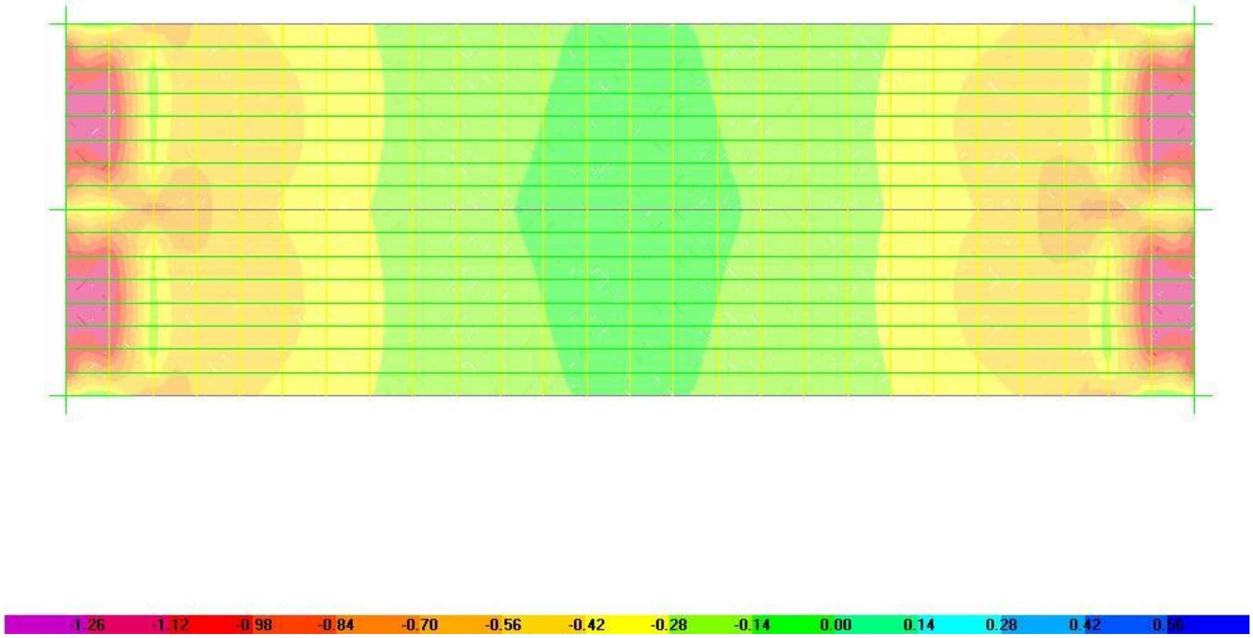

- Transversal Stresses in the Deck

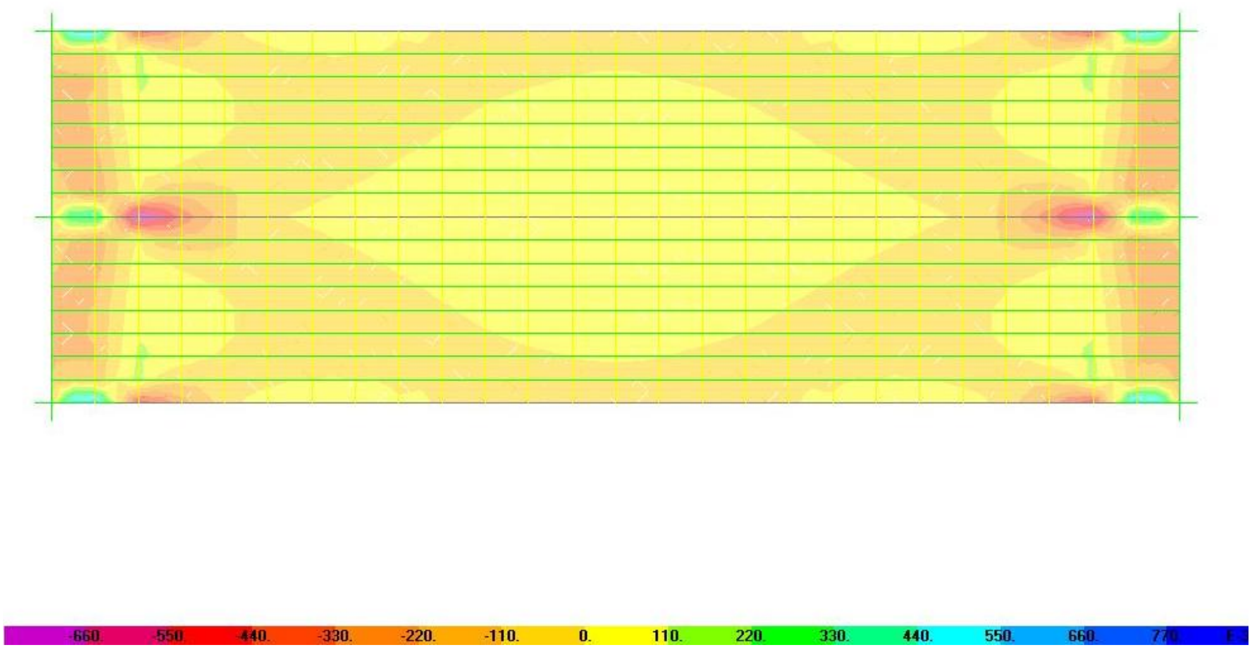

Stage IV: Railing Load

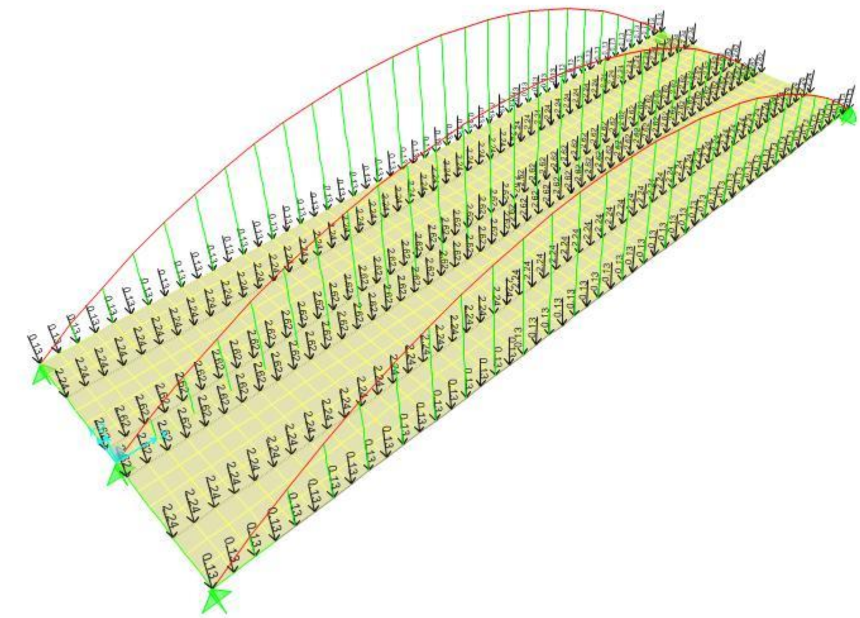

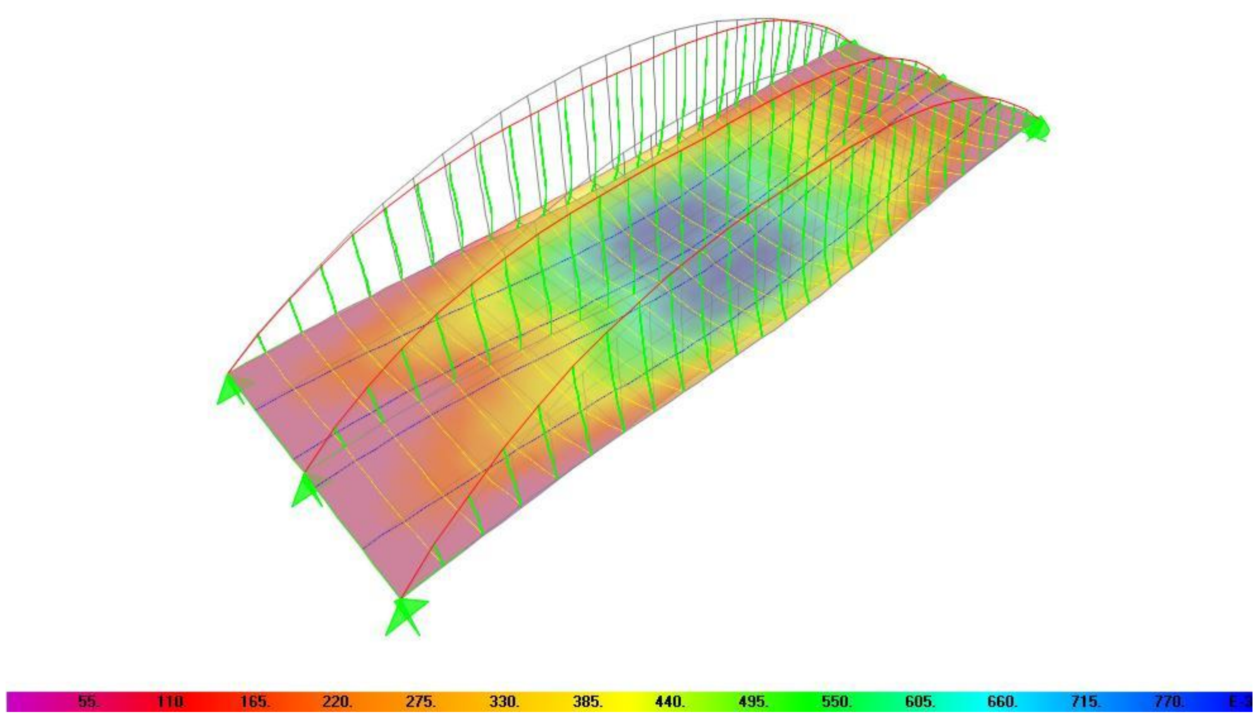

- Median Arch

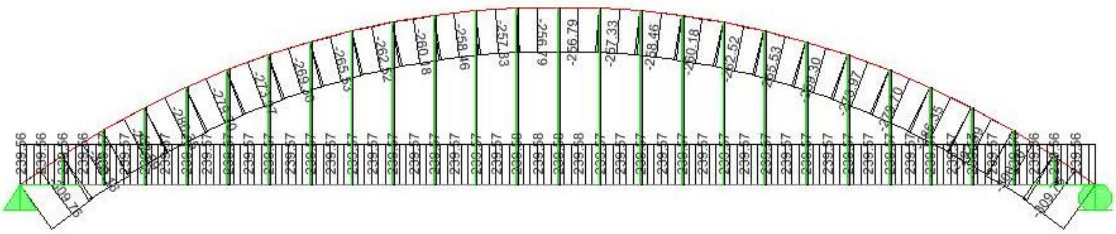

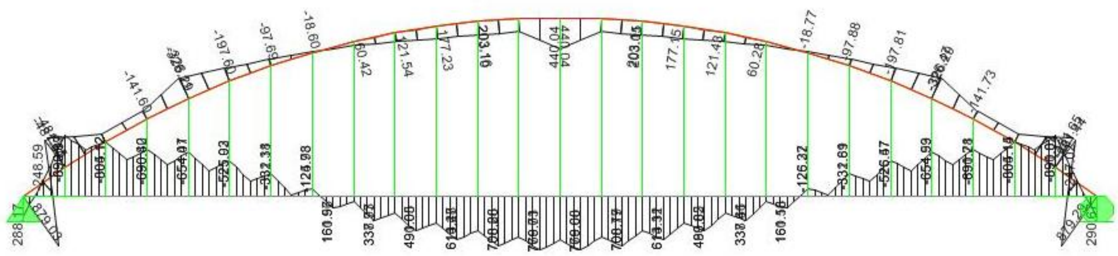

- Outside Arch

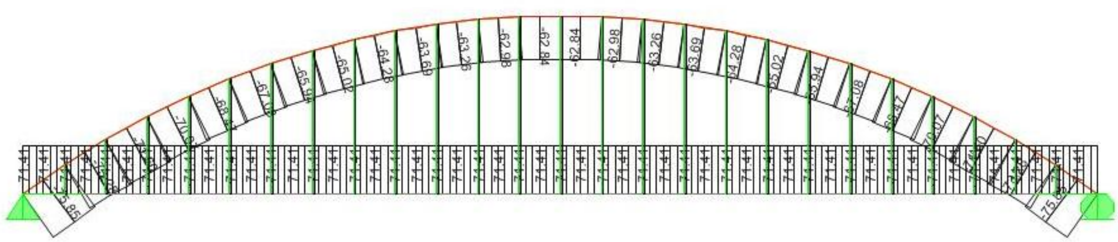

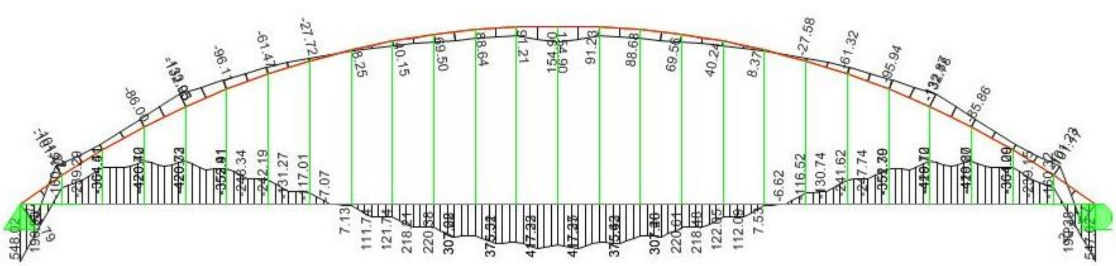

Stage IV: Future Wearing Surface

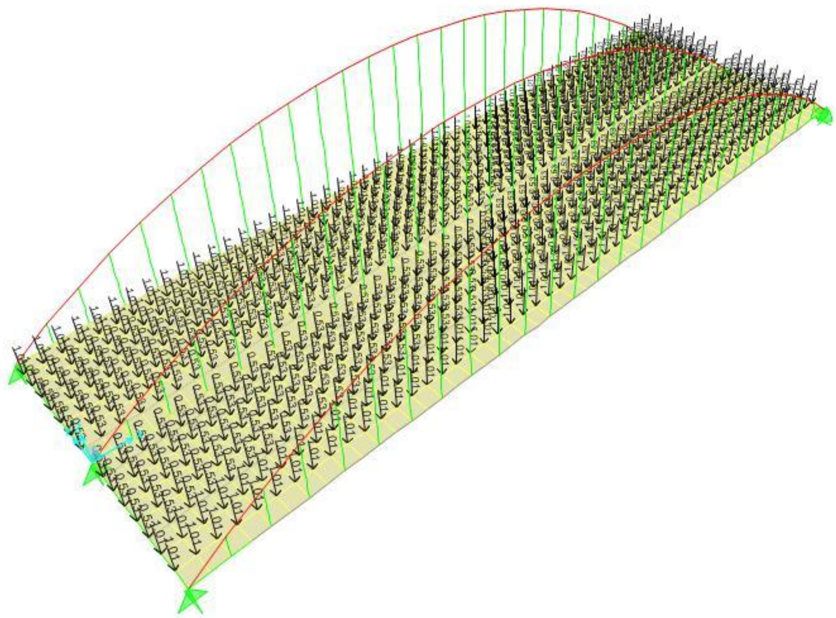

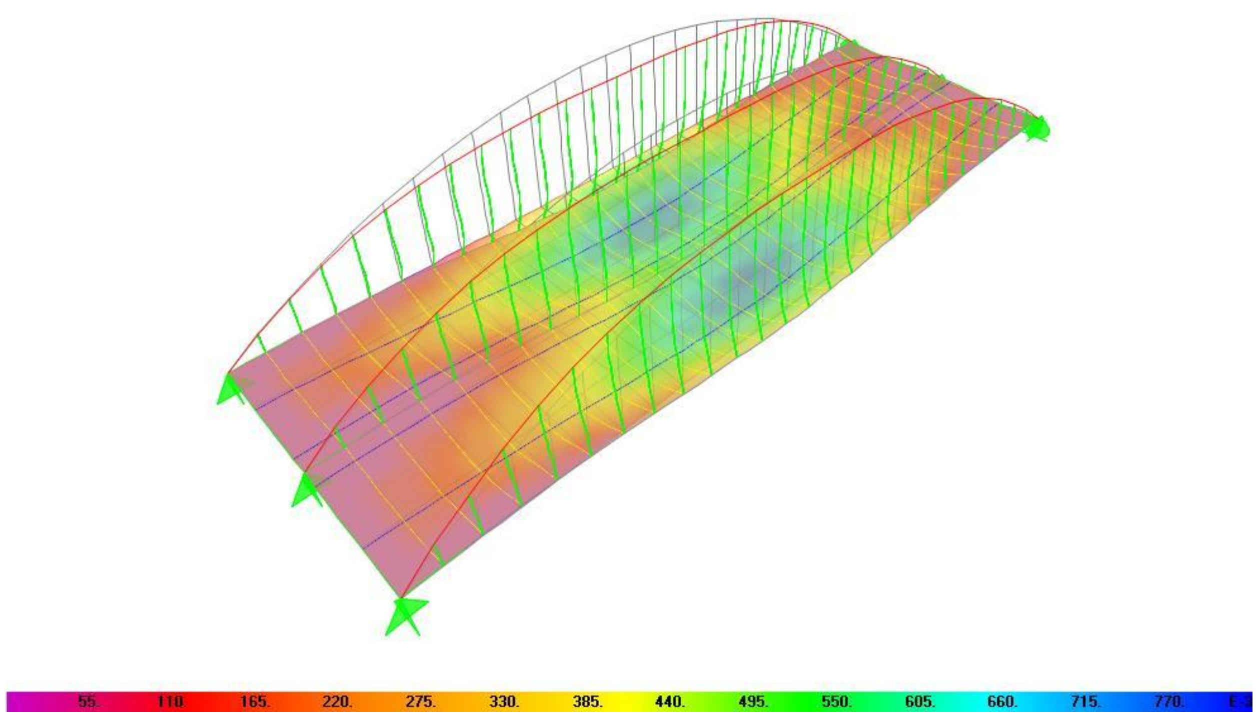

- Median Arch

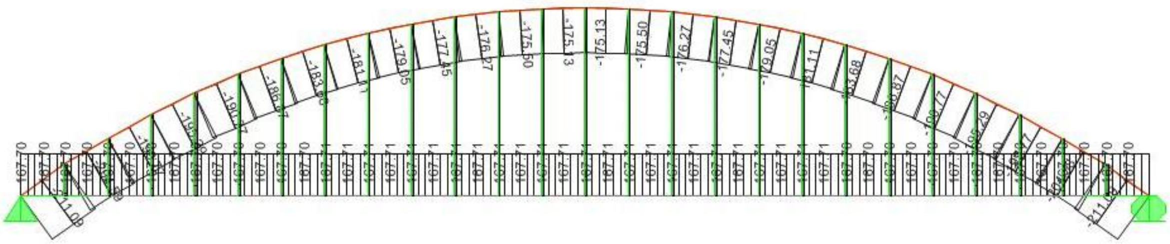

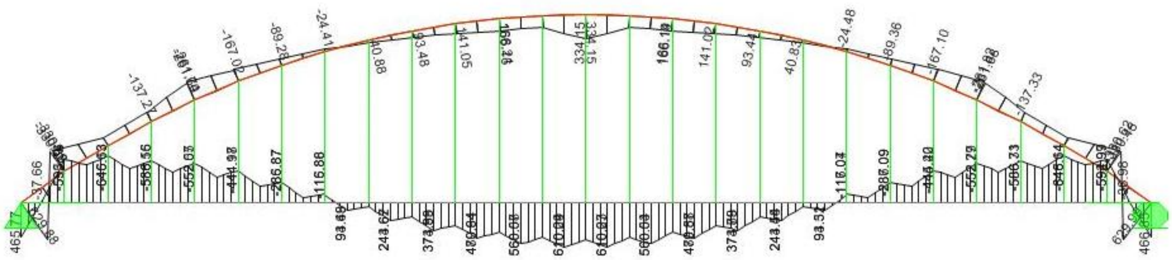

- Outside Arch

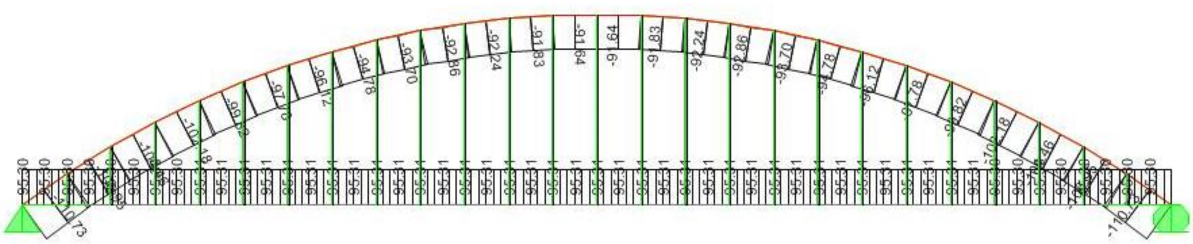

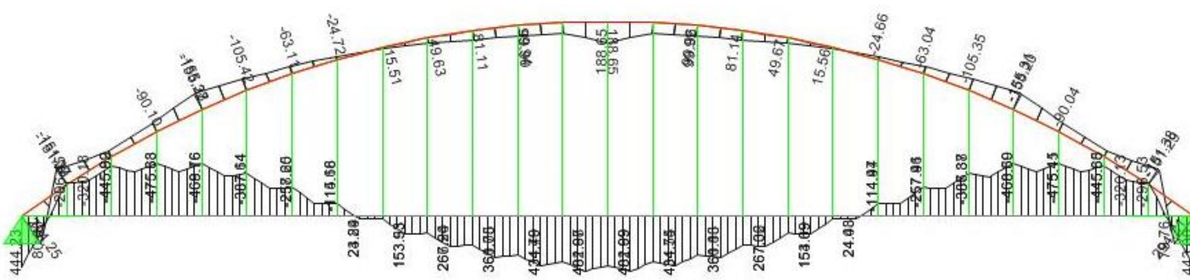

Stage IV: Moving Live Load

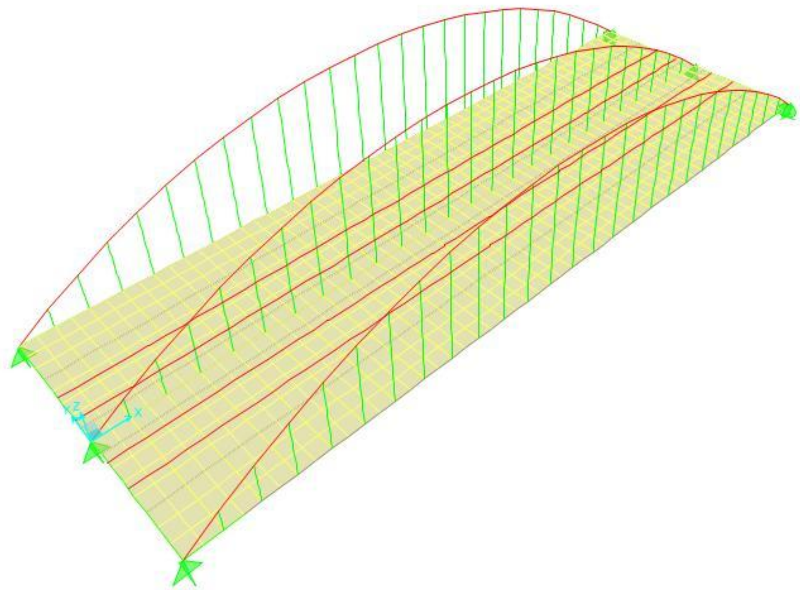

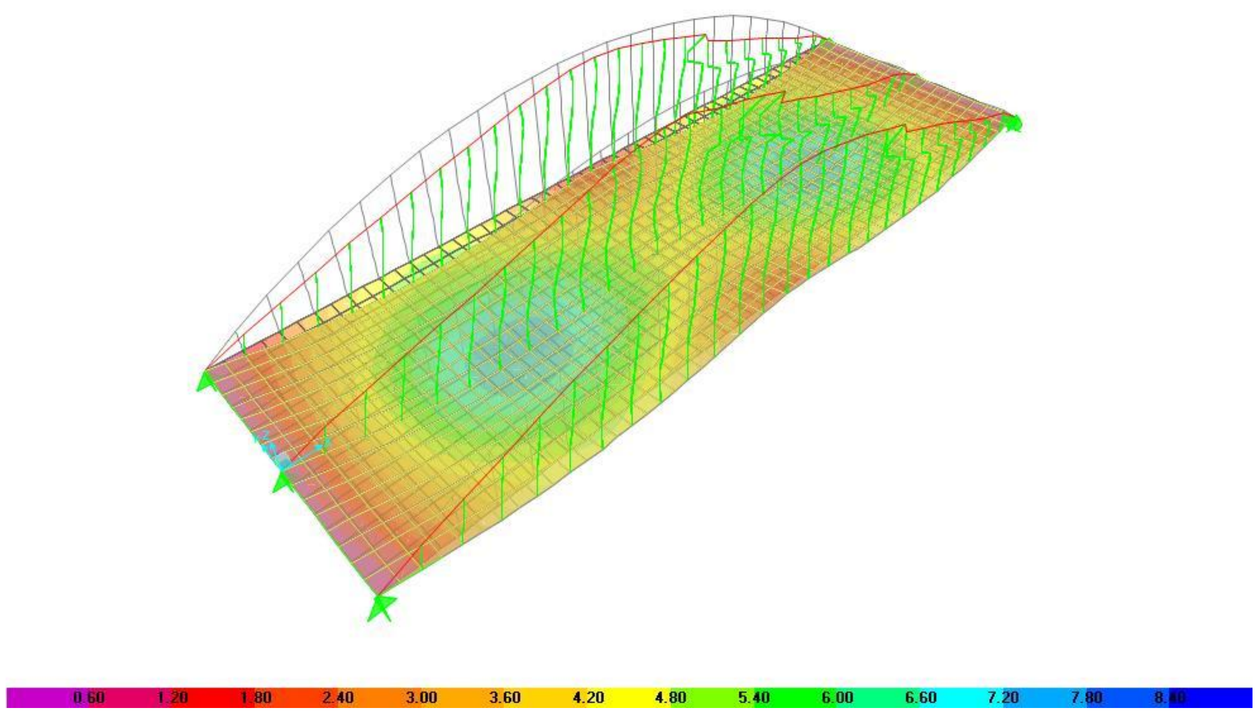

- Median Arch

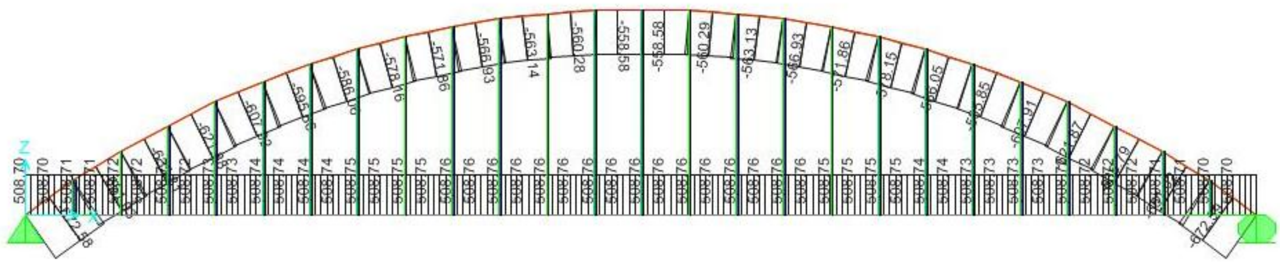

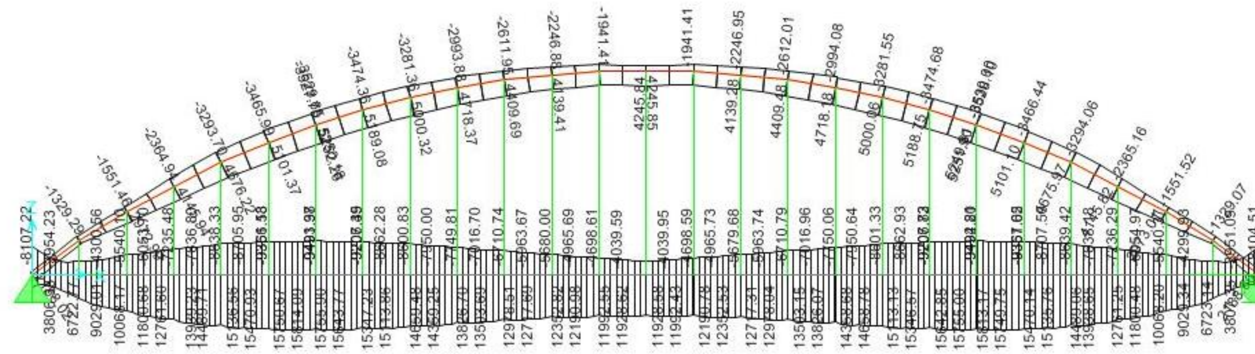

- Outside Arch

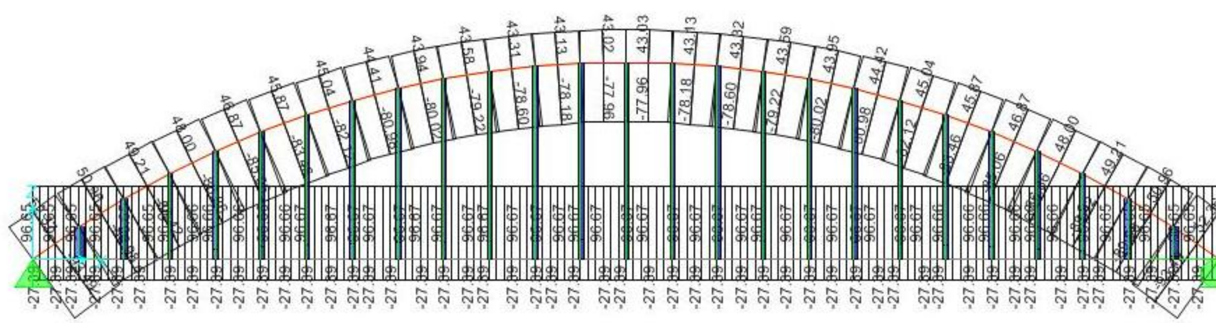

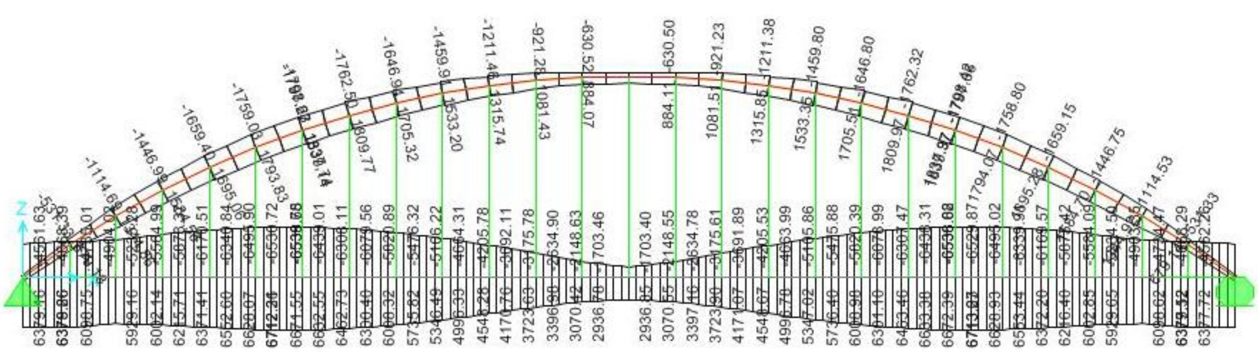

Stage IV: Pedestrian Live Load

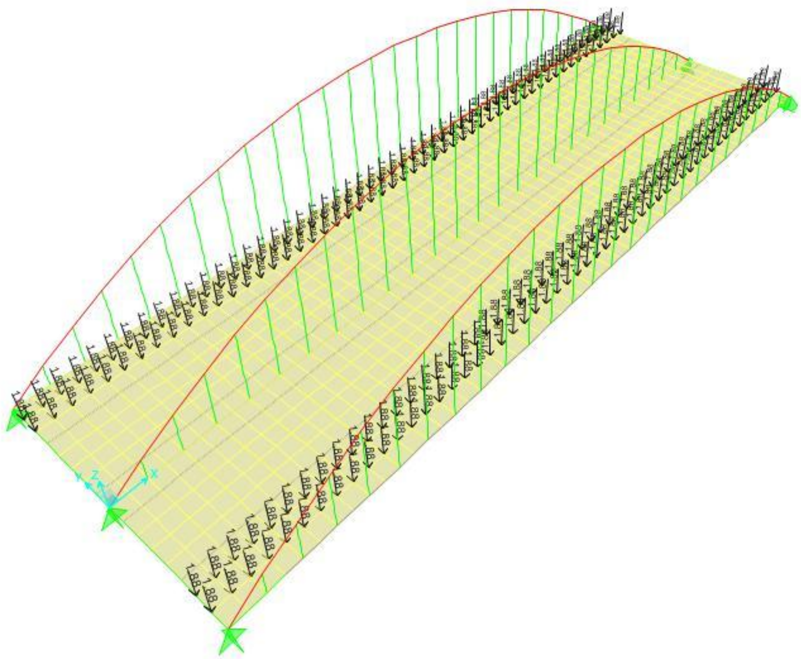

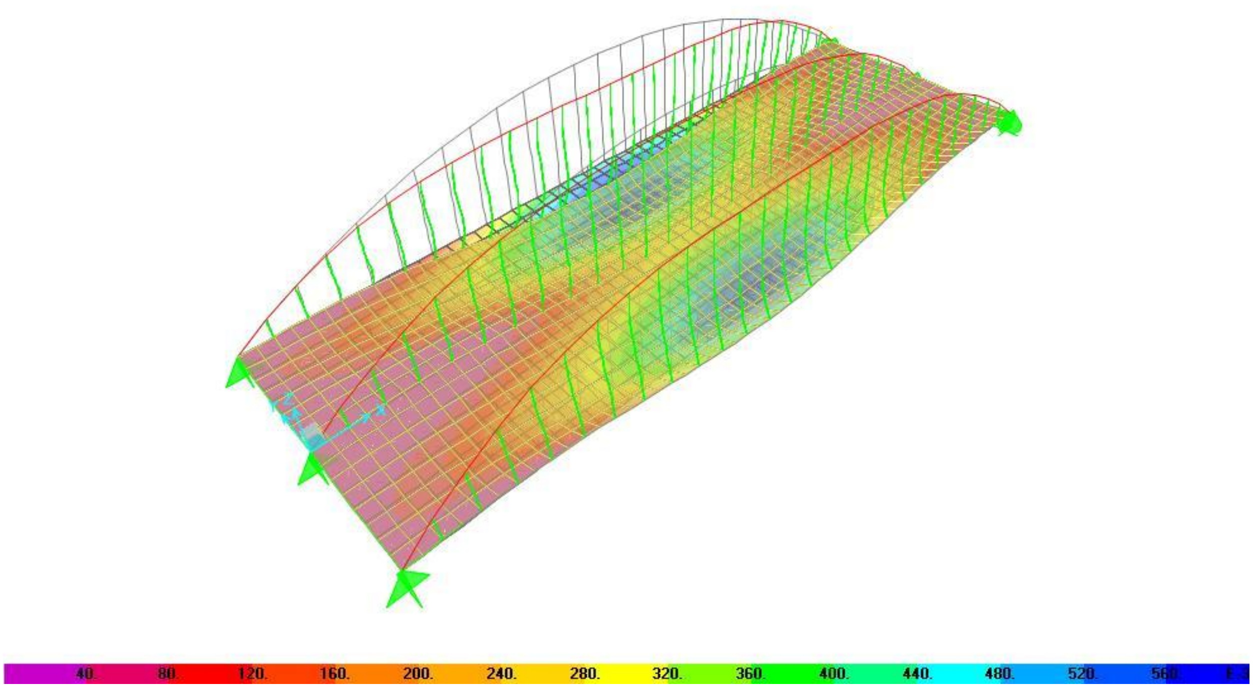

- Median Arch

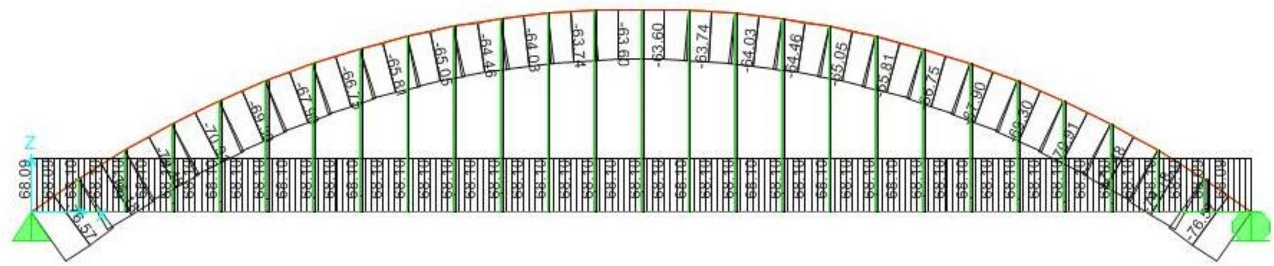

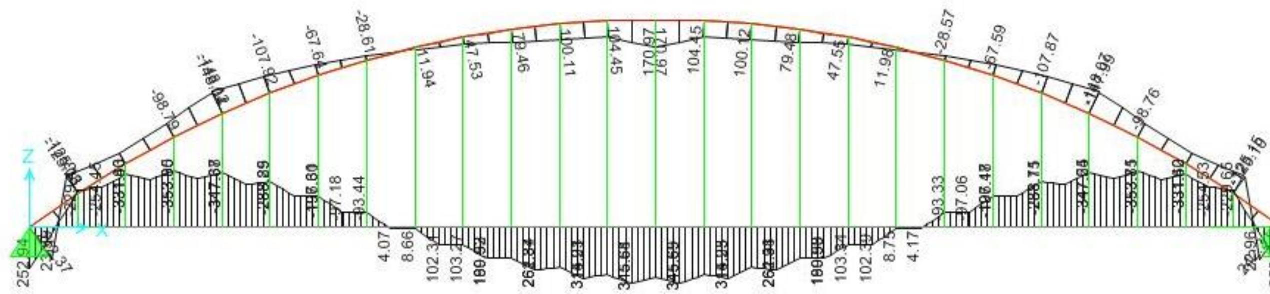

- Outside Arch

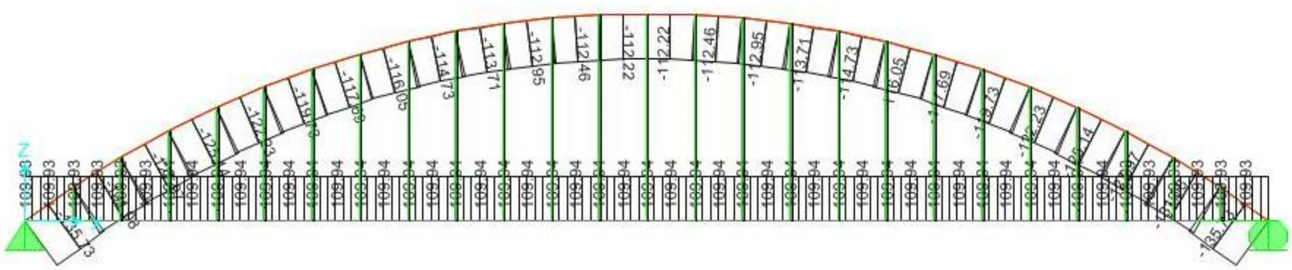

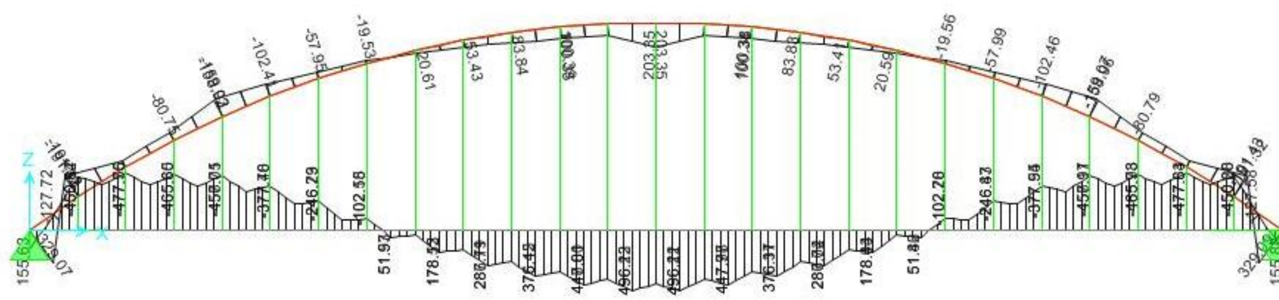

Stage IV: Service I Combination

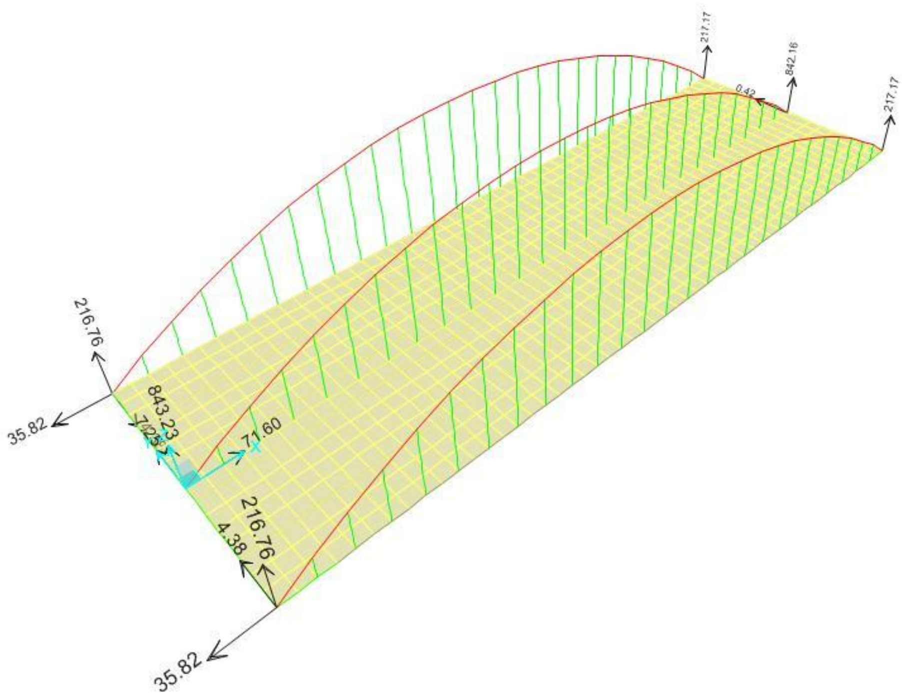

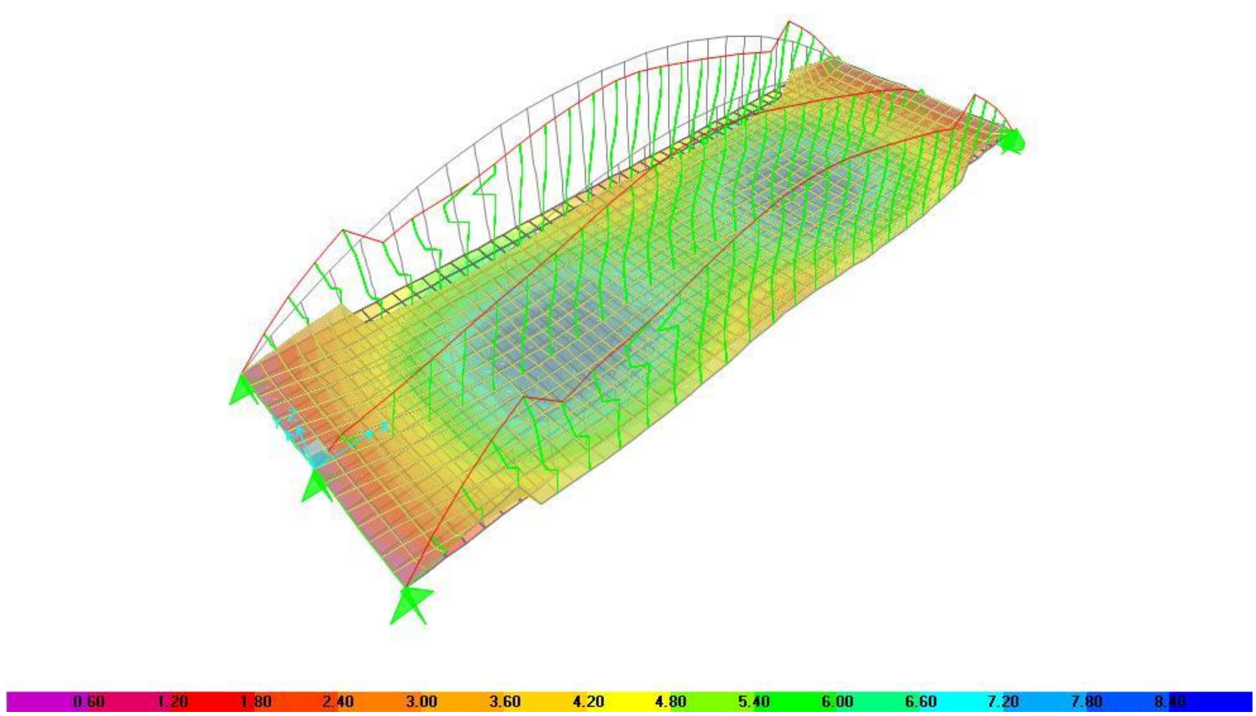

- Median Arch

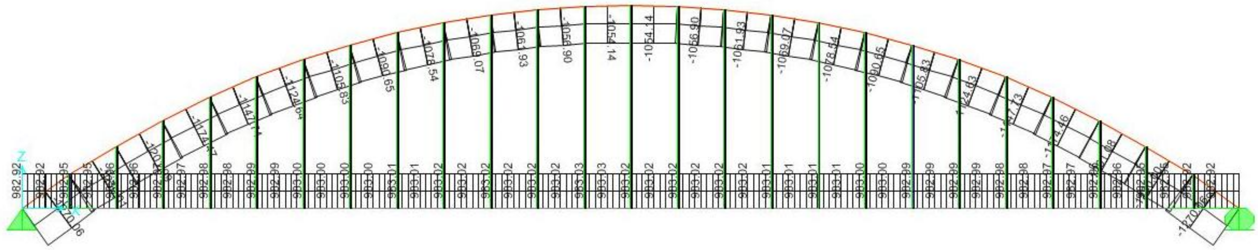

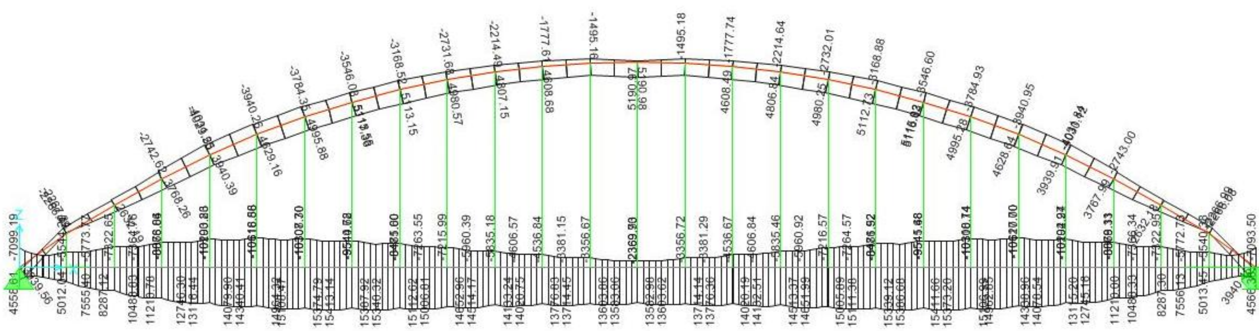

- Outside Arch

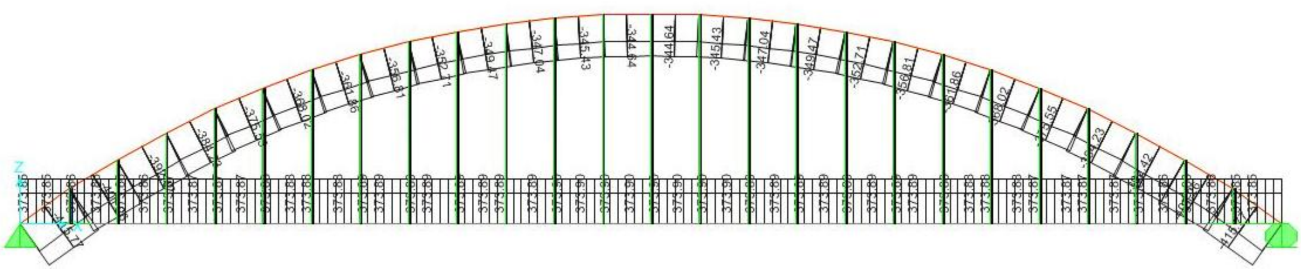

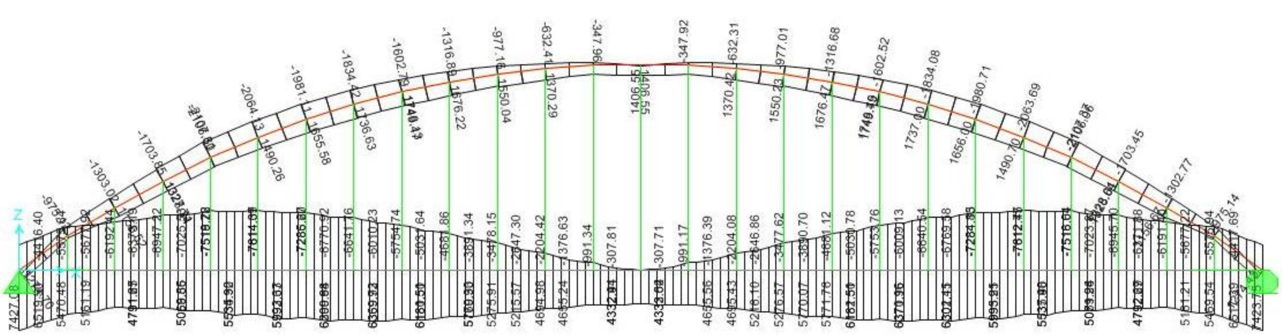

<u>Stage IV: Strength I Combination</u>

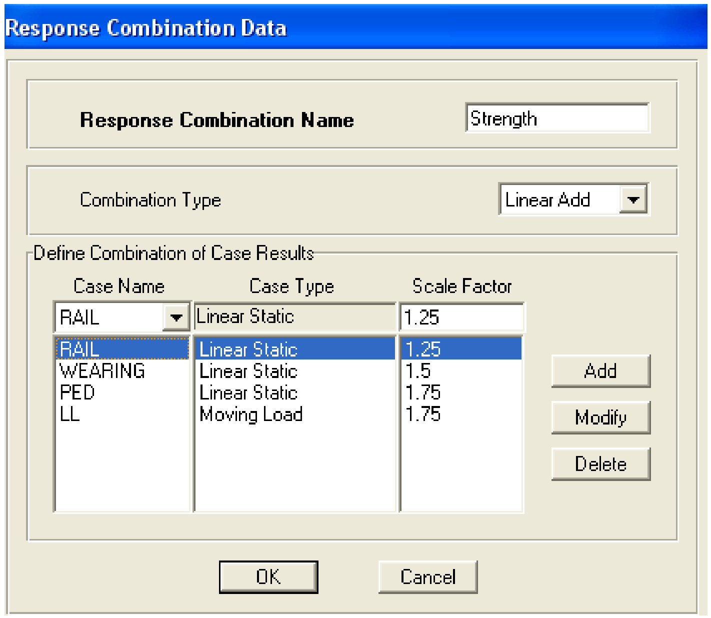

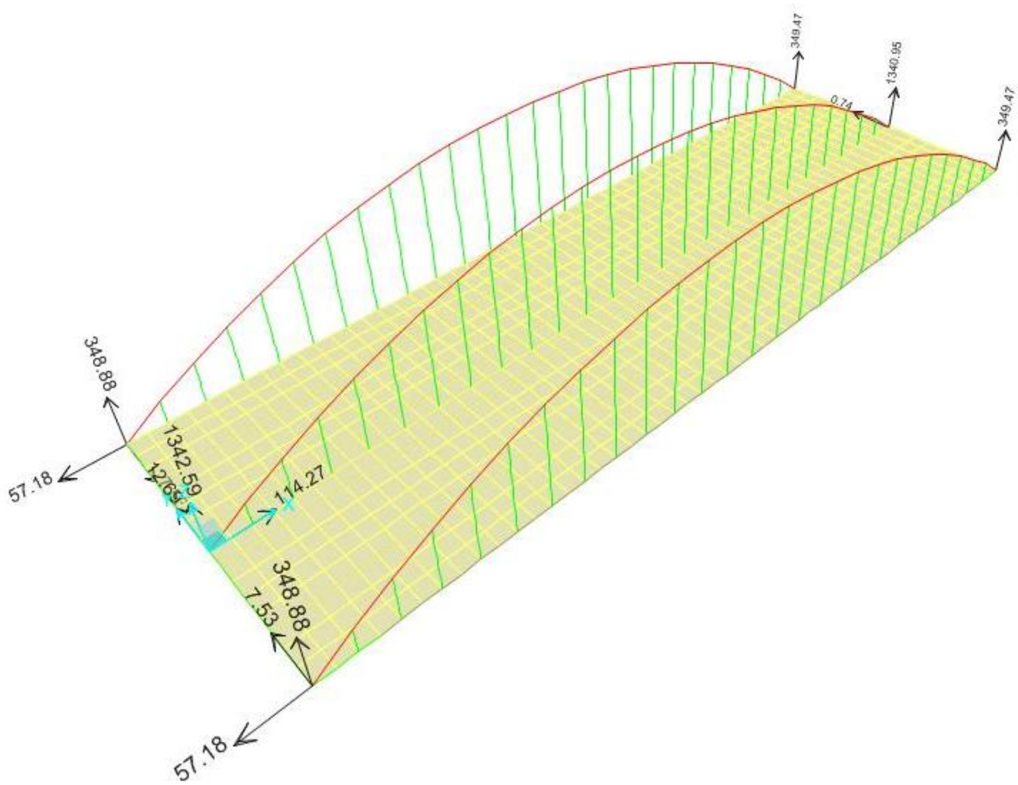

- Median Arch

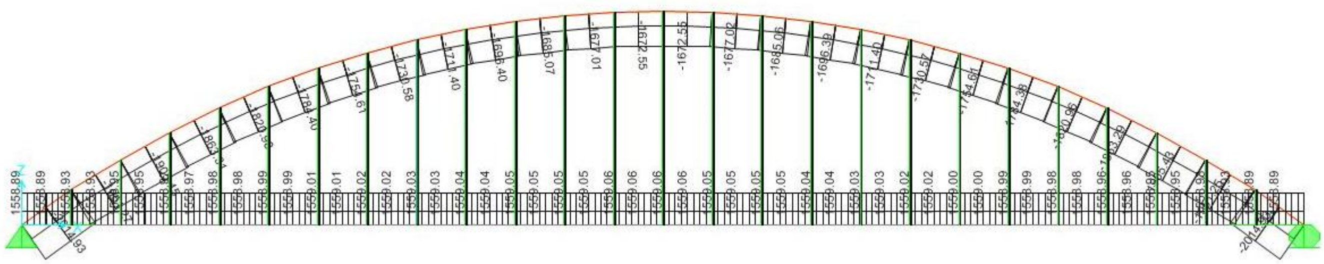

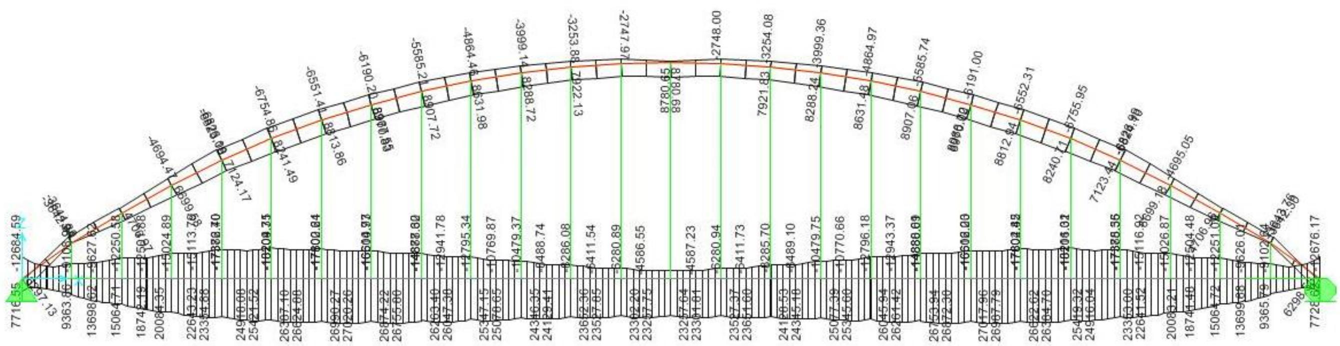

- Outside Arch

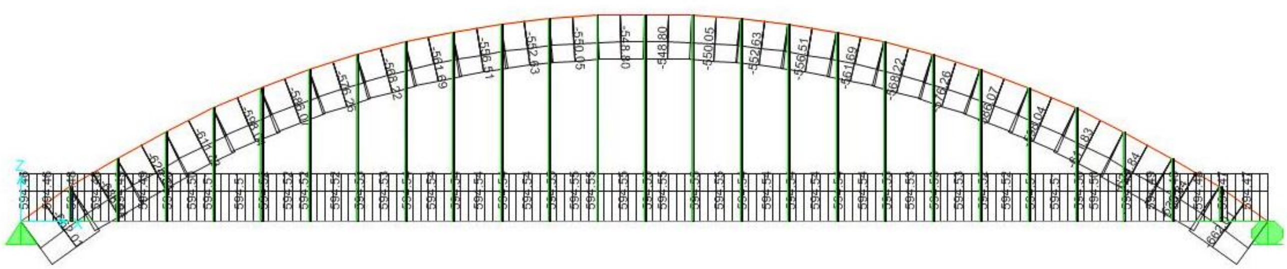

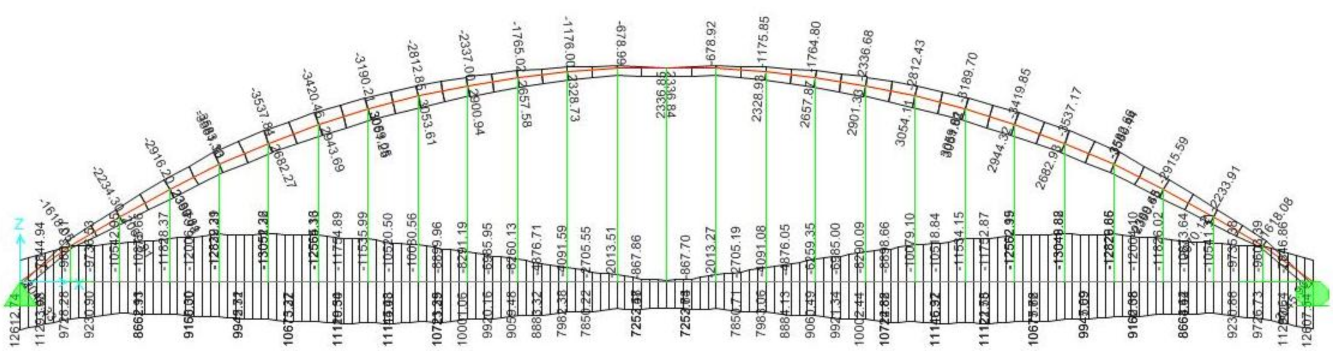

Stage IV: Fatigue Load

- Median Arch

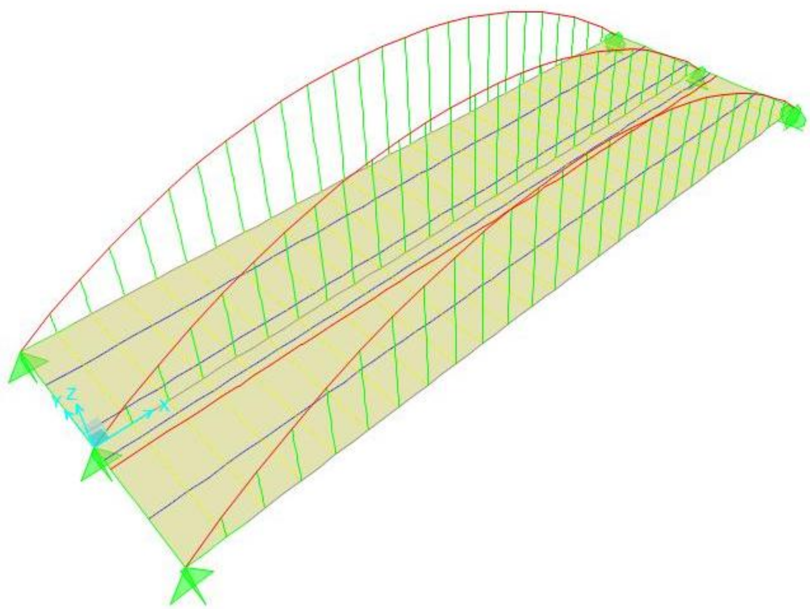

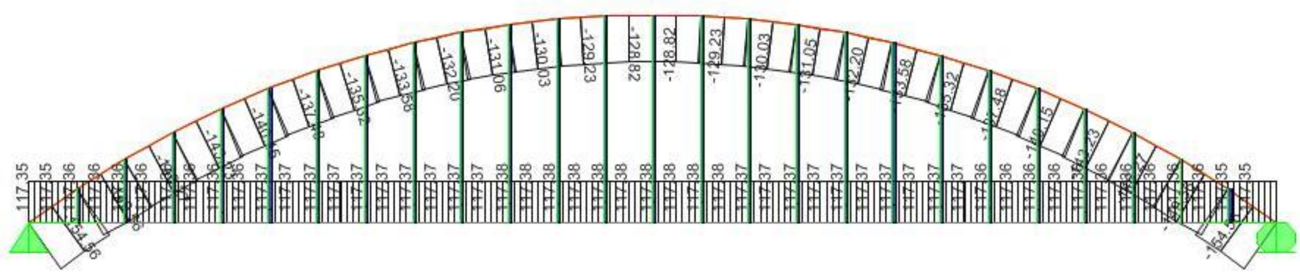

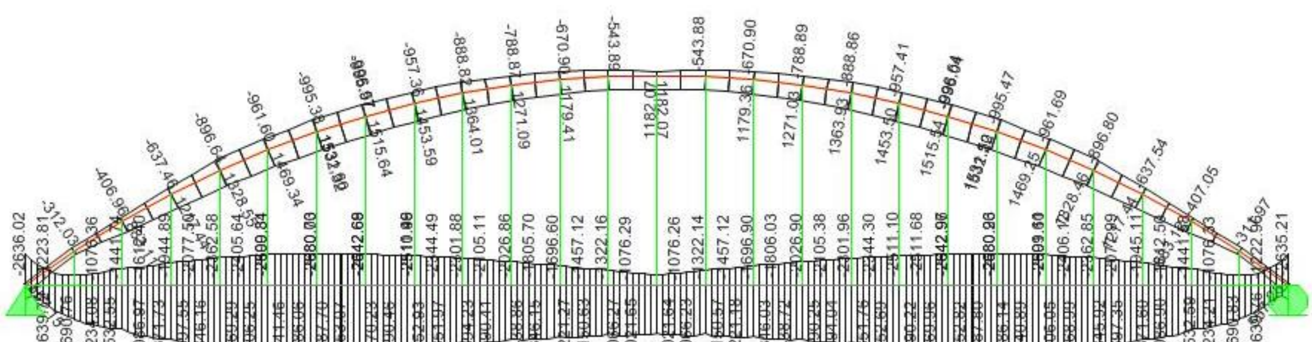

- Outside Arch

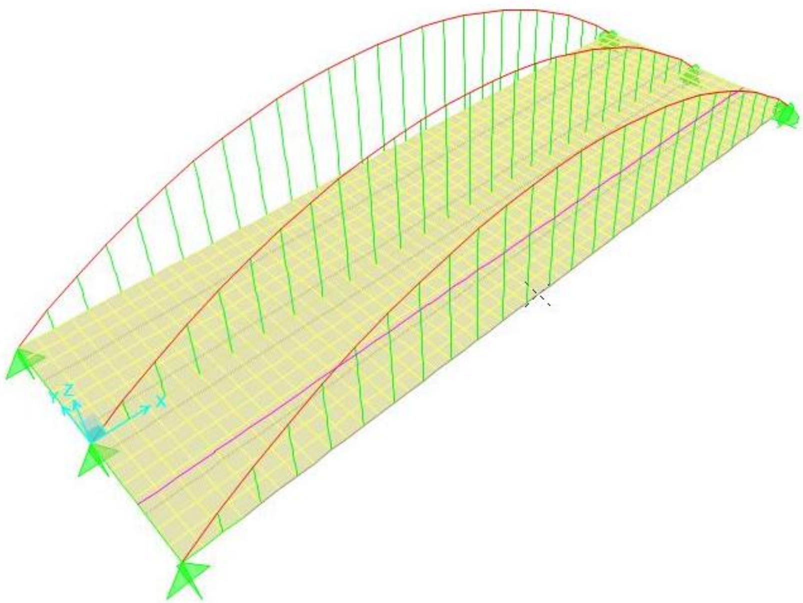

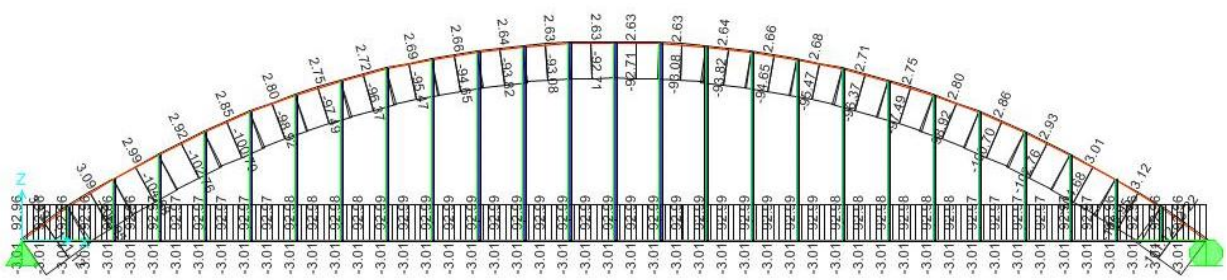

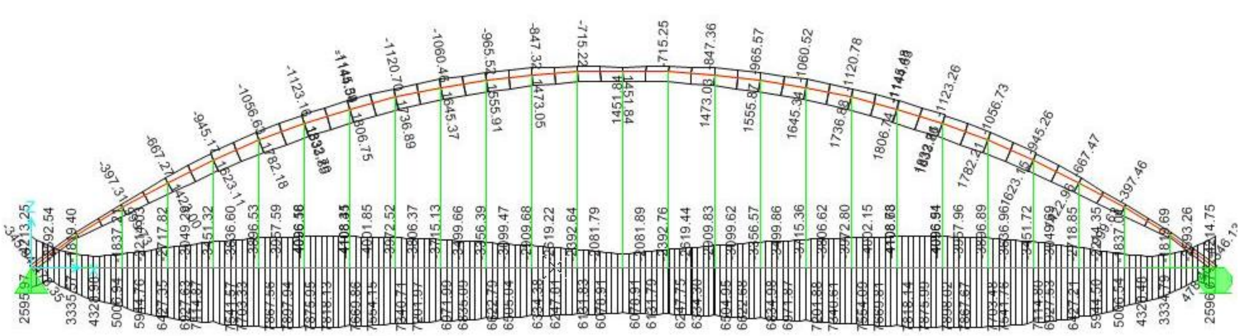

APPENDIX C: SERVICE CHECKS

Job Name:	Columbus Viaduct	Subject:	Median Arch (Sec. 4)		
Job Number:		Originator:		Checker:	

Input Data:

Member Size:
Select:

Member Loadings:

P =	263.50	kips
Mx(max) =	80.80	ft-kips
Mx1 =	0.00	ft-kips
Mx2 =	0.00	ft-kips
My(max) =	0.00	ft-kips
My1 =	0.00	ft-kips
My2 =	0.00	ft-kips

Member Properties:

OD =	18.000	in.
ID =	16.124	in.
A =	50.28	in.^2
t =	0.938	in.
Ix = Iy =	1835.10	in.^4
Sx = Sy =	203.90	in.^3
rx = ry =	6.040	in.
wt./ft. =	171.10	plf.

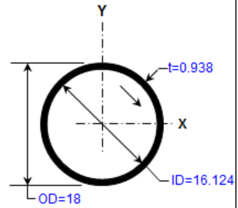

Section ϕ18-0.938"

Design Parameters:

Fy =	46.00	ksi
Kx =	1.00	
Ky =	1.00	
Lx =	10.000	ft.
Ly =	10.000	ft.
Lbx =	10.000	ft.
Lby =	10.000	ft.
Cmx =	0.85	
Cmy =	0.85	
ASIF =	1.000	

Results:

For Axial Compression:

Kx*Lx/rx =	19.87	
Ky*Ly/ry =	19.87	
Cc =	111.55	
fa =	5.24	ksi
Fa =	26.13	ksi
Pa =	1313.64	kips

For X-axis Bending:

Lcx =	63.59	ft.
fbx =	4.76	ksi
Fbx =	30.36	ksi
Mrx =	515.87	ft-kips

For Y-axis Bending:

Lcy =	63.59	ft.
fby =	0.00	ksi
Fby =	30.36	ksi
Mry =	515.87	ft-kips

X-axis Euler Stress:
F'ex = 378.32 ksi

Y-axis Euler Stress:
F'ey = 378.32 ksi

Stress Ratio:
S.R. = **0.347** Eqn. H1-2

Job Name:	Columbus Viaduct	Subject:	Oustide Arch (Sec. 4)		
Job Number:		Originator:		Checker:	

Input Data:

Member Size:
Select:

Member Loadings:

P =	211.00	kips
Mx(max) =	45.80	ft-kips
Mx1 =	0.00	ft-kips
Mx2 =	0.00	ft-kips
My(max) =	0.00	ft-kips
My1 =	0.00	ft-kips
My2 =	0.00	ft-kips

Member Properties:

OD =	18.000	in.
ID =	17.000	in.
A =	27.49	in.^2
t =	0.500	in.
Ix = Iy =	1053.00	in.^4
Sx = Sy =	117.00	in.^3
rx = ry =	6.190	in.
wt./ft. =	93.54	plf.

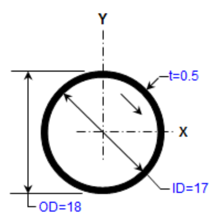

Section ϕ18-1/2"

Design Parameters:

Fy =	46.00	ksi
Kx =	1.00	
Ky =	1.00	
Lx =	10.000	ft.
Ly =	10.000	ft.
Lbx =	10.000	ft.
Lby =	10.000	ft.
Cmx =	0.85	
Cmy =	0.85	
ASIF =	1.000	

Results:

For Axial Compression:

Kx*Lx/rx =	19.39	
Ky*Ly/ry =	19.39	
Cc =	111.55	
fa =	7.68	ksi
Fa =	26.17	ksi
Pa =	719.42	kips

For X-axis Bending:

Lcx =	63.59	ft.
fbx =	4.70	ksi
Fbx =	30.36	ksi
Mrx =	296.01	ft-kips

For Y-axis Bending:

Lcy =	63.59	ft.
fby =	0.00	ksi
Fby =	30.36	ksi
Mry =	296.01	ft-kips

X-axis Euler Stress:
F'ex = 397.35 ksi

Y-axis Euler Stress:
F'ey = 397.35 ksi

Stress Ratio:
S.R. = **0.433** Eqn. H1-2

Stress calculations at section 4 in median and outside arches

Job Name:	Columbus Viaduct	Subject:	Median Arch (Sec. 5)
Job Number:		Originator:	Checker:

Input Data:

Member Size:

Select:

Member Loadings:

P =	292.50	kips
Mx(max) =	72.00	ft-kips
Mx1 =	0.00	ft-kips
Mx2 =	0.00	ft-kips
My(max) =	0.00	ft-kips
My1 =	0.00	ft-kips
My2 =	0.00	ft-kips

Member Properties:

OD =	18.000	in.
ID =	16.124	in.
A =	50.28	in.^2
t =	0.938	in.
Ix = Iy =	1835.10	in.^4
Sx = Sy =	203.90	in.^3
rx = ry =	6.040	in.
wt./ft. =	171.10	plf.

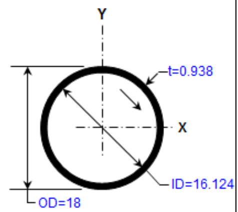

Section ϕ18-0.938"

Design Parameters:

Fy =	46.00	ksi
Kx =	1.00	
Ky =	1.00	
Lx =	10.000	ft.
Ly =	10.000	ft.
Lbx =	10.000	ft.
Lby =	10.000	ft.
Cmx =	0.85	
Cmy =	0.85	
ASIF =	1.000	

Results:

For Axial Compression:

Kx*Lx/rx =	19.87	
Ky*Ly/ry =	19.87	
Cc =	111.55	
fa =	5.82	ksi
Fa =	26.13	ksi
Pa =	1313.64	kips

For X-axis Bending:

Lcx =	63.59	ft.
fbx =	4.24	ksi
Fbx =	30.36	ksi
Mrx =	515.87	ft-kips

For Y-axis Bending:

Lcy =	63.59	ft.
fby =	0.00	ksi
Fby =	30.36	ksi
Mry =	515.87	ft-kips

X-axis Euler Stress:

F'ex = 378.32 ksi

Y-axis Euler Stress:

F'ey = 378.32 ksi

Stress Ratio:

S.R. = **0.350** Eqn. H1-2

Job Name:	Columbus Viaduct	Subject:	Oustide Arch (Sec.5)
Job Number:		Originator:	Checker:

Input Data:

Member Size:

Select:

Member Loadings:

P =	234.50	kips
Mx(max) =	40.75	ft-kips
Mx1 =	0.00	ft-kips
Mx2 =	0.00	ft-kips
My(max) =	0.00	ft-kips
My1 =	0.00	ft-kips
My2 =	0.00	ft-kips

Member Properties:

OD =	18.000	in.
ID =	17.000	in.
A =	27.49	in.^2
t =	0.500	in.
Ix = Iy =	1053.00	in.^4
Sx = Sy =	117.00	in.^3
rx = ry =	6.190	in.
wt./ft. =	93.54	plf.

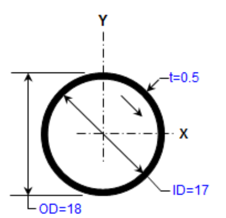

Section ϕ18-1/2"

Design Parameters:

Fy =	46.00	ksi
Kx =	1.00	
Ky =	1.00	
Lx =	10.000	ft.
Ly =	10.000	ft.
Lbx =	10.000	ft.
Lby =	10.000	ft.
Cmx =	0.85	
Cmy =	0.85	
ASIF =	1.000	

Results:

For Axial Compression:

Kx*Lx/rx =	19.39	
Ky*Ly/ry =	19.39	
Cc =	111.55	
fa =	8.53	ksi
Fa =	26.17	ksi
Pa =	719.42	kips

For X-axis Bending:

Lcx =	63.59	ft.
fbx =	4.18	ksi
Fbx =	30.36	ksi
Mrx =	296.01	ft-kips

For Y-axis Bending:

Lcy =	63.59	ft.
fby =	0.00	ksi
Fby =	30.36	ksi
Mry =	296.01	ft-kips

X-axis Euler Stress:

F'ex = 397.35 ksi

Y-axis Euler Stress:

F'ey = 397.35 ksi

Stress Ratio:

S.R. = **0.447** Eqn. H1-2

Stress calculations at section 5 in median and outside arches

Job Name:	Columbus Viaduct	Subject:	Median Arch (Sec. 6)
Job Number:		Originator:	Checker:

Input Data:

Member Size:
Select:

Member Loadings:

P =	317.00	kips
Mx(max) =	56.40	ft-kips
Mx1 =	0.00	ft-kips
Mx2 =	0.00	ft-kips
My(max) =	0.00	ft-kips
My1 =	0.00	ft-kips
My2 =	0.00	ft-kips

Member Properties:

OD =	18.000	in.
ID =	16.124	in.
A =	50.28	in.^2
t =	0.938	in.
Ix = Iy =	1835.10	in.^4
Sx = Sy =	203.90	in.^3
rx = ry =	6.040	in.
wt./ft. =	171.10	plf.

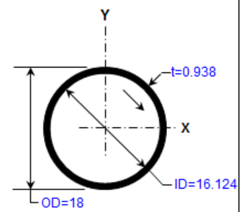

Section ϕ18-0.938"

Design Parameters:

Fy =	46.00	ksi
Kx =	1.00	
Ky =	1.00	
Lx =	10.000	ft.
Ly =	10.000	ft.
Lbx =	10.000	ft.
Lby =	10.000	ft.
Cmx =	0.85	
Cmy =	0.85	
ASIF =	1.000	

Results:

For Axial Compression:

Kx*Lx/rx =	19.87	
Ky*Ly/ry =	19.87	
Cc =	111.55	
fa =	6.30	ksi
Fa =	26.13	ksi
Pa =	1313.64	kips

For X-axis Bending:

Lcx =	63.59	ft.
fbx =	3.32	ksi
Fbx =	30.36	ksi
Mrx =	515.87	ft-kips

For Y-axis Bending:

Lcy =	63.59	ft.
fby =	0.00	ksi
Fby =	30.36	ksi
Mry =	515.87	ft-kips

X-axis Euler Stress:
F'ex = 378.32 ksi

Y-axis Euler Stress:
F'ey = 378.32 ksi

Stress Ratio:
S.R. = **0.338** Eqn. H1-2

Job Name:	Columbus Viaduct	Subject:	Oustide Arch (Sec. 6)
Job Number:		Originator:	Checker:

Input Data:

Member Size:
Select:

Member Loadings:

P =	255.00	kips
Mx(max) =	33.50	ft-kips
Mx1 =	0.00	ft-kips
Mx2 =	0.00	ft-kips
My(max) =	0.00	ft-kips
My1 =	0.00	ft-kips
My2 =	0.00	ft-kips

Member Properties:

OD =	18.000	in.
ID =	17.000	in.
A =	27.49	in.^2
t =	0.500	in.
Ix = Iy =	1053.00	in.^4
Sx = Sy =	117.00	in.^3
rx = ry =	6.190	in.
wt./ft. =	93.54	plf.

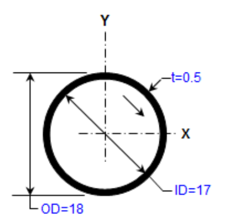

Section ϕ18-1/2"

Design Parameters:

Fy =	46.00	ksi
Kx =	1.00	
Ky =	1.00	
Lx =	10.000	ft.
Ly =	10.000	ft.
Lbx =	10.000	ft.
Lby =	10.000	ft.
Cmx =	0.85	
Cmy =	0.85	
ASIF =	1.000	

Results:

For Axial Compression:

Kx*Lx/rx =	19.39	
Ky*Ly/ry =	19.39	
Cc =	111.55	
fa =	9.28	ksi
Fa =	26.17	ksi
Pa =	719.42	kips

For X-axis Bending:

Lcx =	63.59	ft.
fbx =	3.44	ksi
Fbx =	30.36	ksi
Mrx =	296.01	ft-kips

For Y-axis Bending:

Lcy =	63.59	ft.
fby =	0.00	ksi
Fby =	30.36	ksi
Mry =	296.01	ft-kips

X-axis Euler Stress:
F'ex = 397.35 ksi

Y-axis Euler Stress:
F'ey = 397.35 ksi

Stress Ratio:
S.R. = **0.453** Eqn. H1-1

Stress calculations at section 6 in median and outside arches

Job Name:	Columbus Viaduct	Subject:	Median Tie (Sec. 1)		
Job Number:		Originator:		Checker:	

Input Data:

Member Size:

Select:

Member Loadings:

P =	-527.00	kips
Mx(max) =	224.60	ft-kips
Mx1 =	0.00	ft-kips
Mx2 =	0.00	ft-kips
My(max) =	0.00	ft-kips
My1 =	0.00	ft-kips
My2 =	0.00	ft-kips

Member Properties:

H =	24.000	in.
B =	36.000	in.
t =	0.500	in.
A =	59.00	in.^2
Ix =	5985.00	in.^4
Sx =	498.70	in.^3
rx =	10.100	in.
Iy =	11135.00	in.^4
Sy =	618.60	in.^3
ry =	13.700	in.
wt./ft. =	200.76	plf.

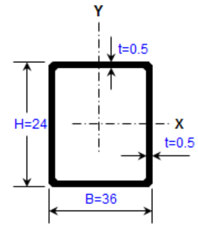

Section 24x36x1/2

Design Parameters:

Fy =	46.00	ksi
Kx =	1.00	
Ky =	1.00	
Lx =	10.000	ft.
Ly =	10.000	ft.
Lbx =	10.000	ft.
Lby =	10.000	ft.
Cmx =	0.85	
Cmy =	0.85	
ASIF =	1.000	

Results:

For Axial Tension:

Kx*Lx/rx =	N.A.	
Ky*Ly/ry =	N.A.	
Cc =	N.A.	
ft =	8.93	ksi
Ft =	27.60	ksi
Pa =	-1628.40	kips

For X-axis Bending:

Lcx =	127.17	ft.
fbx =	5.40	ksi
Fbx =	27.60	ksi
Mrx =	1147.01	ft-kips

For Y-axis Bending:

Lcy =	84.78	ft.
fby =	0.00	ksi
Fby =	27.60	ksi
Mry =	1422.78	ft-kips

X-axis Euler Stress:

F'ex = N.A. ksi

Y-axis Euler Stress:

F'ey = N.A. ksi

Stress Ratio:

S.R. = **0.519** Eqn. H2-1

Job Name:	Columbus Viaduct	Subject:	Outside Tie (Sec. 1)		
Job Number:		Originator:		Checker:	

Input Data:

Member Size:

Select:

Member Loadings:

P =	-422.00	kips
Mx(max) =	215.30	ft-kips
Mx1 =	0.00	ft-kips
Mx2 =	0.00	ft-kips
My(max) =	0.00	ft-kips
My1 =	0.00	ft-kips
My2 =	0.00	ft-kips

Member Properties:

H =	24.000	in.
B =	36.000	in.
t =	0.500	in.
A =	59.00	in.^2
Ix =	5985.00	in.^4
Sx =	498.70	in.^3
rx =	10.100	in.
Iy =	11135.00	in.^4
Sy =	618.60	in.^3
ry =	13.700	in.
wt./ft. =	200.76	plf.

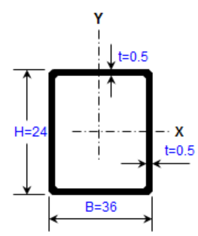

Section 24x36x1/2

Design Parameters:

Fy =	46.00	ksi
Kx =	1.00	
Ky =	1.00	
Lx =	10.000	ft.
Ly =	10.000	ft.
Lbx =	10.000	ft.
Lby =	10.000	ft.
Cmx =	0.85	
Cmy =	0.85	
ASIF =	1.000	

Results:

For Axial Tension:

Kx*Lx/rx =	N.A.	
Ky*Ly/ry =	N.A.	
Cc =	N.A.	
ft =	7.15	ksi
Ft =	27.60	ksi
Pa =	-1628.40	kips

For X-axis Bending:

Lcx =	127.17	ft.
fbx =	5.18	ksi
Fbx =	27.60	ksi
Mrx =	1147.01	ft-kips

For Y-axis Bending:

Lcy =	84.78	ft.
fby =	0.00	ksi
Fby =	27.60	ksi
Mry =	1422.78	ft-kips

X-axis Euler Stress:

F'ex = N.A. ksi

Y-axis Euler Stress:

F'ey = N.A. ksi

Stress Ratio:

S.R. = **0.447** Eqn. H2-1

Stress calculations at section 4 in median and outside ties

Job Name:	Columbus Viaduct	Subject:	Median Tie (Sec. 2)
Job Number:		Originator:	Checker:

Input Data:

Member Size:

Select:

Member Loadings:

P =	-527.00	kips
Mx(max) =	220.30	ft-kips
Mx1 =	0.00	ft-kips
Mx2 =	0.00	ft-kips
My(max) =	0.00	ft-kips
My1 =	0.00	ft-kips
My2 =	0.00	ft-kips

Member Properties:

H =	24.000	in.
B =	36.000	in.
t =	0.500	in.
A =	59.00	in.^2
Ix =	5985.00	in.^4
Sx =	498.70	in.^3
rx =	10.100	in.
Iy =	11135.00	in.^4
Sy =	618.60	in.^3
ry =	13.700	in.
wt./ft. =	200.76	plf.

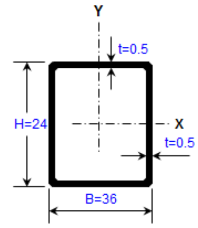

Section 24x36x1/2

Design Parameters:

Fy =	46.00	ksi
Kx =	1.00	
Ky =	1.00	
Lx =	10.000	ft.
Ly =	10.000	ft.
Lbx =	10.000	ft.
Lby =	10.000	ft.
Cmx =	0.85	
Cmy =	0.85	
ASIF =	1.000	

Results:

For Axial Tension:

Kx*Lx/rx =	N.A.	
Ky*Ly/ry =	N.A.	
Cc =	N.A.	
ft =	8.93	ksi
Ft =	27.60	ksi
Pa =	-1628.40	kips

For X-axis Bending:

Lcx =	127.17	ft.
fbx =	5.30	ksi
Fbx =	27.60	ksi
Mrx =	1147.01	ft-kips

For Y-axis Bending:

Lcy =	84.78	ft.
fby =	0.00	ksi
Fby =	27.60	ksi
Mry =	1422.78	ft-kips

X-axis Euler Stress:

F'ex = N.A. ksi

Y-axis Euler Stress:

F'ey = N.A. ksi

Stress Ratio:

S.R. = **0.516** Eqn. H2-1

Job Name:	Columbus Viaduct	Subject:	Outside Tie (Sec. 2)
Job Number:		Originator:	Checker:

Input Data:

Member Size:

Select:

Member Loadings:

P =	-422.00	kips
Mx(max) =	205.40	ft-kips
Mx1 =	0.00	ft-kips
Mx2 =	0.00	ft-kips
My(max) =	0.00	ft-kips
My1 =	0.00	ft-kips
My2 =	0.00	ft-kips

Member Properties:

H =	24.000	in.
B =	36.000	in.
t =	0.500	in.
A =	59.00	in.^2
Ix =	5985.00	in.^4
Sx =	498.70	in.^3
rx =	10.100	in.
Iy =	11135.00	in.^4
Sy =	618.60	in.^3
ry =	13.700	in.
wt./ft. =	200.76	plf.

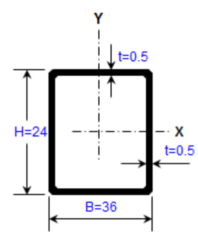

Section 24x36x1/2

Design Parameters:

Fy =	46.00	ksi
Kx =	1.00	
Ky =	1.00	
Lx =	10.000	ft.
Ly =	10.000	ft.
Lbx =	10.000	ft.
Lby =	10.000	ft.
Cmx =	0.85	
Cmy =	0.85	
ASIF =	1.000	

Results:

For Axial Tension:

Kx*Lx/rx =	N.A.	
Ky*Ly/ry =	N.A.	
Cc =	N.A.	
ft =	7.15	ksi
Ft =	27.60	ksi
Pa =	-1628.40	kips

For X-axis Bending:

Lcx =	127.17	ft.
fbx =	4.94	ksi
Fbx =	27.60	ksi
Mrx =	1147.01	ft-kips

For Y-axis Bending:

Lcy =	84.78	ft.
fby =	0.00	ksi
Fby =	27.60	ksi
Mry =	1422.78	ft-kips

X-axis Euler Stress:

F'ex = N.A. ksi

Y-axis Euler Stress:

F'ey = N.A. ksi

Stress Ratio:

S.R. = **0.438** Eqn. H2-1

Stress calculations at section 5 in median and outside ties

Job Name:	Columbus Viaduct	Subject:	Median Tie (Sec. 3)
Job Number:		Originator:	Checker:

Input Data:

Member Size:

Select:

Member Loadings:

P =	-527.00	kips
Mx(max) =	202.20	ft-kips
Mx1 =	0.00	ft-kips
Mx2 =	0.00	ft-kips
My(max) =	0.00	ft-kips
My1 =	0.00	ft-kips
My2 =	0.00	ft-kips

Member Properties:

H =	36.000	in.
B =	36.000	in.
t =	0.500	in.
A =	71.00	in.^2
Ix =	14916.00	in.^4
Sx =	828.70	in.^3
rx =	14.500	in.
Iy =	14916.00	in.^4
Sy =	828.70	in.^3
ry =	14.500	in.
wt./ft. =	241.60	plf.

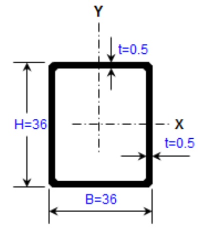

Section 36x36x1/2

Design Parameters:

Fy =	46.00	ksi
Kx =	1.00	
Ky =	1.00	
Lx =	10.000	ft.
Ly =	10.000	ft.
Lbx =	10.000	ft.
Lby =	10.000	ft.
Cmx =	0.85	
Cmy =	0.85	
ASIF =	1.000	

Results:

For Axial Tension:

Kx*Lx/rx =	N.A.	
Ky*Ly/ry =	N.A.	
Cc =	N.A.	
ft =	7.42	ksi
Ft =	27.60	ksi
Pa =	-1959.60	kips

For X-axis Bending:

Lcx =	127.17	ft.
fbx =	2.93	ksi
Fbx =	27.60	ksi
Mrx =	1906.01	ft-kips

For Y-axis Bending:

Lcy =	127.17	ft.
fby =	0.00	ksi
Fby =	27.60	ksi
Mry =	1906.01	ft-kips

X-axis Euler Stress:

F'ex = N.A. ksi

Y-axis Euler Stress:

F'ey = N.A. ksi

Stress Ratio:

S.R. = **0.375** Eqn. H2-1

Job Name:	Columbus Viaduct	Subject:	Outside Tie (Sec. 3)
Job Number:		Originator:	Checker:

Input Data:

Member Size:

Select:

Member Loadings:

P =	-422.00	kips
Mx(max) =	177.30	ft-kips
Mx1 =	0.00	ft-kips
Mx2 =	0.00	ft-kips
My(max) =	0.00	ft-kips
My1 =	0.00	ft-kips
My2 =	0.00	ft-kips

Member Properties:

H =	36.000	in.
B =	36.000	in.
t =	0.500	in.
A =	71.00	in.^2
Ix =	14916.00	in.^4
Sx =	828.70	in.^3
rx =	14.500	in.
Iy =	14916.00	in.^4
Sy =	828.70	in.^3
ry =	14.500	in.
wt./ft. =	241.60	plf.

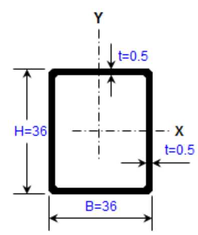

Section 36x36x1/2

Design Parameters:

Fy =	46.00	ksi
Kx =	1.00	
Ky =	1.00	
Lx =	10.000	ft.
Ly =	10.000	ft.
Lbx =	10.000	ft.
Lby =	10.000	ft.
Cmx =	0.85	
Cmy =	0.85	
ASIF =	1.000	

Results:

For Axial Tension:

Kx*Lx/rx =	N.A.	
Ky*Ly/ry =	N.A.	
Cc =	N.A.	
ft =	5.94	ksi
Ft =	27.60	ksi
Pa =	-1959.60	kips

For X-axis Bending:

Lcx =	127.17	ft.
fbx =	2.57	ksi
Fbx =	27.60	ksi
Mrx =	1906.01	ft-kips

For Y-axis Bending:

Lcy =	127.17	ft.
fby =	0.00	ksi
Fby =	27.60	ksi
Mry =	1906.01	ft-kips

X-axis Euler Stress:

F'ex = N.A. ksi

Y-axis Euler Stress:

F'ey = N.A. ksi

Stress Ratio:

S.R. = **0.308** Eqn. H2-1

Stress calculations at section 6 in median and outside ties

APPENDIX D: INTERACTION DIAGRAMS

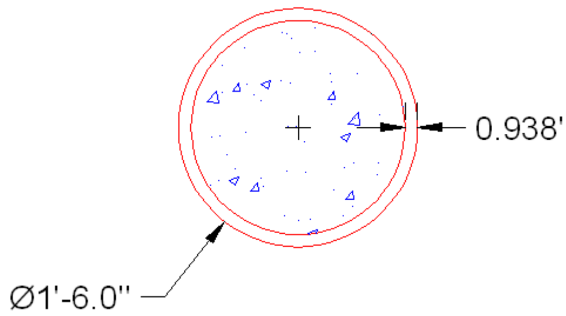

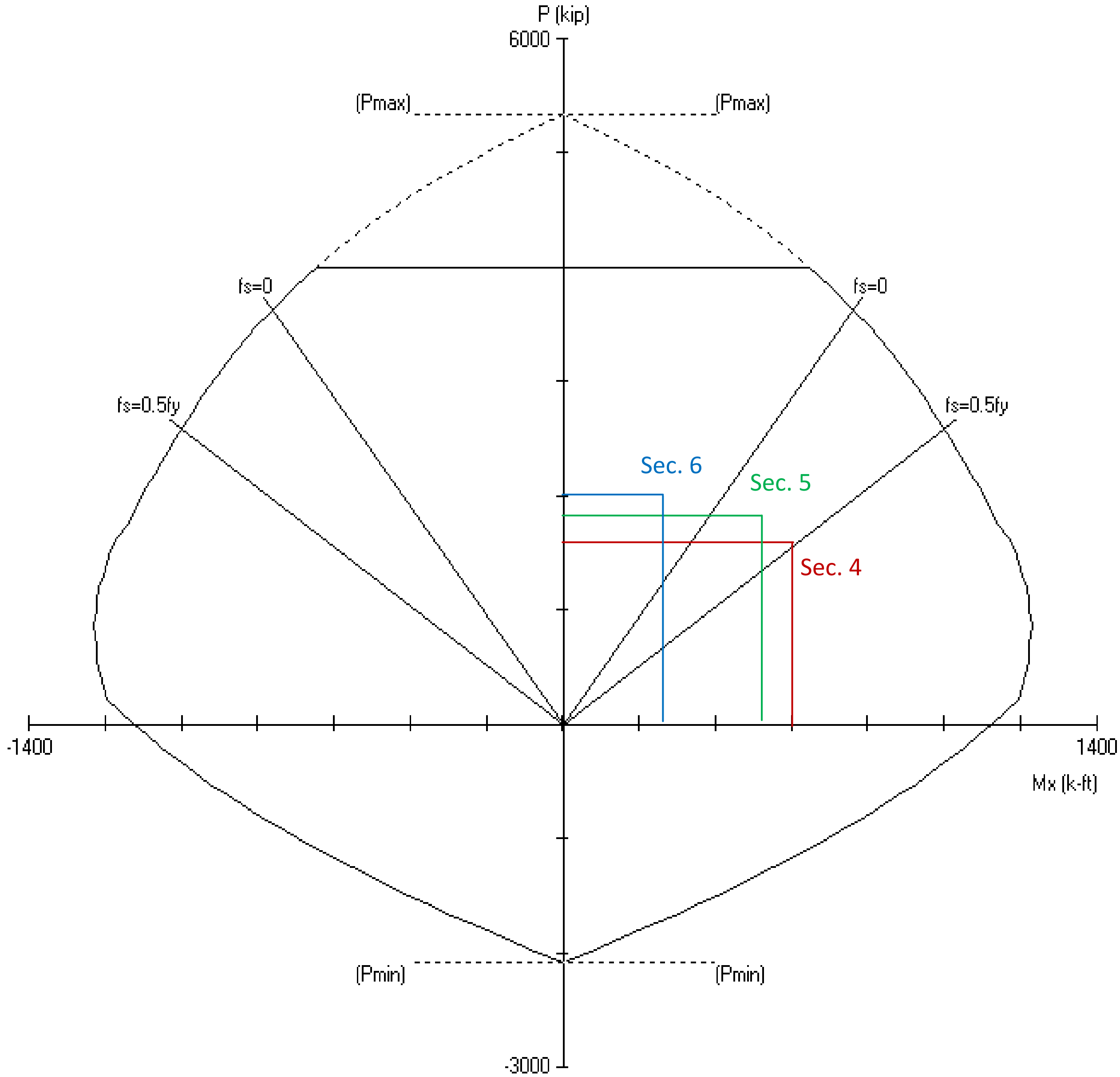

Interaction diagram for median arch

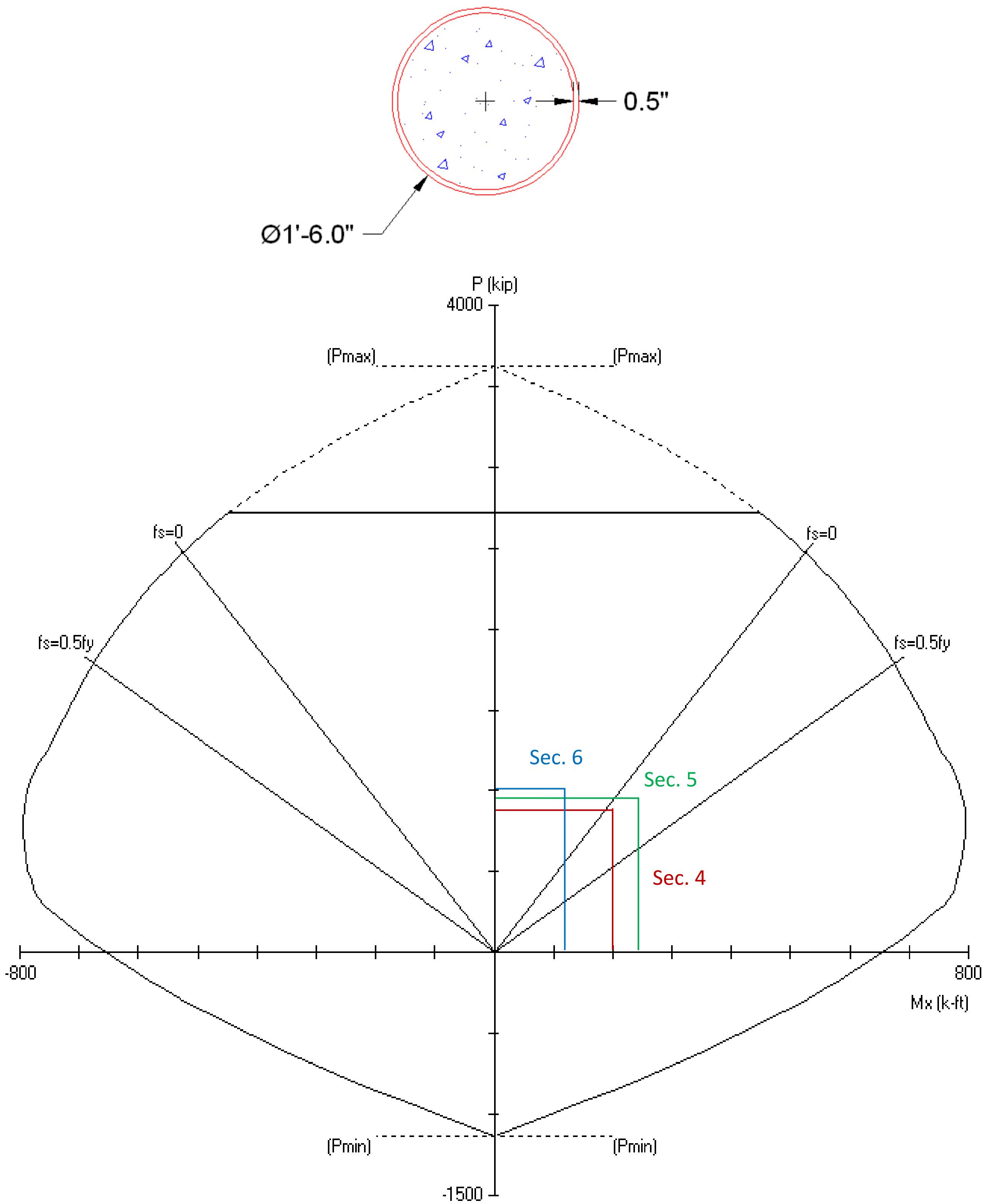

Interaction diagram for outside arch

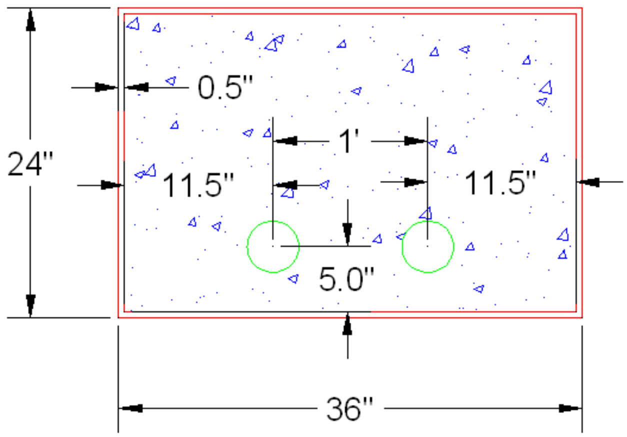

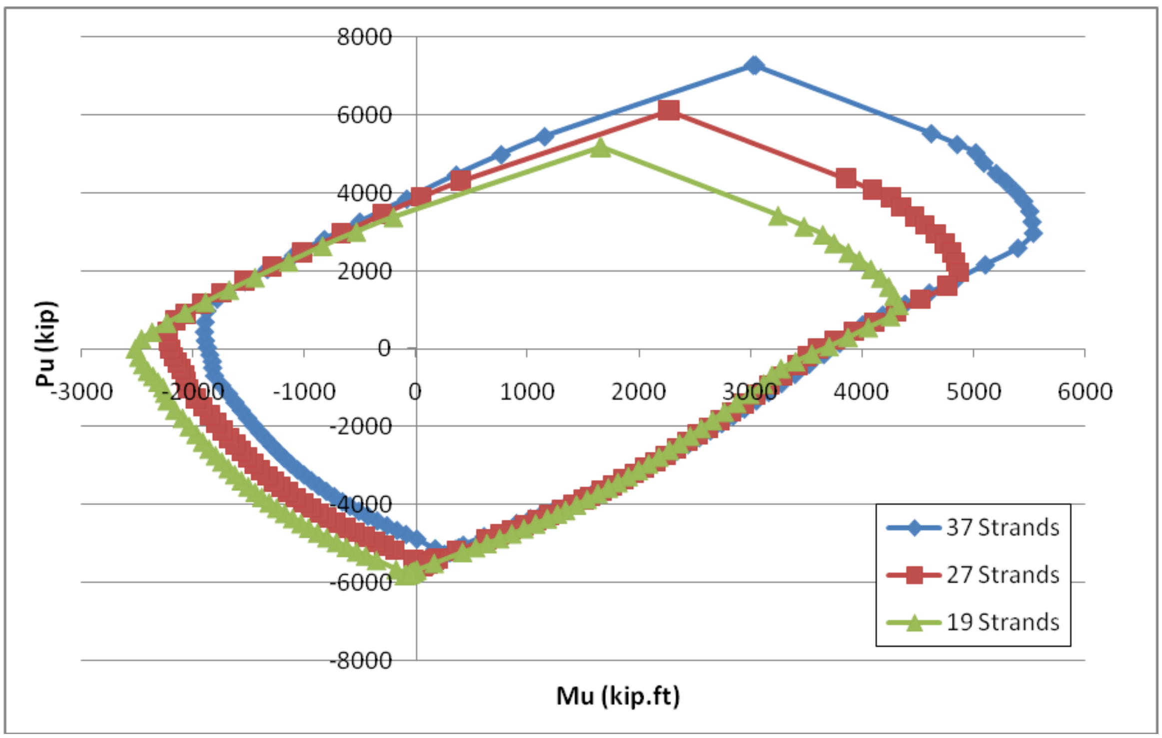

Interaction diagram for the tie mid-section without deck

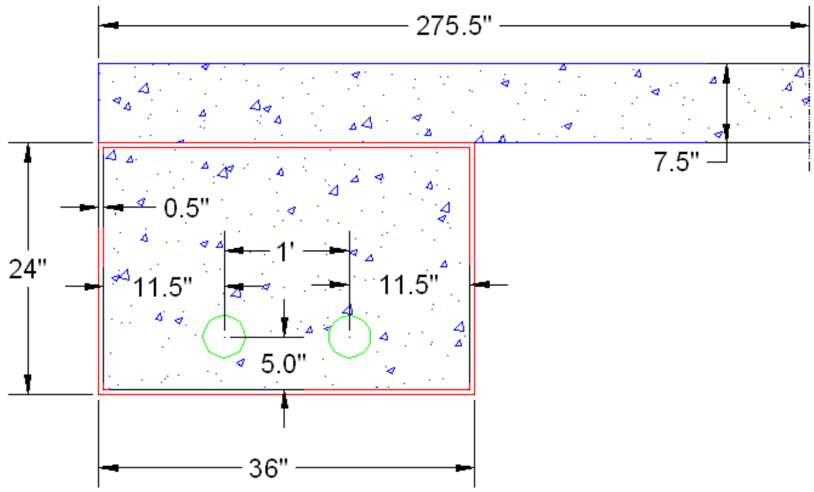

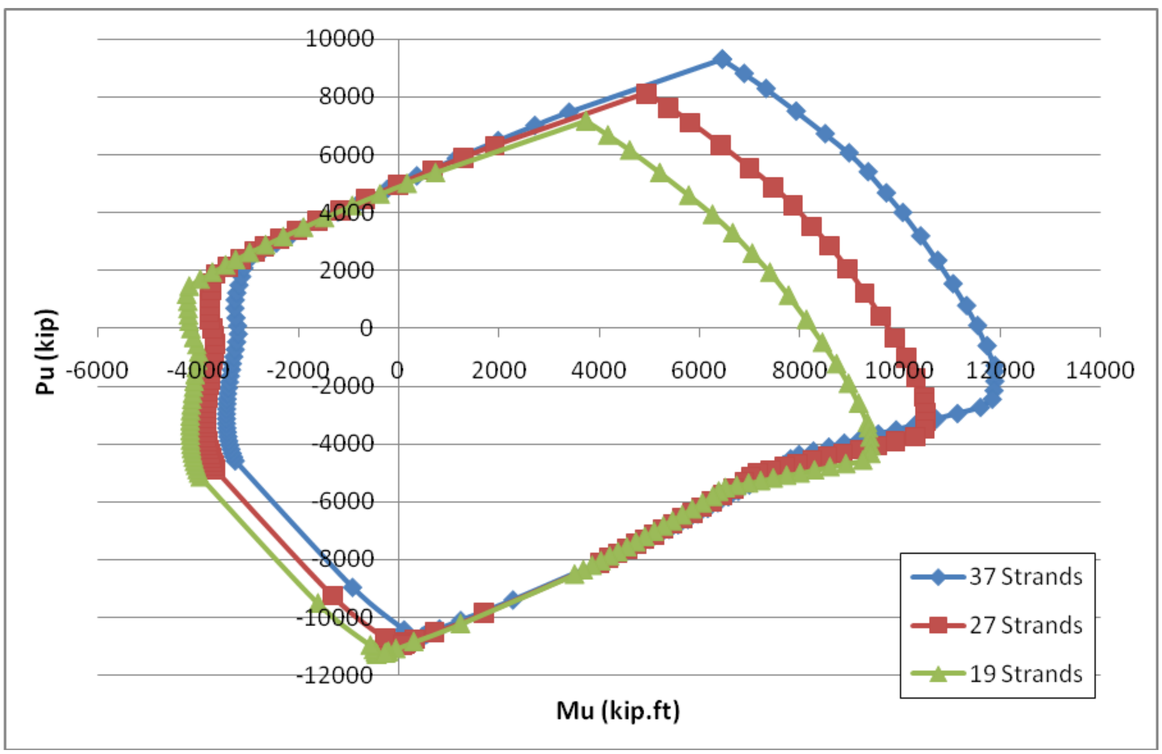

Interaction diagram for the outside tie mid-section with deck

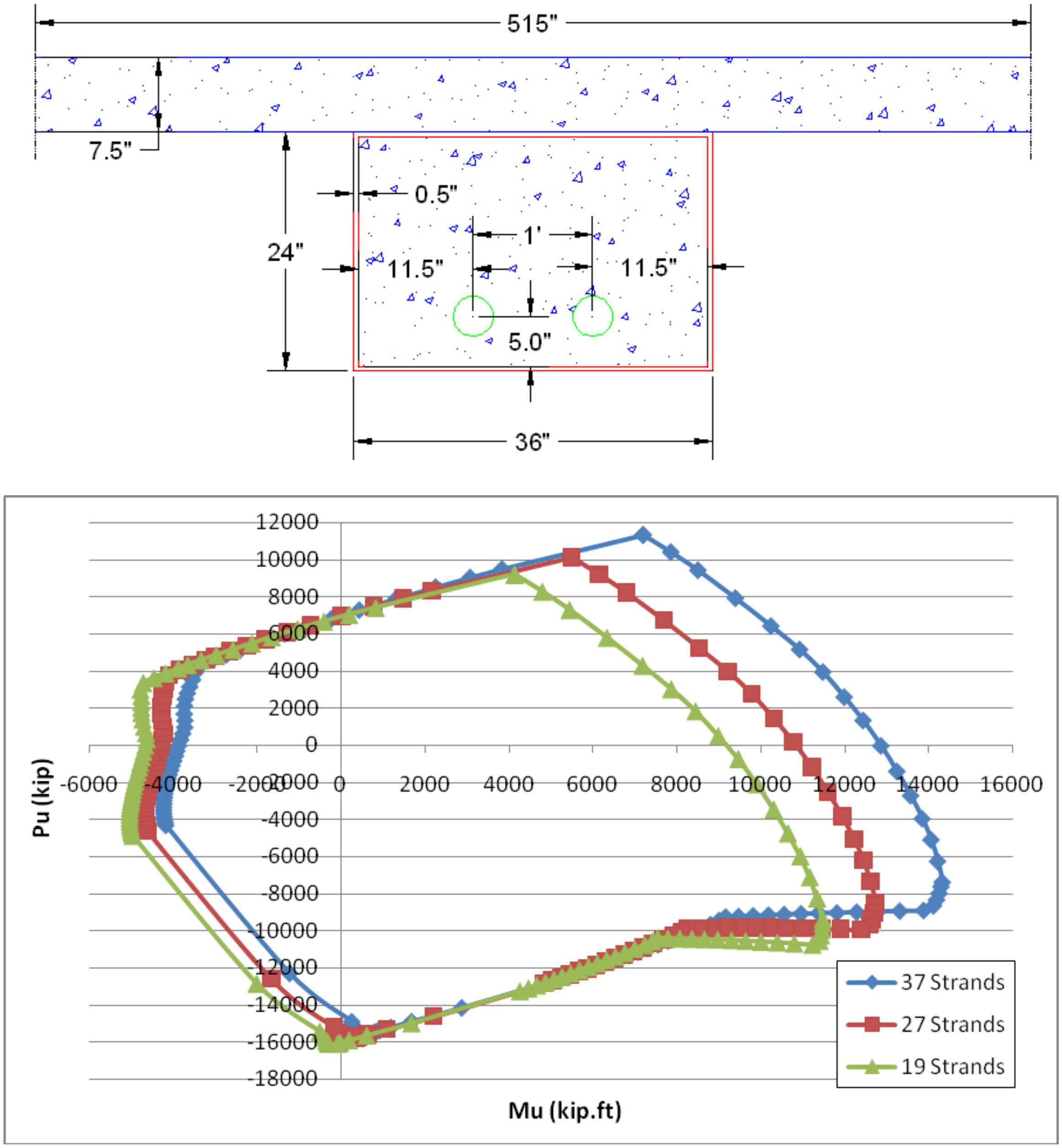

Interaction diagram for the median tie mid-section with deck

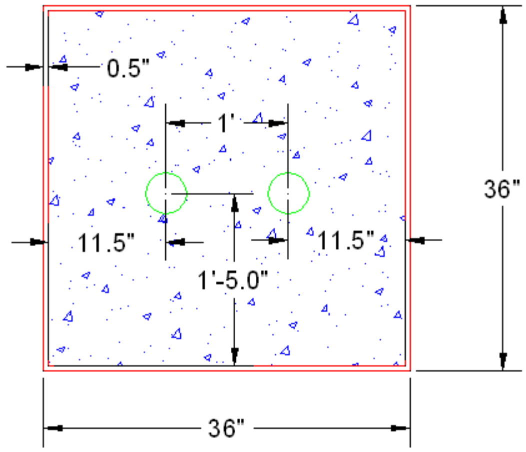

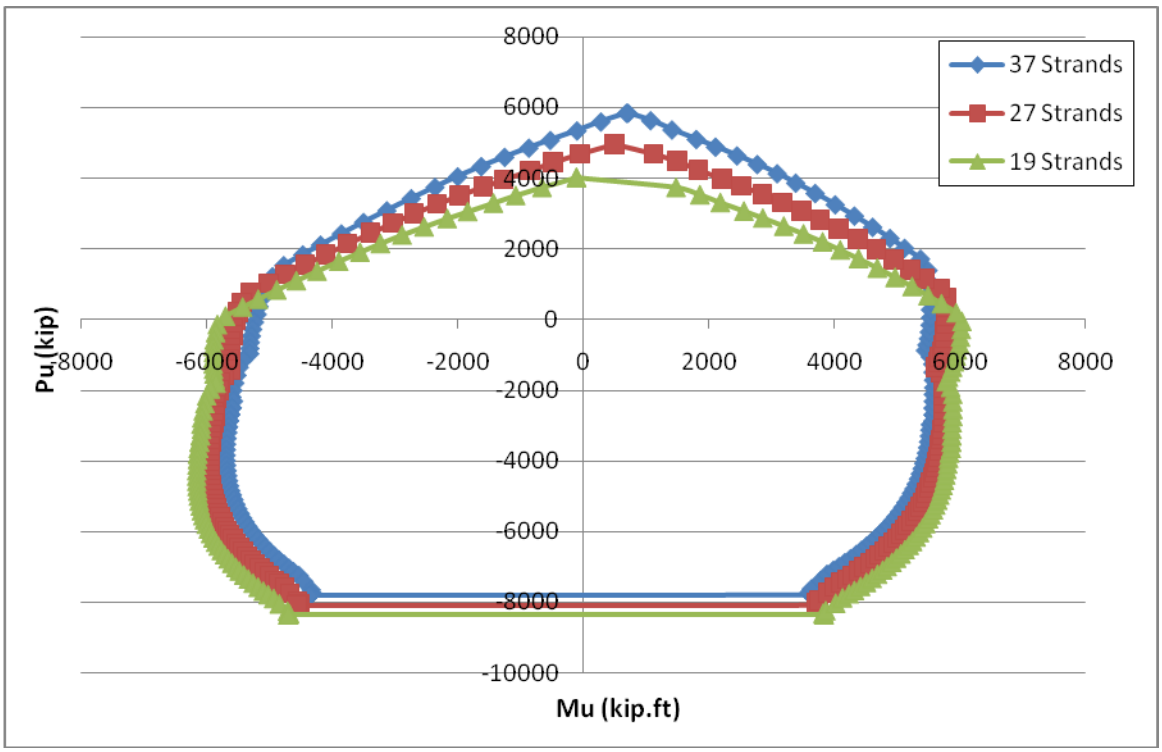

Interaction diagram for the tie end-section without deck

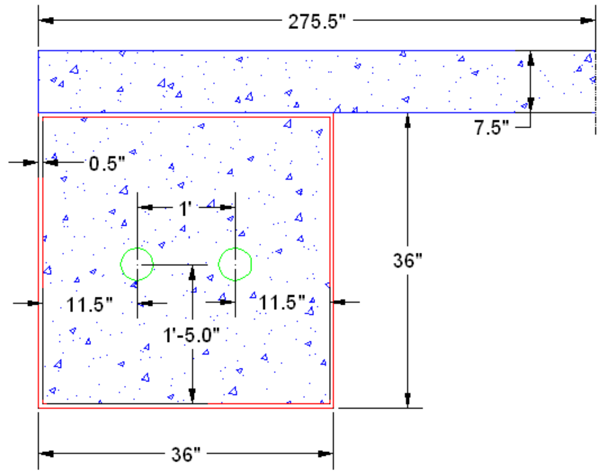

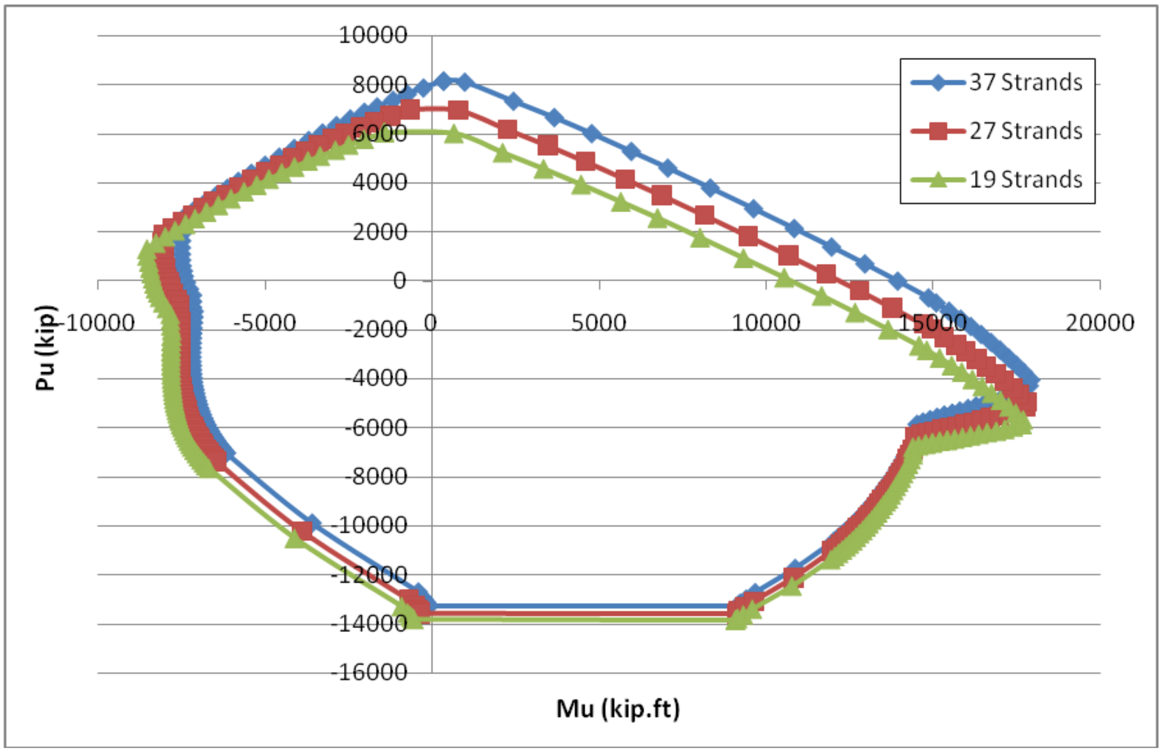

Interaction diagram for the outside tie end-section with deck

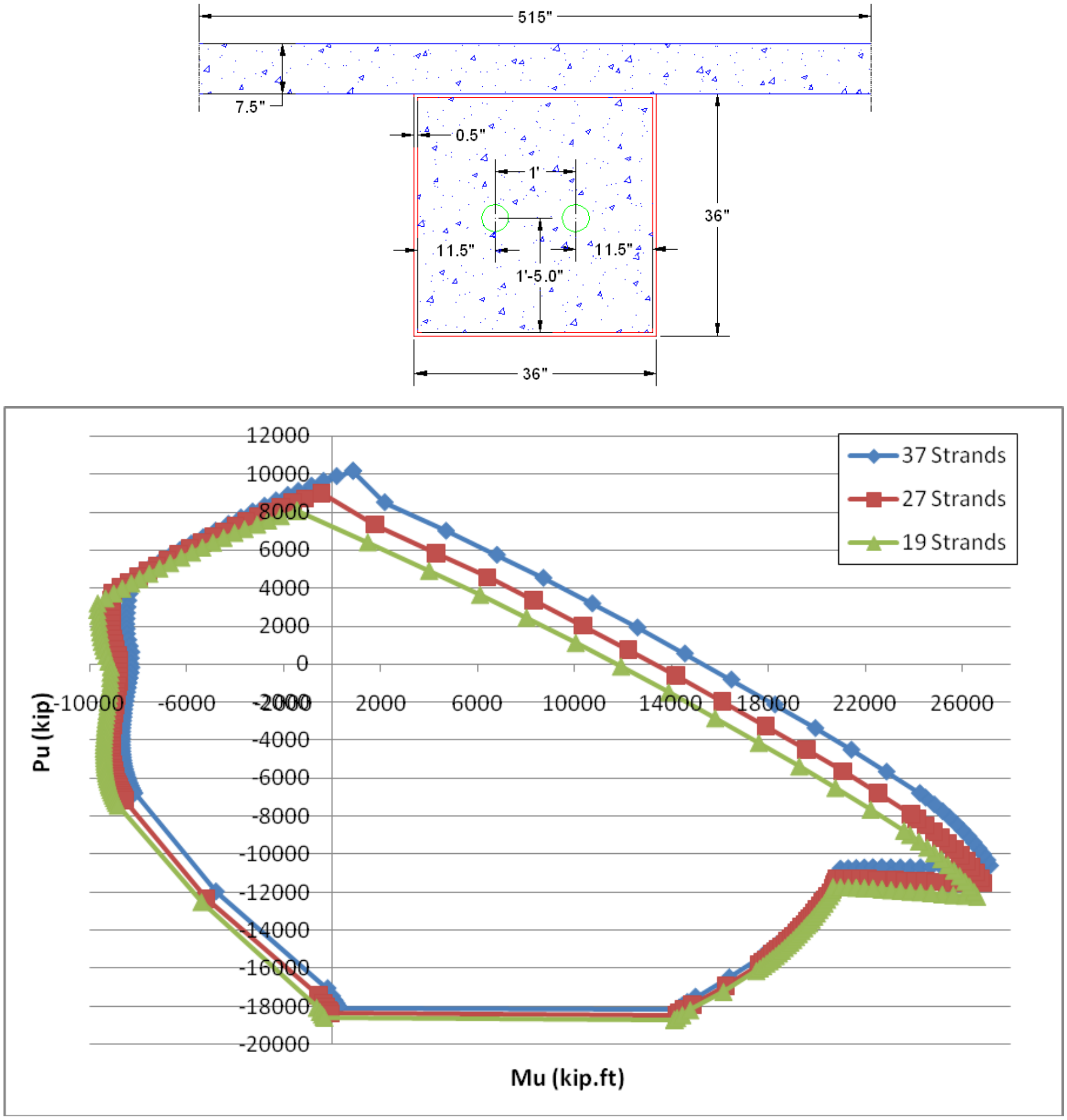

Interaction diagram for the median tie end-section with deck